EFFECTS OF RETINOIC ACID ON SIMPLE HEPATIC STEATOSIS AND DGAT2 EXPRESSION IN NON-ALCOHOLIC FATTY LIVER DISEASE (NAFLD) RATS

BY

NAWAL AHMED MOHAMED BEN-AMER

INTERNATIONAL ISLAMIC UNIVERSITY MALAYSIA

2026

EFFECTS OF RETINOIC ACID ON SIMPLE HEPATIC STEATOSIS AND DGAT2 EXPRESSION IN NON-ALCOHOLIC FATTY LIVER DISEASE (NAFLD) RATS

BY

NAWAL AHMED MOHAMED BEN-AMER

A thesis submitted in fulfillment of the requirement for the degree of Doctor of Philosophy of Health Sciences

Kulliyyah of Medicine
International Islamic University Malaysia

JUNE 2026

ABSTRACT

Non-alcoholic fatty liver disease (NAFLD) is an increasing public health problem worldwide, with limited effective treatment available. The main pathological feature of the disease is the accumulation of triglycerides in hepatocytes. Hepatic triglyceride synthesis is mediated by diacylglycerol acyltransferase-2 (DGAT2). Retinoic acid (RA), the active form of vitamin A, is metabolised and stored mainly in the liver. RA has been implicated in the pathogenesis of NAFLD. However, its effect on hepatic steatosis and its possible regulatory role on DGAT2 expression in NAFLD remain unclear. This study aimed to investigate the effectiveness of RA in a NAFLD animal model, and determine its role in hepatic DGAT2 expression. The study was conducted in two phases: a pilot study to determine the time required to induce liver steatosis using a 12% high cholesterol diet (HCD), followed by the main study using the same diet. Forty-five Sprague–Dawley rats were divided into five groups; control, control + RA, HCD, HCD + vehicle, and HCD + RA. After hepatic steatosis induction, selected groups received RA or vehicle for four weeks. Body weight, liver weight, serum biochemical parameters, hepatic TG content and histopathological changes were assessed. Hepatic DGAT2 expression was determined using immunohistochemistry and ImageJ software, while scanning electron microscope (SEM) was used to assess hepatic sinusoidal endothelial cells fenestration and porosity. Data were analysed using one-way ANOVA. The pilot study demonstrated that animals fed with 12% high cholesterol diet exhibited histopathological progression of NAFLD, from a simple steatosis in the four weeks group to non-alcoholic steatohepatitis (NASH) in the five- and six-week groups. In the second phase, a significant decrease in body weight by 20% was observed in RA-treated animals compared with HCD-fed rats. Liver weight and TG content were also significantly reduced. However, serum TG was not significantly lower in the RA-treated HCD group compared with the untreated HCD group, and RA had no noticeable effect on serum total cholesterol. Histopathological results showed improvement in hepatic steatosis, ballooning, and inflammation in the RA-treated group compared with the HCD group. The NAFLD Activity Score (NAS) and hepatic DGAT2 expression were both significantly reduced in HCD animals receiving RA. SEM analysis revealed significantly diminished fenestration frequency and porosity in all HCD groups, with no significant improvement following RA treatment. In conclusion, the results demonstrate that RA mainly improved hepatic lipid accumulation and histological injury, potentially through reduced hepatic DGAT2 expression, but had limited effects on the serum lipid profile and LSEC ultrastructural changes.

ملخص البحث

يُعدّ مرض الكبد الدهني غير الكحولي مشكلة صحية عامة متزايدة الانتشار في جميع أنحاء العالم، مع محدودية العلاجات الفعالة المتاحة. وتتمثل السمة المرضية الرئيسية لهذا المرض في تراكم الدهون الثلاثية في خلايا الكبد. يتم تصنيع الدهون الثلاثية في الكبد بواسطة إنزيم أسيل ترانسفيراز ثنائي أسيل جليسرول-2 (DGAT2). يُستقلب حمض الريتينويك (RA)، وهو الشكل النشط لفيتامين أ، ويُخزن بشكل رئيسي في الكبد. وقد ثبت تورط حمض الريتينويك في نشأة مرض الكبد الدهني غير الكحولي (NAFLD). مع ذلك، لا يزال تأثيره على التدهن الكبدي ودوره التنظيمي المحتمل على التعبير عن جين DGAT2 في مرض الكبد الدهني غير الكحولي غير واضحين. هدفت هذه الدراسة إلى التحقق من فعالية حمض الريتينويك في نموذج حيواني لمرض الكبد الدهني غير الكحولي، وتحديد دوره في التعبير عن جين DGAT2 في الكبد. هدفت هذه الدراسة إلى التحقق من فعالية حمض الريتينويك في نموذج حيواني لمرض الكبد الدهني غير الكحولي، وتحديد دوره في التعبير عن إنزيم DGAT2 الكبدي. أُجريت الدراسة على مرحلتين: دراسة تجريبية لتحديد الوقت اللازم لتحفيز تراكم الدهون في الكبد باستخدام نظام غذائي عالي الكوليسترول بنسبة 12%، تلتها الدراسة الرئيسية باستخدام النظام الغذائي نفسه. قُسِّمت خمسة وأربعون فأراً من سلالة سبرغ-داولي إلى خمس مجموعات: مجموعة ضابطة، ومجموعة ضابطة مع حمض الريتينويك، ومجموعة نظام غذائي عالي الكوليسترول، ومجموعة نظام غذائي عالي الكوليسترول مع دواء وهمي، ومجموعة نظام غذائي عالي الكوليسترول مع حمض الريتينويك. بعد تحفيز التليف الكبدي الدهني، تلقت مجموعات مختارة حمض الريتينويك أو دواءً وهمياً لمدة أربعة أسابيع. تم تقييم وزن الجسم، ووزن الكبد، ومؤشرات الكيمياء الحيوية في الدم، ومحتوى الدهون الثلاثية في الكبد، والتغيرات النسيجية المرضية. تم تحديد التعبير عن DGAT2 الكبدي باستخدام الكيمياء المناعية وبرنامج ImageJ، بينما تم استخدام المجهر الإلكتروني الماسح (SEM) لتقييم ثقوب ومسامية الخلايا البطانية الجيبية الكبدية. تم تحليل البيانات باستخدام تحليل التباين أحادي الاتجاه (ANOVA). أظهرت الدراسة التجريبية أن الحيوانات التي تغذت على نظام غذائي غني بالكوليسترول بنسبة 12% أظهرت تطورًا نسيجيًا مرضيًا لمرض الكبد الدهني غير الكحولي (NAFLD)، من التدهن البسيط في مجموعة الأسابيع الأربعة إلى التهاب الكبد الدهني غير الكحولي (NASH) في مجموعتي الأسابيع الخمسة والستة. في المرحلة الثانية، لوحظ انخفاض ملحوظ في وزن الجسم بنسبة 20% لدى الحيوانات المعالجة بحمض الريتينويك مقارنةً بالفئران التي تغذت على نظام غذائي عالي الكوليسترول. كما انخفض وزن الكبد ومحتوى الدهون الثلاثية بشكل ملحوظ. مع ذلك، لم يكن مستوى الدهون الثلاثية في الدم أقل بشكل ملحوظ في مجموعة الفئران المعالجة بحمض الريتينويك والتي تغذت على نظام غذائي عالي الكوليسترول مقارنةً بمجموعة الفئران غير المعالجة، ولم يكن لحمض الريتينويك أي تأثير ملحوظ على مستوى الكوليسترول الكلي في الدم. أظهرت نتائج الفحص النسيجي المرضي تحسنًا في التدهن الكبدي، وتضخم الخلايا الكبدية، والالتهاب في المجموعة المعالجة بحمض الريتينويك مقارنةً بمجموعة النظام الغذائي عالي الكربوهيدرات. كما انخفض مؤشر نشاط مرض الكبد الدهني غير الكحولي (NAS) بشكل ملحوظ في الحيوانات المعالجة بحمض الريتينويك، وانخفض تعبير جين DGAT2 الكبدي بشكل كبير في حيوانات النظام الغذائي عالي الكربوهيدرات التي تلقت حمض الريتينويك. أظهر تحليل المجهر الإلكتروني الماسح انخفاضًا ملحوظًا في معدل الثقوب والمسامية في جميع مجموعات النظام الغذائي عالي الكوليسترول، دون أي تحسن ملحوظ بعد العلاج بحمض الريتينويك. وخلصت الدراسة إلى أن حمض الريتينويك حسّن بشكل رئيسي تراكم الدهون في الكبد والضرر النسيجي، ربما من خلال تقليل التعبير عن إنزيم DGAT2 في الكبد، لكن تأثيره كان محدودًا على مستوى الدهون في الدم والتغيرات البنيوية الدقيقة لخلايا بطانة الجيوب الكبدية.

APPROVAL PAGE

The thesis of Nawal Ahmed Mohamed Ben-Amer has been approved by the following:

Zunariah Buyong
Supervisor

Nor Zamzila Abdullah
Co-Supervisor

Asmah Hanim Hamdan
Co-Supervisor

Sirajudeen Kuttulebbai Naina Mohamed Salam
Chairman of Supervisory Committee

Muhammad Lokman Md. Isa
Internal Examiner

Zaitunnatakhin Zamli
Internal Examiner

Mahadeva Rao Uttarkar Sathyanarayana
External Examiner

Mohd Hafiz Arzmi
Chairman

DECLARATION

I hereby declare that this thesis is the result of my own investigations, except where otherwise stated. I also declare that it has not been previously or concurrently submitted as a whole for any other degrees at IIUM or other institutions.

Nawal Ahmed Mohamed Ben-Amer

…… 20 June 2026

Signature Date ……

INTERNATIONAL ISLAMIC UNIVERSITY MALAYSIA

DECLARATION OF COPYRIGHT AND AFFIRMATION OF FAIR USE OF UNPUBLISHED RESEARCH

EFFECTS OF RETINOIC ACID ON SIMPLE HEPATIC STEATOSIS AND DGAT2 EXPRESSION IN NON-ALCOHOLIC FATTY LIVER DISEASE (NAFLD) RATS

I declare that the copyright holders of this thesis/dissertation are jointly owned by the student and IIUM.

Affirmed by Nawal Ahmed Mohamed Ben-Amer

20 June 2026

…… ……

Signature Date

This thesis is dedicated to my loving family, whose unwavering support and encouragement have been my greatest motivation throughout this journey. To my parents, for their endless sacrifices and belief in my potential; to my friends, for their constant encouragement and understanding; and to all those who inspired and guided me along the way. Your faith in me has been invaluable, and this work is a testament to your love and support.

ACKNOWLEDGEMENTS

All praise is due to Allah, the Almighty, whose grace and mercy have constantly been with me throughout the duration of my programme. Although, it has been tasking, His mercies and blessings on me ease the hard task of completing this thesis.

I am deeply grateful to my supervisor, Assoc. Prof. Dr. Zunariah Buyong whose enduring disposition, kindness, promptitude, thoroughness and friendship facilitated the successful completion of my work. I put on record and appreciate her detailed comments, useful suggestions and inspiring queries which have considerably improved this thesis. Her brilliant grasp of the aim and content of this work led to her insightful comments, suggestions and queries which helped me a great deal. Despite her commitments, she took time to listen and attend to me whenever requested. The moral support she extended to me is in no doubt a boost that helped in building and writing the draft of this research work. I am also grateful to my co supervisor, Prof. Sirajudeen Kuttulebbai Naina Mohamed Salam, Assoc. Prof. Dr Nor Zamzila Abdullah, and Asst Prof Dr. Asmah Hanim Hamdan, whose support and cooperation contributed to the outcome of this work.

I extend my deepest gratitude to the International Islamic University Malaysia through IIUM Research Management Centre for providing financial support under RMCG20-064-0064 & RMCG20-069-0069. My thanks also go to the medical laboratory staff, medical laboratory technologists, Department of Basic Medical Sciences, Pathology and Laboratory Medicine, and Postgraduate Office, Kulliyyah of Medicine, International Islamic University Malaysia, Malaysia.

Lastly, my gratitude goes to my beloved husband and lovely children; for their prayers, understanding and endurance while away. Once again, we glorify Allah for His endless mercy on us, enabling me to successfully round off the efforts of writing this thesis. Alhamdulillah.

TABLE OF CONTENTS

LIST OF TABLES

LIST OF FIGURES

LIST OF ABBREVIATIONS

ACAT	Acyl coA Cholesterol Acyl Transeferase
ALP	Alkaline Phosphatase
ALT	Alanine Aminotransferase
ARAT	Acyl coA Retinol Acyl Transferase
AST	Aspartate Aminotransferase
ATRA	All-trans Retinoic Acid
CHO	Cholesterol
CRABP	Cellular Retinoic acid Binding Protein
CVD	Cardiovascular Disease
DGAT2	Diacylglycerol Acyltransferase 2
DAG	DAG Diacyl glycerol
DNL	Denovolipogensis
FXR	Farnesoid X Receptor
G3PAT	Glycerol-3-Phosphate Acyl Transferase
HCD	High Cholesterol Diet
H&E	Haematoxylin and Eosin
HFD	High Fat Diet
HSCs	Hepatic Stellate Cells
HSL	Hormone Sensitive Lipase
IHC	Immunohistochemistry
LRAT	Lecithin: Retinol Acyl Transferase
LSECs	Liver Sinusoidal Endothelial Cells
MAG	Monoacyl Glycerol
MASLD	Metabolic Dysfunction–Associated Steatotic Liver Disease
MT	Masson's Trichrome
NAFLD	Non-alcoholic Fatty Liver Disease
NASH	Non-alcoholic Steatohepatitis
NAS	Non-acoholic Scoring
ORO	Oil Red O Stain
PA	Phosphatidic Acid

PAP	Phosphatidic Acid Phosphatase
PNPLA3	Patatin-Like Phospholipase Domain-Containing Protein 3
RA	Retinoic Acid
RALDH	Retinaldehyde Dehydrogenase
RAR	Retinoic Acid Receptors
RARE	Retinoic Acid Response Elements
RBP	Retinol Binding Protein
RXR	Retinoid X Receptors
SREBPs	Sterol Regulatory Element-Binding Proteins
TG	Triglyceride
T2DM	Type 2 Diabetes Mellitus
VCTE	Vibration-Controlled Transient Elastography
XBP1	X-Box Binding Protein 1

CHAPTER ONE

INTRODUCTION

1.1 BACKGROUND AND EPIDEMIOLOGY OF THE DISEASE

Non-alcoholic fatty liver disease (NAFLD) is a pathological condition determined by the presence of triglycerides (TG) deposition in the liver exceeding 5% of its weight, which is recognised as the hallmark of the disease (Gowda, Shekhar, Gowda, Chen, & Hui, 2023), in absence of other risk factors causing lipid accumulation in the liver such as alcohol and drugs (Kounatidis et al., 2024).

NAFLD is the most prevalent chronic liver disease worldwide. It is estimated to be approximately one-third of the population (Wong, Ekstedt, Wong, & Hagström, 2023). The global prevalence has increased immensely over the last few decades, increasing by more than 50% over the past three decades, from 25.3% in 1990-2006 to 38.0% in 2016-2019 according to a recent systematic review (Targher et al., 2024). This epidemic is in parallel with increased obesity and type 2 diabetes prevalence (Wong et al., 2023). In Malaysia, prevalence rates of 37.4% in a Klang Valley screening population and 72.4% among patients with type 2 diabetes mellitus have been reported (Khammas et al., 2019; Lai et al., 2019). The prevalence is particularly high among individuals with obesity and type 2 diabetes mellitus. NAFLD prevalence in type 2 diabetes is up to 75% , while in severely obese patients prevalence reaches 90% (Grander, Grabherr, & Tilg, 2023).

Additionally, NAFLD was reported to be more frequent in males than in females (Nagral et al., 2022).This widespread prevalence has transformed NAFLD into a public health crisis. Therefore, great advances have been recognized to understand the complex pathogenesis of this disease. In recent years, NAFLD has been identified as a multisystem disease, where the metabolic dysfunction and associated insulin resistance play the major role in the pathogenesis of NAFLD and its related comorbid diseases such as liver cirrhosis, failure, hepatocellular carcinoma, cardiovascular diseases, and

chronic kidney disease. Consequently, a new terminology metabolic dysfunction-associated fatty liver disease (MAFLD) has been used to replace NAFLD in adult individuals (Targher et al., 2024).

NAFLD disease burden is expected to be increased along with rising tendencies in metabolic syndrome and obesity among populations. Moreover, NAFLD mortality in Asian-Pacific regions is predicted to be raised by 65% to 100% in 2030 (Estes et al., 2020). NAFLD is a disease that progresses from the most common manifestation of simple hepatic steatosis to the more serious non-alcoholic steatohepatitis (NASH), present in 10-20% of NAFLD patients. NASH is histologically identified by hepatic inflammation, hepatocytes ballooning and progressive fibrosis, eventually progressing to advanced liver disease with increased mortality, followed by end-stage liver disease and hepatocellular carcinoma (Grander et al., 2023).

1.2 PATHOPHYSIOLOGY OF NAFLD

The rising disease burden and lack of available effective treatments have made understanding the pathophysiology of NAFLD the focus of many researchers, to identify the potential target for future treatment. The development and progression of NAFLD is complex and multifactorial. However, previously Day & James (1998) proposed a two-hit theory to explain the progression of the disease from simple steatosis to NASH. The first hit involves lipid accumulation in the liver, and the second hit includes an oxidative stress, an inflammatory process leading to hepatocellular injury, inflammation and fibrosis.

In recent years, understanding of NAFLD pathogenesis has advanced with complex parallel heterogeneous pathways involved in the development and progression of NAFLD/ NASH. These include dietary habits, genetic predisposition, and environmental factors that predispose to insulin resistance, obesity, and changes in the intestinal microbiome. Insulin resistance leads to an increased hepatic de novo lipogenesis (DNL), adipose tissue dysfunction with secretion of consequent adipokines and inflammatory cytokines, mitochondrial dysfunction, oxidative stress, production of reactive oxygen species (ROS), and endoplasmic reticulum (ER) stress (Buzzetti, Pinzani, & Tsochatzis, 2016).

Alteration in gut microbiota composition has been recognised to play an important role in the pathogenesis of NAFLD. Disruption of gastrointestinal bacteria leads to increased production of free fatty acid (FFA) in the intestine, and enhances intestinal permeability. As the liver continuously receives blood flow mainly from intestinal vessels, exposing it directly to the toxins, antigens from food and gut microbiota products (Olivia et al., 2019).

An unhealthy diet consumed by patients with NAFLD often contains low micronutrients and minerals, predisposing them to vitamin and mineral deficiencies. Moreover, alterations in gut microbiota interrupt micronutrient absorption. Therefore, deficiency of micronutrients is considered to play a role in the pathogenesis of NAFLD. Recent research has focused on some micronutrients such as vitamins A, C, E, resveratrol, pentoxifylline and minerals like iron, copper, selenium, magnesium, and zinc to determine their role in pathogenesis and therapeutic potential (Kang, 2025). In this context, the following section will focus on the role of vitamin A derivatives in the pathogenesis of NAFLD and their efficacy.

1.3 CURRENT TREATMENT OF NAFLD

Non- alcoholic fatty liver disease (NAFLD) is raising global health concerns. Currently there is yet no approved therapy. The primary management of the disease is lifestyle modification, including diet control such as a Mediterranean diet and reducing caloric intake to 500-1000 kcal has been shown to be effective in reducing hepatic staetosis and insulin resistance. Another cornerstone for the management of NAFLD is physical activity. Ultimately, weight loss improves liver histology and even resolves NASH (Paternostro & Trauner, 2022). However, these habits are difficult to keep over a long time.

Vitamin E is a strong anti-oxidant and acts by increasing the activity of antioxidant enzymes. A cross-sectional study reported the protective effect of vitamin E supplementation for NAFLD patients. Moreover, vitamin E supplementation is recommended for non-diabetic NASH patients (Qi et al., 2024). Proper management and glycaemic control in patients with type 2 diabetes is also an effective strategy to slow the progression of NAFLD. Pioglitazone is an anti-diabetic medicine that enhances

insulin sensitivity, used for the management of NAFLD and NASH. A recent meta-analysis on pioglitazone-treated NAFLD patients, reported the effectiveness of the drug in alleviating NAFLD by improving the hepatic histopathology, liver enzymes and serum lipids, with the incidence of oedema reported in treated groups (Wang et al., 2023).

Another treatment option for NAFLD is semaglutid, a glucagon-like peptide-1 receptor agonist. Semaglutide has been reported to reduce body weight, improve blood sugar control, reduce liver enzymes, and inflammatory markers for NASH-treated patients with some adverse effects such as gastrointestinal symptoms (nausea, constipation, abdominal pain) (Liava & Sinakos, 2021). Additionally, the Farnesoid X receptor (FXR) agonist holds great potential for the treatment of NAFLD. FXR is an endogenous receptor for bile acids, and activation of FXR receptors enhances the peroxisome proliferator-activated receptor α (PPARα), a nuclear receptor that promotes fatty acid oxidation. Clinical studies on FXR agonist-treated NASH exhibiting beneficial effects regressing the NASH by reducing hepatic steatosis, inflammation and fibrosis (Tang et al., 2024).

The hallmark of NAFLD is triglyceride deposition in the liver. Diacylglycerol acyltransferase 2 (DGAT 2) enzyme, catalyses the last reaction for triglyceride synthesis in the liver, making it an attractive target for pharmacologic intervention in NAFLD. Ervogastat, a selective DGAT2 inhibitor has been recently used in clinical trials for the treatment of NASH patients, demonstrating a promising efficacy in reducing the hepatic TG , serum TG, and improving hepatic steatosis (Amin et al., 2022).

1.4 VITAMIN A DERIVATIVE (RETINOIC ACID)

Vitamin A is an essential fat-soluble vitamin for humans and other vertebrates. The liver is the principal storage site of vitamin A in the form of retinyl ester packed in lipid droplets inside the cytoplasm of hepatic stellate cells (HSCs). Retinoids are naturally occurring compounds that cannot be de novo synthesised in the human body. The term vitamin A comprises provitamin A carotenoids that are dietary precursors of retinol. There are three known food compositions, which are α-carotene, β-carotene, and β-cryptoxanthin. The term retinoids refer to retinol, its metabolites, and synthetic analogues that have a comparable structure. Two isomers of the retinoids exist: cis and all trans isomers, the latter is the most common and stable form (the form used in this research). The major sources of vitamin A from foods are grains and vegetables. β-carotene intake primarily comes from cantaloupe, broccoli, squash, peas, and spinach, while α-carotene is mainly derived from carrots (51%). β-cryptoxanthin is obtained solely from fruits, followed by dairy and meat products as retinyl esters (Shirakami, Lee, Clugston, & Blaner, 2013).

Retinoic acid is the main physiological metabolite of vitamin A, which is transiently produced and promptly excreted. It is present in the serum as various fatty acids, and transported bound to albumin. Additionally, it effectively binds to retinol binding protein (RBP). Another specific intracellular binding protein, namely cellular retinoic acid binding protein (CRABP), promotes RA to bind to nuclear elements and alters gene transcription (Dawson & Okamura, 1990). RA then bind to nuclear retinoic acid receptors (RAR) and forms a heterodimer with Retinoid X receptors (RXR) (Duong & Rochette-egly, 2011). The complex RAR-RXR binds to retinoic acid Response Elements (RARE), which regulate the expression of different target genes that are involved in cellular differentiation, regeneration, proliferation and apoptosis (Abbott et al., 2007; Haaker et al., 2020). Excess all-trans retinoic acid (ATRA) is oxidised and gradually excreted from the body through the kidneys or the liver into bile or urine (Adamantidi et al., 2025).

1.5 DISTURBANCE OF VITAMIN A DERIVATIVE IN NAFLD

Insufficient serum retinol was observed in 11-36% morbidly obese patients with NAFLD (Chaves et al., 2008, 2014). Hepatic retinol content was also stated to be low in 68% of NAFLD (Chaves et al., 2014). A serum protein (RBP) was stated to be raised in NAFLD and obese patients. This was explained primarily by increased hepatic expression of this protein (Thompson et al., 2017) and impaired kidney excretion might be another contributing factor. While the adipose tissue origin of RBP is locally acting protein and does not contribute to raised circulating RBP (Lee et al., 2016). A recent meta-analysis included 8423 participants, and reported significantly higher levels of circulating RBP in NAFLD patient compared to non-NAFLD individuals (Hu et al.,2023).

Retinoids are involved in the metabolism of vital biological molecules such as lipids (Chen & Chen, 2014), carbohydrates (Johnson & Wolf, 1961) and proteins (Esteban-Pretel et al., 2010). An experimental study demonstrated the role of retinoids in lipid metabolism, which reported that vitamin A-deficient animals had increased lipid deposition and increased hepatic content of triglyceride. This was explained by decreased gene expression of mitochondrial oxidation enzymes and reversed by administration of All trans retinoic acid (ATRA) (Kang et al., 2007). A cross-sectional study on NAFLD patients revealed a significant decrease in serum RA in NAFLD patient groups when compared to the controls, and the lowest level was reported in NASH patients with fibrosis. Subsequently, the use of serum RA level was recommended in assessing the degree of NAFLD (Allam et al., 2020).

Another cross-sectional study on NAFLD reported that low serum vitamin A correlated with the degree of steatosis (Makbol et al., 2025). Similarly, a cross-sectional study involving 3537 American adult patients with NAFLD reported a positive correlation of serum retinol with the degree of NAFLD. While serum retinol negatively correlated with the grade of fibrosis (Niu et al., 2023). Furthermore, a cohort study involving US population reported that depleted serum retinol level was associated with hepatic fibrosis and hepatic-related mortality in chronic liver disease (J. Song & Jiang, 2023). Ultimately, it is clearly evidenced from the above research that low serum retinoids are strongly related to the extent of steatosis and advanced fibrosis. Consequently, the role of retinoids in NAFLD animal models has been studied

extensively to determine their therapeutic efficacy and underlying mechanism, which will be addressed in detail in the next chapters.

1.6 PROBLEM STATEMENT

NAFLD is the most common chronic liver disease worldwide, with a rising prevalence driven by increasing rates of obesity, insulin resistance, and metabolic syndrome globally. Besides, it has a serious clinical impact, with potential progression to NASH, fibrosis, cirrhosis, liver failure, and predisposes to hepatocellular carcinoma. Despite extensive research to understand the complex pathophysiology of the disease, there is still no approved effective treatment available and current management has limitations in long-term adherence, efficacy, and adverse effects, as discussed in Section 1.3 The pathogenesis of NAFLD mainly involves TG accumulation in the liver, insulin resistance, oxidative stress, and inflammation. Hepatic DGAT2 is the key enzyme that catalyses the final step for TG synthesis, making it directly relevant to hepatic steatosis and lipid accumulation in NAFLD**.** Recent studies highlighted the potential role of selective DGAT2 inhibitors for the treatment of NAFLD and promising results have been reported. Therefore, DGAT2 is considered as a potential therapeutic target for NAFLD.

The role of vitamin A in the pathogenesis of NAFLD has been studied substantially, and its deficiency has been reported in both NAFLD patients and animal models, suggesting a possible link between RA depletion and disease progression. Moreover, serum RA levels have been shown to correlate with the severity of the disease and were highlighted as a biomarker to determine the degree of the disease. Among vitamin A derivatives, retinoic acid (RA) has been studied extensively to determine its role in regulating lipid metabolism in NAFLD animal models. Retinoic acid is an active metabolite of vitamin A and has been shown to reduce hepatic TG accumulation and inflammation in animal models, mainly through optimizing insulin sensitivity, modulating oxidative stress pathways, increasing fatty acid oxidation and decreased fatty acid de novo-synthesis. However, the mechanism of RA action on TG metabolism, particularly via DGAT2, remains unclear, and the findings are inconsistent across studies.

The duration required to establish simple hepatic steatosis before progression to NASH remained uncertain. Therefore, Phase 1 determined the appropriate duration of high-cholesterol diet exposure before initiating RA treatment. Subsequently, this study investigated whether RA can ameliorate hepatocyte damage caused by high cholesterol diet at early stage of NAFLD, through its regulatory effect on DGAT2. Moreover, to date, there is a lack of studies on the effect of RA on hepatic endothelial cells, which are highlighted to play a role in the pathogenesis of NAFLD and are considered treatment targets as well. This research focused on the knowledge deficit on the role of RA in the NAFLD animal model. Specifically, this study determined the effect of RA on biochemical parameters including liver enzyme, serum lipids, and tissue TG. Additionally, the study assessed changes in body weight, liver weight, and histopathological scoring. Furthermore, this study aimed to provide a better understanding of the underlying mechanism of RA in improving hepatic steatosis by investigating DGAT2 expression in liver tissue, as well as examining hepatocytes and LSECs' ultrastructural changes.

1.7 RESEARCH QUESTIONS

The main question of this research was what is the effect of the RA on non-alcoholic fatty liver disease? Following that the subsequent specific questions are:

1. Can non-alcoholic fatty liver disease (NAFLD) be successfully induced in Sprague-Dawley rats through a high cholesterol diet?
2. Does RA treatment affect body and liver weight in NAFLD rats?
3. Does the RA treatment alter the level of hepatic TG, serum ALT, cholesterol and TG of NAFLD rats?
4. Does the RA treatment improve the hepatic histopathological features of NAFLD rats?
5. Does the RA treatment reduce the expression of the DGAT2 enzyme in NAFLD rats?

6. Does the RA treatment affect the hepatic ultrastructure and sinusoidal fenestration in NAFLD rats?

1.8 RESEARCH OBJECTIVES

1.8.1 General Objective

To evaluate the effects of RA treatment on simple hepatic steatosis and DGAT2 expression in the NAFLD rat model.

1.8.2 Specific Objectives

1. To establish non-alcoholic fatty liver disease (NAFLD) in Sprague-Dawley rats through a high cholesterol diet.
2. To compare the body and liver weight of RA-treated NAFLD rats and the control groups.
3. To compare the level of hepatic TG, serum ALT, cholesterol and TG of RA-treated NAFLD rats and the control groups.
4. To compare the hepatic histopathological features of RA-treated NAFLD rats and the control groups.
5. To compare the expression of the DGAT2 enzyme in RA-treated NAFLD rats and control groups.
6. To compare the hepatic ultrastructure and sinusoidal fenestration of RA-treated NAFLD rats and the control groups.

1.8.3 Research Hypothesis

This research hypothesis had aimed to test retinoic acid (RA) treatment in NAFLD animal model and whether RA would improve the liver function, hepatic histopathological features through modulation of DGAT2 expression in NAFLD and the impact of RA on hepatic endothelial integrity.

1. A high cholesterol diet can induce non-alcoholic fatty liver disease (NAFLD) in Sprague-Dawley rats.
2. The body and liver weights of NAFLD rats are decreased by RA treatment compared with those of the control groups.
3. The levels of hepatic TG, serum ALT, cholesterol, and TG in NAFLD rats are decreased by RA treatment compared with the control groups.
4. The hepatic histopathological features of NAFLD rats are improved by RA treatment compared to the control groups.
5. The expression of the DGAT2 enzyme in NAFLD rats is decreased by RA treatment compared to the control groups.
6. The hepatic ultrastructure and sinusoidal fenestration of NAFLD rats are improved by RA treatment compared to the control groups.

1.9 CONCEPTUAL FRAMEWORK

The research was designed to evaluate the efficacy of RA in the treatment of NAFLD in an animal model. This study focused on a specific enzyme, DGAT2, which is responsible for the development of hepatic steatosis and triglyceride accumulation in the liver. The effect of RA on this enzyme was assessed following the induction of NAFLD, particularly during the early stage of the disease (simple steatosis) prior to progression to steatohepatitis. The study aimed to determine whether RA could regress the progression of the disease and prevent the development of non-alcoholic steatohepatitis.

It was hypothesised that RA would prevent weight gain, improve liver function and serum lipid profile, and prevent progression of the disease to a more advanced stage.

In addition, RA was hypothesised to improve histopathological features and restore the ultrastructure of hepatocytes and liver sinusoidal endothelial cells (LSECs). Figure 1.1 illustrates the conceptual framework of this research.

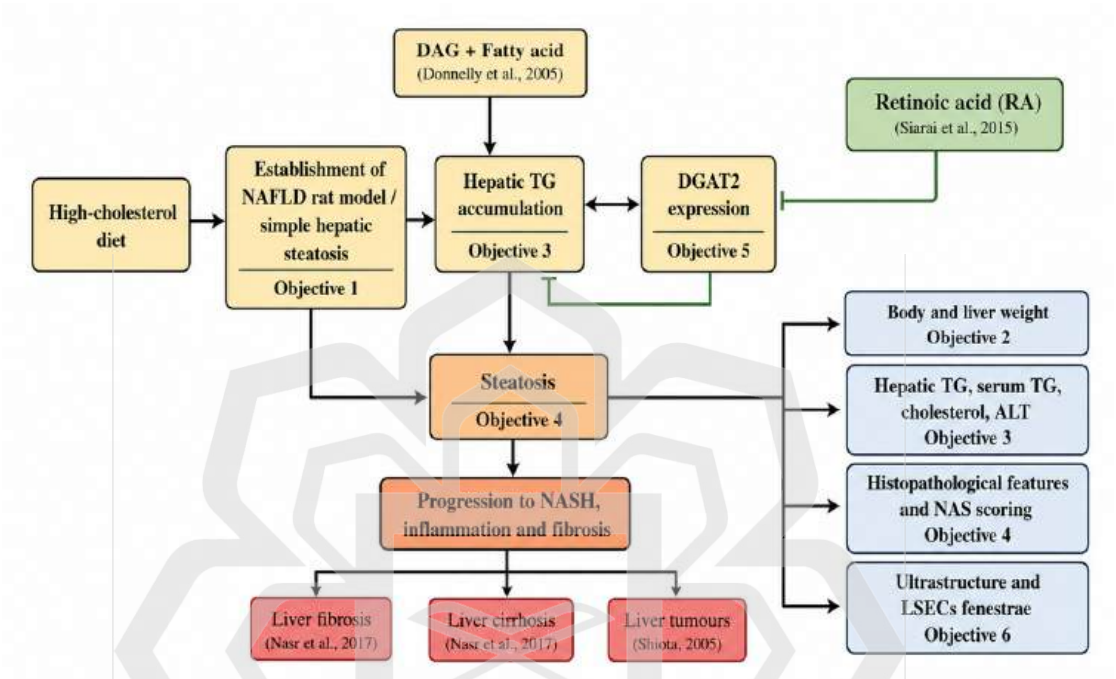

Figure 1.1 The Conceptual Framework of the Study.

DAG: Diacylglycerol, TG: triglyceride, DGAT2: diacylglycerol acyltransferase, LFT: liver function test, NAS: non-alcoholic scoring system, NASH: non-alcoholic steatohepatitis, LSECs: liver sinusoidal enothelial cells.

CHAPTER TWO

REVIEW OF LITERATURE

2.1 NON-ALCOHOLIC FATTY LIVER DISEASE (NAFLD)

2.1.1 Risk Factors and Comorbidities

Non-alcoholic fatty liver disease (NAFLD) is a major cause of chronic liver disease globally. NAFLD is a spectrum of disease categorised by simple hepatic steatosis in the absence of other coincidental causes for the development of liver fat accumulation such as excess alcohol consumption. The early stage of the disease is a benign condition, which is non-alcoholic fatty liver (NAFL), which may progress to a more severe non-alcoholic steatohepatitis (NASH). Consequently, this may lead to the development of the liver fibrosis, cirrhosis.and even liver failure (Pouwels et al., 2022). Individuals with NAFLD frequently have other concomitant diseases. The most common are. dyslipidaemia,. obesity, type 2 diabetes mellitus (T2DM), all of which are collectively known as the metabolic syndrome. These are considered prominent risk factors for NAFLD (Pouwels et al., 2022). It has been shown that NAFLD patients have an increased prevalence of cardiovascular disease (CVD) both with and without diabetes (Kim et al., 2024).

Metabolic syndrome exposes patients to widespread end-organ injury as evidenced by CVD and NAFLD. This had been attributed to ectopic lipid accumulation leading to fat-derived toxic metabolites. These toxic products provoke systemic and organ inflammation thereby precipitating the development and progression of NAFLD, CVD, and malignancy (Richie Manikat et al., 2023). Additionally, gastrointestinal infection with *Helicobacter pylori* increases the risk of development of NAFLD by 36%. This is due to raised inflammatory markers such as tumour necrosis factor-α, in *H. pylori*-infected persons, which predisposes to the development of NAFLD. Other cardiovascular diseases associated with NAFLD are arrhythmias, including atrial fibrillation, with an increased risk for development of atrial fibrillation among NAFLD

patients, which was estimated to be almost two-fold. A dangerous arrhythmia also has a related risk in NAFLD patients, including ventricular arrhythmias (Chen et al., 2021).

The ethnic and racial differences have been demonstrated to play a crucial role in the development, progression and outcomes of NAFLD. These differences have been attributed to genetic, environmental, and dietary factors. The Hispanic population has shown a higher occurrence of steatohepatitis and cirrhosis, while those who are African American have a lower likelihood of developing liver failure. Furthermore, genetic study in Hispanic NAFLD patients who possess a homozygous allele of patatin-like phospholipase domain-containing protein 3 (PNPLA3), have higher hepatic lipid content by two-fold compared to non-PNPLA3 Hispanic patients (Benedict & Zhang, 2017).

Furthermore, other co-morbid diseases linked to NAFLD are chronic kidney diseases (CKD), as reported by a cross-sectional study, where the prevalence of CKD and raised albumin excretion in urine was higher in patients with NAFLD than in individuals without NAFLD (Cao et al., 2021). Additional comorbidities include, obstructive sleep apnea, hypothyroidism (Pouwels et al., 2022). Besides, a retrospective study on 211,955 patients with NAFLD compared with matched healthy individuals reported that patients with NAFLD had significantly increased rates of the subsequent extrahepatic malignancies such as colon, gastric, uterine, prostate and breast cancers (Abu-freha et al., 2023). Consequently, NAFLD is a complex metabolic liver disease associated with multiple comorbid diseases. Therefore, screening of patients with NAFLD has been proposed to detect early cancers and decrease mortality (Song & Wong, 2023).

2.1.2 Symptoms and Signs

Most patients with NAFLD do not experience any warning symptoms. Meanwhile, some patients have complained of fatigue, right hypochondrial discomfort, enlarged liver, acanthosis nigricans, and developing lipomas. A notable percentage of patients presented with cirrhosis or end-stage liver disease. Splenomegaly has been reported in 25% of patients with NAFLD (Rotbain et al., 2017). Additionally, hepatomegaly can be seen during clinical examination, which is due to liver fatty infiltration. Abnormal liver function tests such as the level of aminotransferases (ALT and AST), can be an early indication of NASH or NAFLD. Incidental abdominal radiological scanning may also detect fatty liver (Pouwels et al., 2022).

2.1.3 Radiological Imaging for NAFLD

Different imaging methods can be used to support the diagnosis of NAFLD and NASH. However, while imaging can detect NAFLD, it cannot reliably differentiate between NASH and NAFLD; histopathological examination remains the gold standard. Ultrasound scan is the often-used tool to diagnose NAFLD by revealing a hyperechoic texture or bright hepatic tissue due to diffuse fatty accumulation. The ultrasound scanning showed a hyperechogenic liver, which, when compared to the spleen or kidney echogenicity, is suggestive of steatosis. Additionally, computed tomography and magnetic resonance imaging can identify hepatic steatosis, although they are not sensitive in detecting the inflammation or fibrosis of the liver. Vibration-controlled transient elastography (VCTE) is a non-invasive procedure used to detect the fibrotic changes in the liver by measuring liver stiffness, and evaluating the extent of liver damage (Pouwels et al., 2022). Another imaging procedure is the magnetic resonance spectroscopy (MRS) with non-invasive high accuracy in the diagnosis of NAFLD (Nakeep et al., 2024).

2.2 ANIMAL MODELS USED IN NAFLD RESEARCH

Non-alcoholic fatty liver disease becomes a very common condition worldwide, due it to its link to a frequently seen diseases such as obesity, insulin resistance and metabolic syndrome. However, the mechanisms driving the development and progression of the disease into a more severe condition, is not completely understood. Moreover, the unavailability of an effective treatment has made researchers focus on animal models resembling the human condition. Therefore, different animal models have been used to study the pathogenesis and efficacy of new therapies for NAFLD. The common animal models of NAFLD include dietary, genetic, and chemically induced models, which are described below.

2.2.1 Nutritionally Induced NAFLD Models

Bad dietary habits are predominantly responsible for the development of NAFLD in humans. Therefore, diet is a crucial component in the development of the disease in animals. The pathogenesis and progression of the disease can be imitated in animals by simulating poor dietary habits.

2.2.1.1 Methionine and Choline Deficient (MCD)

Diet deficient in some essential elements has been used to induce NAFLD in animals resembling human disease. Among these elements are methionine and a choline-deficient diet (MCD). Methionine is an essential amino acid, while choline is an essential micronutrient for membrane lipids and an important neurotransmitter that is primarily metabolised and stored by the liver (Zhong et al., 2024). The major benefit of this model is the rapid induction of steatosis and inflammation in a few weeks. The precise pathophysiology of the development of NAFLD in this model is not completely understood, although, it is suggested that abnormal phospholipid synthesis, and aberrant lipoprotein secretion lead to mitochondrial dysfunction in liver cells, progressing to fatty liver and liver injury (Zhong et al., 2024). The disadvantage of this model is that

the metabolic changes are opposite to those of NAFLD in humans as mice fed on the MCD diet develop weight loss, decreased blood glucose levels and increased insulin sensitivity (Rinella & Green, 2004).

2.2.1.2 High-Fructose Diet

Animal fructose consumption in the form of corn syrup drinks boosts intestinal bacterial overgrowth, which leads to increased bacterial endotoxin in portal circulation. Consequently, activation of Kupffer cells and hepatic lipid accumulation. Therefore, high fructose-fed rodents develop obesity and NAFLD with insulin resistance, oxidative stress, and simple steatosis. In contrast, this model develops no ballooning degeneration and inflammatory infiltration. Additionally, combining high fructose with high fat and high cholesterol diets has been promoted for the development of hepatocellular ballooning, and progression to fibrosis (Zhong, Zhou, Xu, & Gao, 2020).

2.2.1.3 High-Fat Diet (HFD)

This is the most widely used model of NAFLD, and a variety of fat content diet regimens have been used to induce NAFLD with insulin resistance, marked hepatic steatosis, inflammation, and fibrosis, but without ballooning degeneration (Kirsch et al., 2003). The advantage of the high fat-diet animal models is their similarity in pathogenesis of human NAFLD, which is reflected by significantly increased body weight and liver weight. While liver damage in this model is not serious, there is no considerable fibrosis seen in hepatic tissue. The disadvantage of the HFD model is a longer time needed to develop NAFLD compared to other models, such as MCD (Zhong et al., 2024).

2.2.1.4 High Cholesterol and Cholate Diet

A cholesterol-rich diet is a risk factor for hypercholesterolemia and the development of NAFLD. Addition of cholic acid enhances the absorption of cholesterol and prevents its conversion to bile acids, consequently reducing the elimination of cholesterol and raising its levels (Ibrahim, Hirsova, Malhi, & Gores, 2016). Caballero et al. (2006) were the first to report that a high-cholesterol diet precedes to a selective depletion of mitochondrial glutathione, which has promoted the expression of TNF-α in hepatic tissue, raising the hepatic inflammatory response, and enhancing the development of NASH. Rats fed on 1% high cholesterol diet (HCD) significantly increased liver weight, triglycerides, and free fatty acids in the liver (Zhong et al., 2024).

Furthermore, a 12% HCD-fed rats was reported to successfully induce NASH within 6-week duration, with prominent fatty liver changes, hepatic inflammation, hepatocyte ballooning degeneration, perisinusoidal fibrosis, together with raised serum alanine aminotransferase (ALT), and insulin resistance (Abdul Rahim et al., 2019). This experimental model effectively represents the histopathological and metabolic manifestation of NASH that is observed in humans at a considerably earlier duration of time. Additionally, animal models fed on high-fat and high-cholesterol (HFHC) diets with 15% fat and 1% cholesterol, showed considerable weight gain, and increased percentage of hepatic fat deposition with prominent fibrosis. Therefore, in HFHC experimental animals reported more advanced disease than that produced by only HFD or HCD animals (Savard et al., 2013).

Therefore, this model is relevant to the present study because it allows RA treatment to be assessed during early hepatic steatosis before progression to NASH.

2.2.2 Genetic Models of NAFLD

2.2.2.1 Leptin-Deficient Mice (ob/ob)

This is a frequently used mouse model in metabolic and NAFLD research. Leptin is a hormone expressed mainly in adipose tissue and responsible for satiety. A point mutation in the gene for leptin (*ob* gene) produces a leptin-deficient model with hyperphagia, obesity, insulin resistance, and hyperlipidaemia when fed on a control chow diet. This model produces only steatosis and does not progress to NASH (Leclercq et al., 2002). For the development of the full disease spectrum, HFD or MCD-feeding is required (Jahn, Kircher, Hermanns, & Geier, 2018).

2.2.2.2 Leptin Receptor-Deficient Mice (db/db)

This model is physiologically similar to *ob/ob* mice. *Db/db* mice are resistant to the physiological effects of the leptin hormone. Other related genetic models include low-density lipoprotein receptor-deficient mice (Ldlr-/-) and apolipoprotein E-deficient mice (Apoe-/-). The low-density lipoprotein receptor (LDLR) is a cell surface receptor expressed mainly on hepatocytes. The receptors mediate the endocytosis of cholesterol-rich LDL particles. This pathway is defective in LDLR-deficient mice (Ldlr-/-) leading to an impairment of cholesterol clearance from the circulation and, consequently, severe hypercholesterolemia. These mice have been frequently used in atherosclerosis research. However, it has also been found to be a useful model in NAFLD research (Bieghs et al., 2012). Apolipoprotein (apo) E is an important protein in lipid metabolism; its role is binding to lipid complexes in blood or intestinal fluids to mediate its uptake by specific cell surface receptors. Therefore apo E participates in the distribution of lipids among various tissues and cells of the body (Huang & Mahley, 2014).

The absence of ApoE in Apoe-/- mice results in defective clearance of lipoproteins from the serum and, subsequently, leads to severe hyperlipidaemia and hypercholesterolemia, an important risk factor for developing NAFLD in humans and

cholesterol is increasingly recognised as a direct mediator for inflammation (Jahn et al., 2018). However, this model does not exhibit hepatic fibrosis, as leptin is essential for hepatic fibrosis. Subsequently, ob /ob mice are fundamentally resistant to the development of hepatic fibrosis. In this regard, deletion or resistant leptin receptors are infrequently seen in obese patients with NAFLD, limiting their ability to simulate human NAFLD associated with obesity and insulin resistance (Zhong et al., 2024).

2.2.2.3 Mutation in the Alms1 Gene Model (Foz/Foz mice)

The *Foz/Foz* mice have a mutation in the *Alms1* gene, a widespread protein crucial for the proper functioning of the primary cilium. The coded protein in the *Alms1* gene plays a significant role in intracellular transport and appetite regulation. *Foz / Foz* mutant mice exhibit obesity, IR and steatosis. Feeding mice with HFD contributed to NASH with severe fibrosis (Zhong et al., 2024). However, an adverse reaction was observed affecting other organs producing proteinuria overtime (Liu et al., 2020).

2.3 GROSS LIVER STRUCTURE AND CELLULAR COMPOSITION

The liver is the largest organ in the human body, weighing around 1.5 kg, and is surrounded by a capsule called Glisson's capsule. It is located at the right hypochondrial area and epigastric area, often reaching the left hypochondrial area. Most of its surface is protected by the visceral peritoneum, excluding the posterior surface called the 'bare area', which is in contact with the diaphragm. Porta hepatis is the entry point for the blood vessels (i.e. portal vein, hepatic artery), common bile duct, nerves, and lymphatic vessels (Cotoi & Quaglia, 2016). The liver is divided into lobes and segments. The falciform ligament separates the liver into right and left lobes. The right lobe is divided into the caudate and quadrate lobes by a plane through the gallbladder and inferior vena cava. The liver can be further divided into eight functional segments, each segment has its own vascular inflow, outflow, and biliary drainage. The significance of the functional anatomy of the liver lies in the planning for anatomic resection.

The liver has a dual blood supply, which includes the portal vein and the hepatic artery. The portal vein provides roughly 80% of the liver's blood supply and carries venous blood rich in nutrients drained from the spleen, gastrointestinal tract, and associated organs. The hepatic artery supplies the arterial blood. Both the portal vein and hepatic artery pass into the liver through its hilum, where bile ducts also exit. Branches of the portal vein, hepatic artery, and bile ducts are distributed together in the liver parenchyma within the portal tracts, which can only be seen microscopically. The functional unit of the liver is the hepatic lobule. which consists of hepatocytes arranged in cords or sheets separated by sinusoids (Figure 2.1). A central vein located at the centre of the lobule, while portal tracts located at its periphery consists of a portal venule, bile duct, and hepatic arteriole (Sourianarayanane & Nanchal, 2018). The liver consists of different cell types, as described in the following sections.

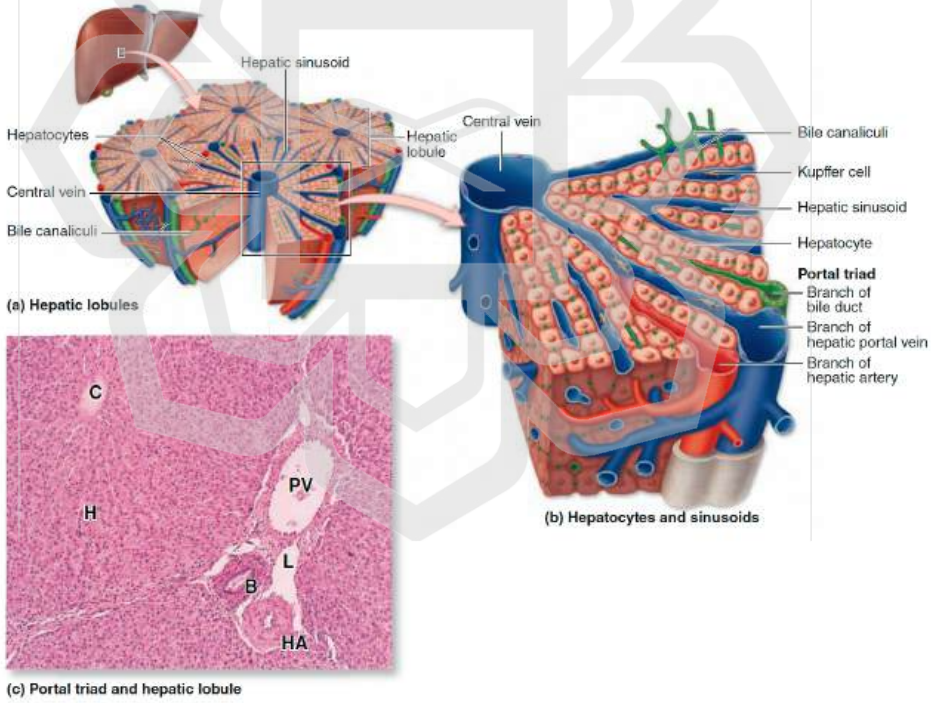

Figure 2.1 The schematic images (a) and (b) representing the gross liver anatomy and its construction unit (hepatic lobule) with microscopic structures. (c) Micrograph of a lobule shows the central vein, C, plates of hepatocytes, H and a portal area with lymphatic, L and components of the portal triad; portal venule, PV, hepatic arteriole, HA and bile ductule, B. Reproduced from Mescher,. (2016)

2.3.1 Hepatocytes

Hepatocytes are the main parenchymal cells forming the liver. They have a polyhedral shape with many facets, usually six in number. Hepatocytes have many organelles, as many as 100 mitochondria, approximately 50 Golgi apparatus, and around 200-300 peroxisomes, more than found in any other cells (Dunnington, 2021). Hepatocytes play an important role in various cellular functions, including carbohydrate, lipid, and protein metabolism, detoxification, and immune cell activation to preserve liver homeostasis (Gong et al., 2023). Hepatocytes are organised in unicellular plates (Remak's plates). This liver plate branch and anastomose with each other to form a maze-like assembly with barriers between the hepatocyte plates and the sinusoids. The surface of the hepatocyte is covered with microvilli (Rodés & Benhamou, 2007).

The presence of numerous endoplasmic reticulum and Golgi bodies reflects their high secretory capacity. The major proteins secreted from hepatocytes are albumin, fibrinogen, transferrin, and clotting factors. Additionally, hepatocytes play a predominant role in the production of bile, which is then transported into the bile canaliculi. The produced bile is transported to the bile ductule and eventually to the bile duct through an osmotic gradient. The bile is further modified by cholangiocytes and ductular epithelium, stored in the gall bladder and released into the intestine once required.(Dunnington, 2021). The liver is the first organ that comes in contact with the nutrients that are absorbed from the gastrointestinal tract. It is also involved in detoxifying and filtering unwanted material by the process of endocytosis (Dunningto, 2021).

2.3.2 Sinusoidal cells

Non-parenchymal cells form about 6% of the lobular parenchyma. These include the hepatic sinusoids which are Kupffer cells, hepatic stellate cells, and liver sinusoidal endothelial cells (LSECs) which are involved in the pathogenesis of many liver diseases (Cain & Hubscher, 2019). LSECs are difficult to see with a conventional light microscope, because of their exclusive, very thin cell structure, small, and definite location within the liver. They are also abundant with transmembrane pores, to form a

permeable barrier, making them appear almost transparent or invisible alongside the greatly bigger, and dense hepatocytes (Mönkemöller, Øie, Hübner, Huser, & Mccourt, 2015). However, LSECs can be seen with an electron microscope or immunocytochemical methods. LSECs are distinctive cells because of their very tiny processes, which cover a huge area of the liver with fenestrations that are arranged in clusters (Figure 2.2A). LSECs control the two-directional interchange of substrates between the lumen of the hepatic sinusoid and the hepatocytes (Cogger, Hunt, & Couteur, 2020).

The transport function of LSEC is principally operated by the transcellular fenestra. These fenestrae are arranged in clusters of a few to more than 50 fenestrations called liver sieve plates, which are separated by ridges of non-fenestrated cytoplasm. The fenestrations have an oval or round shape with diameters ranging from 50 to 500 nm (Mak & Lieber, 1984). The fenestration size and number are decreased in chronic disease and ageing (Figure 2.2B). Furthermore, loss of fenestration is found to be associated with hyperlipidemia and insulin resistance (Couteur et al., 2008), which represent the metabolic manifestation of NAFLD (Hunt et al., 2019). Specifically, the high-fat diet model of NAFLD reported remarkably dilated and damaged hepatic fenestration compared to the control diet (Peng et al., 2014). Similarly, high-fat fed rats developed a reduction in endothelial porosity (Miyao et al., 2015; Cogger et al., 2016).

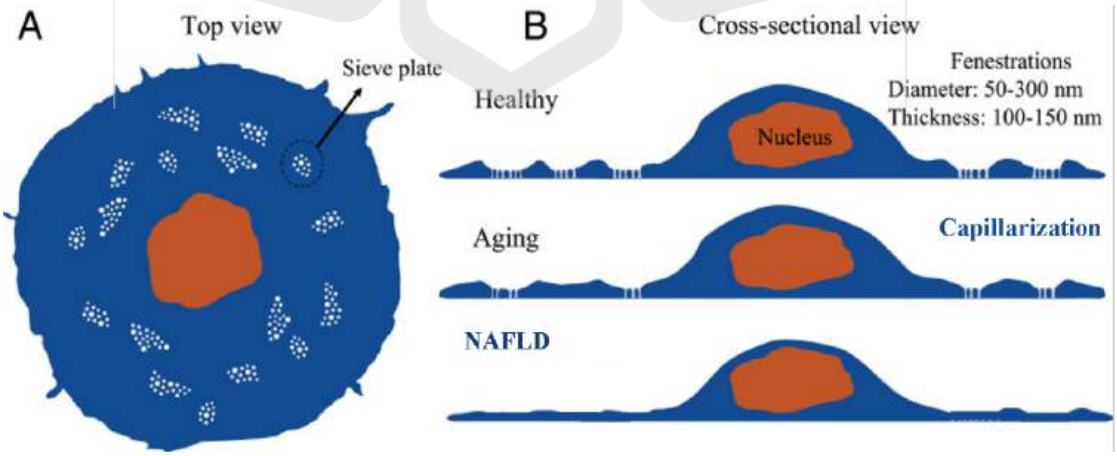

Figure 2.2 Schematic illustration for liver sinusoidal endothelial cells (LSECs) (Adapted from Butola et al., 2021)

2.3.3 Kupffer cells

Kupffer cells are the macrophages that are located in the liver and the most common macrophages in the human body reside in the sinusoids and function to remove pathogens from the circulation efficiently. It acts as a barrier against immunoreactive substances that enter from the gastrointestinal tract into the portal circulation. Therefore, Kupffer cells protect the liver from inflammation caused by these immunoreactive substances. Additionally, Kupffer cells play a primary role in clearing dead red blood cells (Dunnington, 2021).

2.3.4 Cholangiocytes

Cholangiocytes are epithelial cells that line the intrahepatic and extrahepatic bile ducts (Figure 2.3). They are highly specialised cells that participate in bile production and homeostasis. Cholangiocytes play an important role in liver regeneration especially in chronic liver disease, as they contain stem cell niche or progenitor-like cells that are activated in many liver pathologies. Moreover, cholangiocytes can be converted to activated cells and contribute to the inflammatory process by secreting chemokines and cytokines. They can also directly influence the physiology of myofibroblasts, which are responsible for collagen deposition within the liver (Banales et al., 2019).

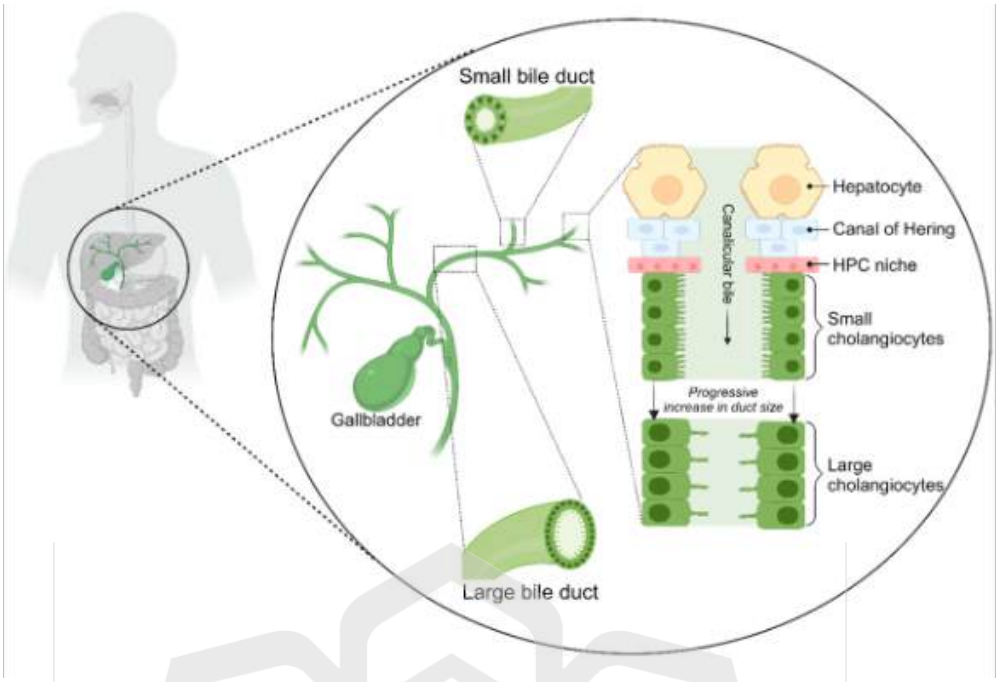

Figure 2.3 Bile Ductules Lined by Cholangiocytes.
(Reproduced from Babboni et al.,2024)

2.3.5 Hepatic Stellate Cells (HSCs)

Hepatic stellate cells (HSCs) are a type of myofibroblast. HSCs are a non-parenchymal liver cell that are situated perisinusoidally in the space of Disse. The most distinctive morphological feature of this cell in a normal liver, is the presence of many cytoplasmic retinoid-containing lipid droplets. For a healthy individual, the liver contains approximately 70% of the total retinoid present in the body. Therefore, HSCs contain the majority of retinoid body stores. When there is significant dietary retinoid intake, the number and size of lipid droplet increases to adapt to excess retinoid. In times of inadequate dietary retinoid consumption, the lipid droplets of HSCs decrease in number and size due to mobilisation of retinoid stores to meet body retinoid needs.

The main function of hepatic stellate cells is extracellular matrix synthesis which contributes to the process of fibrogenesis, and regulates the flow of sinusoidal blood (Dunnington, 2021).When HSCs become activated in liver injury, they lose their lipid droplets and retinoid stores. However, the underlying molecular mechanism of why or

how the lipid droplets and their contents are lost is not yet explained (Blaner et al., 2009).

2.4 HISTOPATHOLOGICAL MANIFESTATIONS OF NAFLD

Liver tissue biopsy remains the gold standard method for diagnosis and scoring of NAFLD (Liang et al., 2014). The liver biopsy is helpful in assessing the amount of fatty changes and the extent of liver damage. For accurate interpretation of pathological changes in the liver, normal liver microscopic features were discussed in the earlier section (see Section 2.3). The classic hepatic lobule was first described by Kiernan in 1833 (Chan et al., 2014). The liver is formed of a distinct hexagonally arranged hepatocyte. The hepatic acinar pattern was proposed by Rappaport in 1954, in which the hepatic acinus is subdivided into three zones according to their distance to the terminal hepatic venules at the periphery of the acinus (Rappaport et al., 1952). Hepatic acinus is used to describe the spread and the progression of the pathology, as the initial phases of NAFLD, and the most severe changes are seen in acinar zone 3 (Brown & Kleiner, 2015).

2.4.1 Histopathological Initiation and Progression of NAFLD

The histopathological changes in NAFLD are divided into NAFL, which commonly involves hepatocytes with macro-vesicular steatosis with or without non-specific inflammation and the more progressive disease form which is NASH. The latter is characterised by macro-vesicular steatosis, hepatocyte balloon degeneration mainly lobular, inflammation, apoptotic bodies, and Mallory-Denk bodies (MDBs). Additionally, some fibrosis could be seen but it is not necessary for diagnosis due to diagnosis of NAFLD is based on the underlying cause, and the fibrosis considered as consequent complication of the disease (Brown & Kleiner, 2015).

In the initial phase of NAFLD, the histologic changes show a characteristic scattering pattern, with the most severe changes seen in acinar zone 3 due to its high capacity for lipogenesis, making it the first area affected by hepatic steatosis (Figure 2.4). In addition, hepatocytes in zone 3 have lower oxygen concentration, making them more susceptible to cell damage from ischemia and metabolic stress (Kietzmann, 2017). Steatosis is defined as the deposition of lipid in vacuoles within hepatocytes (Chalasani & Szabo, 2015). This histological manifestation is seen in all forms of NAFLD. However, it is a common non-specific feature of other liver diseases. Steatosis is considered to be clinically significant when it involves at least 5% of the hepatocytes. In NAFLD, steatosis is mainly macro-vesicular, but it can be a mixture of micro-vesicular and macro-vesicular changes. A foamy cytoplasm is the characteristic appearance of micro-vesicular steatosis which can be noticed in a single hepatocyte or in a small area (Levene et al., 2012).

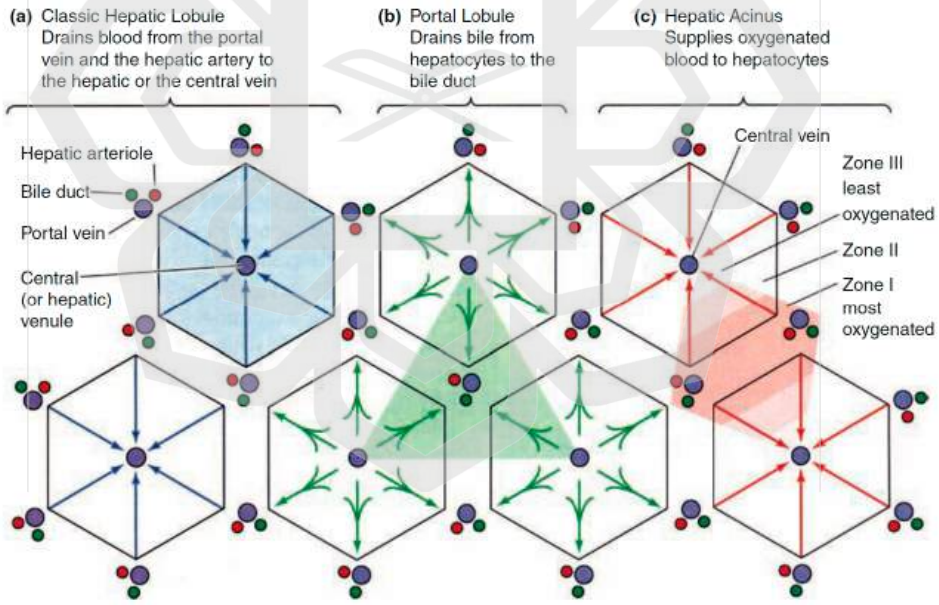

Figure 2.4 Schematic representation of the classic hepatic lobule (a), portal lobule (b) and hepatic acinus (c). Hepatic acinus shows zones 1, 2 and 3 and the decreasing oxygen gradient towards the central vein. Reproduced from Mersher (2016)

2.4.2 Histopathological Scoring Systems for NAFLD

Numerous scoring systems have been established to evaluate NAFLD severity with or without liver biopsy. The most accurate is the invasive biopsy scoring system. One of them, the NAFLD Activity Score (NAS), is an established score that has been used to grade the activity of the disease in patients with NAFLD. Kleiner et al. (2005) developed and validated a semi-quantitative scoring system ranging from 0 to 8, as summarised in Table 2.1. The reproducibility of the histological features was assessed using inter-rater agreement statistics, including weighted kappa values. The NAS is widely used in human and animal studies to assess disease activity and treatment response. It has three components: Steatosis scoring from 0 to 3 (Score 0 = <5% affected hepatocytes; Score 1 = 5-33%; Score 2 = 34-66%; Score 3 = >66%).

Lobular inflammation scoring from 0 to 3 (Score 0= no foci of inflammation, Score 1= < 2 foci per 200x field, Score 2= 2-4 foci per 200x field, Score 3= >4 foci per 200x field) and hepatocellular ballooning scoring from 0 to 2 (Score 0= none, Score 1 = few ballooned hepatocytes, Score 2 = many or prominent ballooning). The score is determined by the weighted sum of its component scores for steatosis (0-3), lobular inflammation (0-3), and ballooning (0-2); it ranges from 0 to 8. NAS scoring level more than five, the diagnosis of steatohepatitis is established, a score of 3- 4 is considered as borderline, and NAS score < 2 suggests simple steatosis or non-NASH (Brunt et al., 1999; Kleiner et al., 2005).

Fibrosis in NAFLD is due to the progression of the disease, resulting from abnormal accumulation of connective tissue and liver structural remodelling. Many scoring systems have been recommended for determining the degree of fibrosis in NASH (Brunt et al., 1999). In recent years, non-invasive vibration controlled transient elastography (VCTE), have been introduced to assess liver stiffness, have been introduced to assess the degree of fibrosis. Furthermore, new biomarkers for liver fibrosis have been proposed and have not yet been used, such as a Mac 2-binding protein glycan isomer (M2BPGi), which is secreted by HSCs to work as a messenger for Kupffer cells during fibrosis progression (Heyens et al., 2021). Another extracellular

matrix (ECM) biomarker is hyaluronic acid (HA), fibronectin, elastin, and laminin (Iqbal et al., 2019).

The most commonly used histopathological staging system for fibrosis in NAFLD poposed by Brunt et al. (1999), which includes four stages: Stage 1: The initial site of NASH fibrosis is pericellular fibrosis. Stage 2: Added to the previous stage some degree of portal fibrosis. Stage 3: This stage is manifested by the bridging fibrosis detected as fibrous septa between any of the vascular structures (i.e., portal-portal, central-central, central-portal), and may be described as focal or extensive involvement of liver tissue. Stage 4: Demonstrating cirrhosis, which is the last stage of advanced fibrosis. Representing fibrous septa separating hepatic nodules formed of regenerated hepatocytes (Brunt et al., 2021).

Table 2.1 NAFLD Activity Score (NAS)

Category	Features	Score	Definition
Steatosis	Percentage of affected hepatocytes	0	<5%
		1	5–33%
		2	34–66%
		3	>66%
Lobular inflammation	Number of foci per 200x field	0	No foci
		1	< 2 foci
		2	2–4 foci
		3	>4 foci
Ballooning	Hepatocyte injury	0	None
		1	Few ballooned cells
		2	Prominent ballooning

The total NAS score is the sum of the above scores, ranging from 0 to 8.

2.5 LIPID METABOLISM AND ITS RELEVANCE TO NAFLD

Non-alcoholic fatty liver disease (NAFLD) is now referred to as metabolic dysfunction-associated steatotic liver disease (MASLD). Due to its association with other metabolic diseases, and it is considered a disorder of hepatic lipid metabolism, characterised by excess accumulation of the triglycerides in liver cells. The liver plays a central role in lipid homeostasis, controlling lipid uptake, synthesis and oxidation. Abnormal intracellular lipid accumulation leads to toxic lipid products (lipotoxicity), organelle dysfunction, cellular damage, chronic inflammation and disease progression (Pei et al., 2020).

2.5.1 Overview of Lipid Digestion and Absorption

Liver plays a central role in lipid digestion and absorption. Lipids are organic substances present in our body in three forms: triglycerides, which form 90% of lipids, phospholipids, and cholesterol. Triglycerides and phospholipids are composed of fatty acids, but cholesterol is not. Cholesterol acts as a precursor for vitamin D synthesis, bile acids and steroid hormones, whereas phospholipids are used in the synthesis of cell membranes, and triglycerides are mainly utilised for energy storage in the form of adipose tissue (Salih et al., 2021).

2.5.2 Fatty Acid Metabolism

There are three main substrates in any organism required for metabolic homeostasis: glucose, fatty acids and amino acids. They are important for energy generation and biosynthesis of building blocks for macromolecules. Fatty acids are the building block for different kinds of lipids. The primary pathway for fatty acid degradation is mitochondrial fatty acid β-oxidation (FAO). FAO is the main metabolic pathway for energy homoeostasis in organs such as the liver, heart and skeletal muscle (Houten & Wanders, 2010).

2.5.2.1 Fatty Acid Absorption

The food source of fatty acids is in form of triglycerides. A triglyceride contains three fatty acid molecules linked by ester bonds to a glycerol molecule. Details of triglyceride absorption, including fatty acid absorption, are discussed in the next section (2.5.3.1)

2.5.2.2 Fatty Acid Biosynthesis

Hepatic *de novo* lipogenesis (DNL) is the biosynthesis of lipid from carbon substrates. Several key enzymes are involved in this process, including acetyl-CoA carboxylase (ACC), ATP-citrate lyase, and fatty acid synthase. The newly formed lipid is stored or excreted by hepatocytes. Physiological regulation of hepatic DNL remains incompletely determined. Raised hepatic DNL contributes to a variety of metabolic disorders including insulin resistance, dyslipidaemia, hypertension and systemic inflammation (Lawitz et al., 2022). Plasma fatty acids have three sources, which are produced by lipolysis of the peripheral adipose tissue, fatty acids produced in the liver from carbohydrates through hepatic *de novo* lipogenesis (DNL), and fatty acids that come from the diet. The absorbed fatty acid is mainly from the hydrolysis of triglyceride contained in food, which is broken down to MAG, and free fatty acid, then rejoins MAG in the liver to produce TG (Borén & Taskinen, 2021).

2.5.3 Triglyceride Metabolism

Most of dietary fat is in the form of triacylglycerols (90-95%) with a small portion in the form of cholesterol and phospholipid (Gurr, Frayn, & Frayn, 2008). Triglyceride has hydrophobic molecules, to be transported in aqueous fluid (plasma) need to be combined with lipoprotein particle along with other components. Additionally, dietary triacylglycerols need to be partially hydrolysed before the body can integrate them into lipoproteins. Gastric lipase hydrolyses the triacylglycerols (TAG) into monoacylglycerols (MAG), diacylglycerols (DAG) and non-esterified fatty acids.

2.5.3.1 Triglyceride Absorption

The hydrolysis of TG will be completed in the small intestine by pancreatic lipase into-monoacylglycerols and non-esterified fatty acids, which are then surrounded by bile salt and combined with cholesterol and fat-soluble vitamins. The formed compact particle is called a micelle, which starts to be absorbed in the distal duodenum and is completed in the jejunum through enterocytes of the intestine (Salih et al., 2021). Re-esterification of MAG to TAG occurs in the enterocyte via the monoacylglycerol acyltransferase enzyme (MGAT). Newly generated TG with some cholesterol and cholesteryl ester combine with a special protein and form chylomicron, which is transferred to the blood through the lymphatics.

In the circulation, chylomicrons react with high-density lipoprotein to join the ApoC-II. This protein activates the lipoprotein lipase. Chylomicrons also acquire ApoE from HDL, which plays a role in liver recognition later. In the capillaries of muscle and adipose tissue, lipoprotein lipase hydrolyses most of the triglycerides in chylomicrons into free fatty acids and glycerol. The free fatty acids are used by cells, while glycerol is returned to the liver. When chylomicrons reach their final destination, the remnants are taken-up by the liver, where they can be utilised again to rebuild VLDL or excreted in bile (Gugliucci., 2024)

2.5.3.2 Triglyceride Biosynthesis

There are two main pathways for TG biosynthesis in humans: First, the glycerol phosphate pathway, which is the most common. Second, the monoacylglycerol (MG) pathway. The MG pathway is present in some tissues such as the intestine, liver, and adipose tissue, where it participates in the re-esterification of hydrolysed absorbed TG. Triglyceride is also produced endogenously in hepatic tissue from fatty acids, glycerol and stored in adipose tissue for later use (Figure 2.5).

The components of TG are synthesised from both fatty acids and glycerol. Glycerol must be activated to glycerol 3-phosphate by glycerol kinase (Yen et al., 2008). Then, the activated fatty acids (fatty acyl-CoA) serve as substrates for fatty acid

addition to glycerol 3-phosphate to generate lysophosphatidic acids through glycerol 3-phosphate acyltransferase (GPAT) enzyme. One more CoA-activated fatty acid is added to lysophosphatidic acids, producing 1,2-diacylglycerol phosphates, which are commonly known as phosphatidic acid (PA). The phosphate group of phosphatidic acid is removed by phosphatidic acid phosphatase (PAP) to produce 1,2-diacylglycerols (DAG). DAG, together with fatty acyl-CoA, acts as a substrate for diacylglycerol O-acyltransferase (DGAT) enzyme, forming triglyceride (Michael., 2025).

There are two DGAT enzymes (DGAT1 and DGAT2), which are different at the level of DNA and protein sequences. DGAT1 is found to catalyse the different esterification reactions, such as retinol acyl CoA: Retinol acyltransferase (ARAT) function which acts for the biosynthesis of retinyl esters from retinol. Therefore, DGAT1 activity plays an important role in the absorption of vitamin A from the intestine. Additionally, DGAT1 also possesses MGAT activity *in vitro* assays, revealing its ability to catalyse the esterification of MG. Moreover, DGAT2 has been identified as the most potent DGAT with elevated affinity to its substrates compared to DGAT1. Overexpression of DGAT2 yields significantly more TG accumulation than DGAT1 overexpression. Sterol-regulatory element binding proteins (SREBPs) stimulate the transcription of enzymes responsible for adipogenesis, but these transcriptions have not been shown to regulate DGAT1 or DGAT2 gene expression. The transcription factor X-box binding protein 1 (XBP1), is the key regulator of the unfolded proteins response, and activates the expression of lipogenic genes, involving DGAT2, in the hepatocytes (Yen et al., 2008).

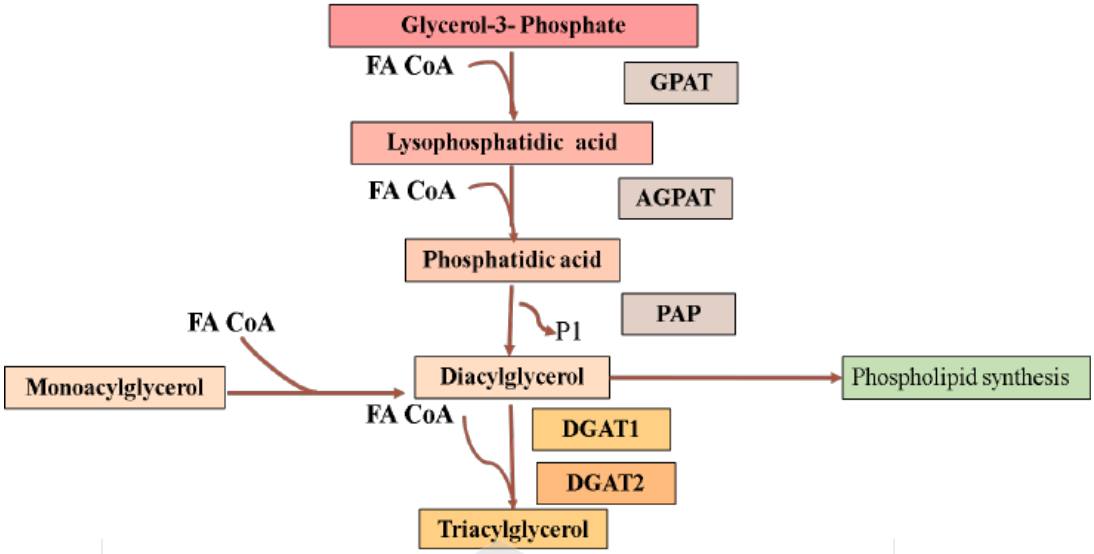

Figure 2.5 Schematic Diagram for Triacylglycerol Synthesis Catalysed by Glycerol-3-Phosphate Acyltransferase (GPAT) Enzymes, Phosphatidic Acid Phosphatase (PAP), and Diacylglycerol O-Acyltransferase 1,2 (DGAT), Phosphate Group (P1).

2.5.4 Cholesterol Metabolism

2.5.4.1 Cholesterol Absorption

The liver has the main role in producing and controlling circulating lipoproteins that carry cholesterol in the circulation. Additionally, liver excretion of cholesterol in bile, as bile acid, represents the critical pathway of removing excess body cholesterol (Ioannou, 2015). Cholesterol is a natural compound that is found mainly in animal tissues, with the highest concentrations in the brain and nerve tissues. It also exists in considerable amounts in the liver, kidneys, and skin. Cholesterol is a crucial component in the nervous system for the formation of synapses and myelin sheaths (Zhang et al., 2024). Excessive cholesterol contributes to a variety of serious diseases including atherosclerosis, gallstones, metabolic dysfunction–associated steatotic liver disease (MASLD), cardiac and vascular diseases, diabetes mellitus, malignancy, and Alzheimer disease.

The human body requires about 1 gram of cholesterol, of which about 600–900 mg comes from endogenous biosynthesis and about 300–500 mg is absorbed from the diet. Absorbed cholesterol comes from the diet and bile. Most animal-origin food, such as meats, shrimp, dairy products, and egg yolks, is recognised to have high cholesterol content. Most of the cholesterol in the diet (85%) is present in non-esterified form, while the residual amount exists in the form of cholesterol esters. Cholesterol ester requires an enzymatic hydrolysis to be absorbed in the small intestine in the form of free cholesterol (Zhang et al., 2024).

The free cholesterol combines with bile acids to form water-soluble micelles, which can be absorbed through the surface of enterocytes. NPC1L1, a 13-transmembrane protein that is highly expressed on the enterocyte, is recognised as a protein that facilitates the absorption of cholesterol. After cholesterol is entered into the enterocytes, the majority of it is re-esterified. The reaction is mediated by the enzyme cholesterol esterase, which is acyl-CoA cholesterol acyltransferase (ACAT). The enzyme catalyses the formation of cholesterol esters from cholesterol and long-chain fatty acids. The formed cholesterol ester assembled together with triglycerides, phospholipids, and a small amount of free cholesterol to form chylomicrons. Eventually, the formed chylomicron arrived in the circulation and cholesterol can be utilised by relevant tissue or used by the liver to synthesise bile salts (Zhang et al., 2024).

2.5.4.2 Cholesterol Biosynthesis

The *de novo* synthesis of cholesterol is the biosynthesis of only sterol by a living cell. However, the majority of cholesterol biosynthesis occurs in the liver, in the endoplasmic reticulum of the hepatocytes. It is a complex process, where the synthesis of cholesterol needs several constituents, including acetyl-CoA, ATP, oxygen, and nicotinamide adenine dinucleotide phosphate (NADPH). This process includes more than twenty enzymes and approximately thirty enzymatic reactions, which start with acetyl-CoA and can be allocated into three stages.

Stage one in cholesterol synthesis is the formation of mevalonate, which starts with acetyl-coenzyme A derived from mitochondria and transported to the cytosol. One molecule of acetyl-coenzyme A and one molecule of acetoacetyl-CoA are converted to 3-hydroxy-3-methylglutaryl-CoA (HMG-CoA). In stage two, HMG-CoA is then reduced to mevalonate by HMG-CoA reductase. Mevalonate is further phosphorylated to isopentyl pyrophosphate, which is transformed to geranyl pyrophosphate. Condensation with another isopentyl pyrophosphate yields farnesyl phosphate. Squalene synthase catalyses the condensation of two molecules of farnesyl pyrophosphate to yield form the linear 30-carbon hydrocarbon, squalene (Tricarico, Crovella, & Celsi, 2015). In stage three, squalene is then cyclised to form lanosterol. Finally, lanosterol undergoes a series of approximately 18-20 enzymatic reactions to be converted to cholesterol (Tricarico et al., 2015). The regulation of cholesterol biosynthesis in the hepatocytes is mediated by a family of transcription factors known as sterol regulatory element-binding proteins, and post transcriptional negative feedback regulation (Zhang et al., 2024).

2.6 MOLECULAR MECHANISMS LINKING LIPID METABOLISM AND NAFLD

The key of NAFLD pathogenesis is the accumulation of triglycerides (TGs) in the hepatocytes. The main enzyme for TG synthesis is the DGAT2, which present mainly in the hepatocyte.

2.6.1 Key Enzymes Regulating Triglyceride Accumulation

The main pathology in NAFLD is TG accumulation in hepatocytes. The principal enzyme responsible for TG biosynthesis in the liver is the DGAT enzyme. Therefore, DGAT2 plays a significant role in the development and pathogenesis of NAFLD. A study on diet-induced NAFLD mice reported that overexpression of hepatic DGAT2 developed steatotic liver, but not insulin resistance, suggesting that DGAT2 induces fatty liver through TG accumulation rather than insulin resistance (Kantartzis et al., 2010).

In a large group of NAFLD patients, evaluation of the expression of lipid metabolism-related genes in liver biopsies reported a two-fold increase in the expression of diacylglycerol O-acyltransferase when compared to normal liver expression (Kohjima et al., 2007). Similarly, knockout mice for hepatic DGAT2 transcript revealed lower hepatic TG content by around 70%; the decrease in hepatic steatosis was not associated with increased hepatic inflammation or fibrosis (Gluchowski et al., 2019).

2.6.2 Role of Diacylglycerol O-Acyltransferase 2 (DGAT2) in NAFLD

A clinical study on DGAT2 inhibition reported a reduction in hepatic TG content in healthy people after 2 weeks and in patients with NASH after 6 weeks (Amin et. al, 2023). Another recent detailed study on an animal model of NAFLD treated with a DGAT2 inhibitor reported a reduction in the liver weight by 11% and a noticeable decrease in hepatic TG concentration by 51%, while hepatic cholesterol content had not been affected by DGAT2 inhibitor treatment, along with reduced serum cholesterol and TG levels. This study uncovers the impactful result by revealing that, the expression of SREBP-1c-regulating genes for fatty acid synthesis enzymes and PNPLA3 in hepatocytes of iDgat2-treated mice was significantly reduced. This indicates that the DGAT2 inhibitor suppresses the expression of SREBP regulating *de novo* lipogenesis and shunting diacylglycerol into phospholipid biosynthesis (Rong et al., 2024).

Although DGAT2 inhibition has shown therapeutic potential in reducing hepatic triglyceride accumulation, most studies focus on pharmacological inhibitors. The possible regulation of DGAT2 by RA remains insufficiently explored, representing an important knowledge gap in understanding RA-mediated improvement of hepatic steatosis.

2.6.3 Vitamin A (Retinoid) Metabolism in the Liver

Vitamin A is a naturally occurring compound that cannot be *de novo* synthesised in the human body and needs to be taken from the diet. The liver is the most important storage site for retinoids. The chief organ for dietary retinoid uptake accounts for 66–75% of retinoid absorbed in the intestine. The liver is also the principal site for retinol-binding protein (RBP) synthesis and secretion, forming 70–80% of all RBP that is normally present in the circulation. Thus the liver is central organ in the body involved in retinoid storage and metabolism (Shirakami et al., 2013).

2.6.3.1 Uptake and Storage of Dietary Retinoids

Consumed dietary retinyl esters are hydrolysed into retinol and free fatty acid in the intestinal lumen, namely, the enterocyte brush-border by retinyl ester hydrolase enzyme. Then these molecules combined into micelles in the intestinal lumen before their absorption. Retinol is believed to be picked up into enterocytes by a brush border membrane transporter. In contrast, dietary carotenoids go into enterocytes through passive diffusion, which neither requires cell membrane transporters nor energy consumption (Chen & Chen, 2014; Haaker et al., 2020).

In the enterocyte, the majority of β-carotene undergoes symmetrical split by 15,15′-dioxygenase to generate retinal. The remains of intact β-carotene can be transported to the liver, where a similar enzyme in hepatocytes catalyses β-carotene cleavage. The resulting retinal from β-carotene hydrolysis is reduced to retinol, which is converted into retinol by retinal reductases. Retinol in enterocytes binds to Cellular Retinol-Binding Protein II (CRBP-II) and then is esterified back to retinyl esters by two distinct enzymes, Lecithin: Retinol Acyltransferase (LRAT) and Intestinal Acyl-CoA: Retinol Acyltransferase (ARAT). Retinyl esters are packed with dietary fat and cholesterol into nascent chylomicrons for entrance into the lymphatic circulation system (Haaker et al., 2020; Shirakami et al., 2013). The majority (66-75%) of chylomicron retinyl ester is taken up by the liver. The remainder of the chylomicron will be removed

from circulation by other organs such as skeletal muscle, adipose tissue, heart, spleen, and kidney (Shirakami et al., 2013).

The liver secretes vitamin A forms mainly as retinol/RBP4, which also binds to the transporter protein TTR (transthyretin) to stabilise the complex and to prevent filtration through the kidney (Braverman et al., 2001; Lerner, 2024). The complex enters the blood circulation to reach and meet the target required organs. The release of retinol from HSC stores into the serum is a tightly controlled process. However, few details are known about the mechanism. Retinol movement from HCS lipid droplets is catalysed by REHs, and some other enzymes are involved in this process, such as patatin-like phospholipase domain-containing 3 (PNPLA3), and hormone-sensitive lipase (HSL) (Saeed et al., 2018).

Within the liver retinol is converted to active retinoic acid by two oxidative processes. The first oxidative step is the oxidation of retinol to retinaldehyde (or retinal). This process is catalysed by enzymes called retinol dehydrogenases (RDHs). CRBPI has proposed to regulate the oxidation of retinol to retinaldehyde. The second step includes irreversible oxidation of retinaldehyde to retinoic acid by mean of retinaldehyde dehydrogenases (RALDHs). Newly synthesised retinoic acid has been found to bind to cellular retinoic acid binding protein, type II (CRABPII), which acts to facilitate cellular uptake and is a co-regulator of retinoic acid signalling in the nucleus (Shirakami et al., 2013).

2.6.3.2 Retinoic Acid Receptors (RARs and RXRs)

The biologically active metabolite of the retinoids is RA, which produces its action by bonding to nuclear retinoid receptors, which includes three: retinoic acid receptors (RARs) alpha, beta, and gamma, (activated by all-trans and 9-cis RA) and another three retinoid X receptors (RXRs) alpha, beta, and gamma (RXRs are activated by 9-cis retinoic acid). Retinoid receptors must dimerise in order to produce their biological action. Combinations of RAR–RXR and RXR–RXR dimers are common, while there is no observed combination of RAR–RAR dimers. Retinoid receptors are primarily

located in the nucleus and different combinations of the hetero- or homodimers bind to various and distinctive DNA sequences, called retinoic acid response elements (RAREs). Binding of retinoids to these receptor–RARE complexes triggers the expression of numerous genes, resulting in different cellular responses (Abbott et al., 2007; Haaker et al., 2020).

2.6.4 Role of Retinoic Acid in NAFLD Pathophysiology and Animal Models

Non-alcoholic fatty liver disease is increasing in prevalence and burden worldwide. Despite this, effective treatment for NAFLD is still limited. In recent years, retinoic acid (RA) has gained notable attention for its role in lipid metabolism, and inflammation in liver cells. Several studies have used RA to treat different NAFLD animal models to determine its therapeutic efficacy and the underlying mechanism behind the improvement of liver steatosis and decreasing the hepatic TG content.

Amengual et al., (2010) were the earliest researchers to demonstrate the effect of RA on the NAFLD animal model. They used 100 mg/kg of RA to treat HFD model of NAFLD for 4 days, resulting significant reduction in body weight, and hepatic TG content, which was explained by increased expression levels of peroxisome proliferator-activated receptor alpha (PPARα) which is the key for controlling transcription of hepatic fatty acid oxidation, and reduction in the mRNA expression levels of sterol regulatory element binding protein 1c (SREBP-1c) responsible for controlling of hepatic fatty acid synthesis.

In another animal study, Kim and colleagues (2014) had reported an *ob /ob* mice model of NAFLD treated with 15 mg/kg/day orally for seven days. They reported that the reduction of hepatic steatosis was mediated by inhibition of *PPAR γ* gene transcription. The PPAR γ plays a role in adipogenesis, and induction of this gene is considered the main factor contributing fat accumulation in the livers of animal models. Also, *PPAR γ* in NAFLD patients is associated with obesity and diabetes. Additionally, increased transcription of a new gene, which is liver-specific Sirtuin 1 (Sirt 1), was

proposed to mediate reduction in hepatic steatosis in HFD mice treated with 7.5 mg/kg RA for 4 weeks. Sirtuin 1 is a protein that regulates fatty acid metabolism through several nutrient sensors, such as AMP-activated protein kinase (AMPK), and sterol regulatory element binding protein-1 (SREBP-1(Geng et al., 2017). In addition, a rabbit model of NAFLD induced by a high cholesterol diet treated with RA orally (5 mg/kg/day) for one week, reported that RA improved antioxidant capacity, decreased hepatic steatosis, reduced the production of cholesterol in the liver, and increased cholesterol clearance (Zarei et al., 2020)

Furthermore, RA treatment in HFD and HFHC animal models has been reported to reduce body weight, liver TG and cholesterol content, intrahepatic liver enzymes, hepatocyte fatty acid uptake and lipid droplet formation, while improving glucose tolerance and insulin sensitivity (Zhu et al., 2022; Bawa et al., 2022). Fenretinide, a synthetic retinoid, has been shown to prevent obesity, improve insulin sensitivity, inhibit hepatic triglyceride accumulation, ballooning and steatosis in the HFHC mice model of NAFLD. Fenretinide also decreased the expression of hepatic genes responsible for inflammation and fibrosis in NAFLD animals (Thompson et al., 2023).

Recently, the effect of RA (10 mg/kg twice weekly for 4 weeks) on lipophagy in the adipose tissue in mice was investigated. Lipophagy is defined as a lipolysis by degrading lipid droplets via autophagy. The result revealed that RA decreased body weight by 10%, with no significant change in plasma TG and NEFA levels. RA also induced the expression and activation of the gene (*AMPK-Beclin1*) that is responsible for lipolysis and autophagy. Concluding that RA modulates lipid deposition not only in the liver but also influences lipid in subcutaneous fat by promoting lipophagy (Mori et al., 2024) .

Collectively, these studies suggest that RA may improve NAFLD through the regulation of hepatic lipid metabolism. However, direct evidence linking RA treatment to changes in DGAT2 expression remains limited, despite the central role of DGAT2 in catalysing the final step of hepatic triglyceride synthesis. This knowledge gap supports the investigation of DGAT2 regulation as a potential mechanism through which RA reduces hepatic triglyceride accumulation and ameliorates NAFLD.

CHAPTER THREE

MATERIALS AND METHODOLOGY

3.1 STUDY DESIGN

The present study is an experimental animal research, which evaluated the drug effect on an animal model through quantitative and semi-quantitative analyses, conducted in compliance with ethical standards..

3.2 EXPERIMENTAL SITES

The research experiments were conducted in several laboratories as follows:

a. Animal Retention Area, Level 3, Kulliyyah of Medicine – animals were kept under optimal temperature and feeding conditions throughout the study period.
b. Pharmaco-Physiology Laboratory, Animal Room, Level 3, Kulliyyah of Medicine – animals received treatment, underwent euthanasia, and liver tissues were harvested.
c. Histology Laboratory, Level 1, Kulliyyah of Medicine – tissues were processed, embedded, sectioned, and stained with haematoxylin and eosin, and Masson's trichrome.
d. Department of Basic Medical Sciences (BMS), IIUM – general laboratory facilities.
e. Integrated Research Laboratory, Level 1, Department of Pathology and Laboratory Medicine (PALM), Kulliyyah of Medicine, and Department of Pathology and Laboratory Medicine, SASMEC @ IIUM – immunohistochemistry and Oil Red O (ORO) staining of cryosectioned liver tissues.
f. Biochemical Laboratory, Level 2, Department of Basic Medical Sciences (BMS), IIUM – liver lipid extraction.

g. Integrated Laboratory, Level 1, Department of Pathology and Laboratory Medicine (PALM), SASMEC @ IIUM – blood sample separation and analysis of serum lipids and liver enzymes.
h. Electron Microscopy Laboratory, Level 1, Kulliyyah of Medicine – liver samples for SEM were fixed and processed.
i. Microscopy Laboratory, Universiti Malaysia Pahang (UMP), Gambang, Kuantan – processed liver samples were viewed under the scanning electron microscope.

3.3 SAMPLE SIZE CALCULATION

Sample size was calculated using G*Power version 3.1 downloaded from the link (http://www.psycho.uni-duesseldorf.de/abteilungen/aap/gpower3/download-and-register) (Faul et al., 2007).Using a statistical power of 95%, the sample size was calculated based on the mean and standard deviation of serum triglyceride level in the control and treated animal group as reported by Geng et al. (2017). Accordingly, eight rats were allocated to each group, giving a total sample size of 40 rats. To account for a 10% attrition rate for potential unexpected death. Therefore, the final sample size was increased to 45 rats, as illustrated in Figure 3.1.

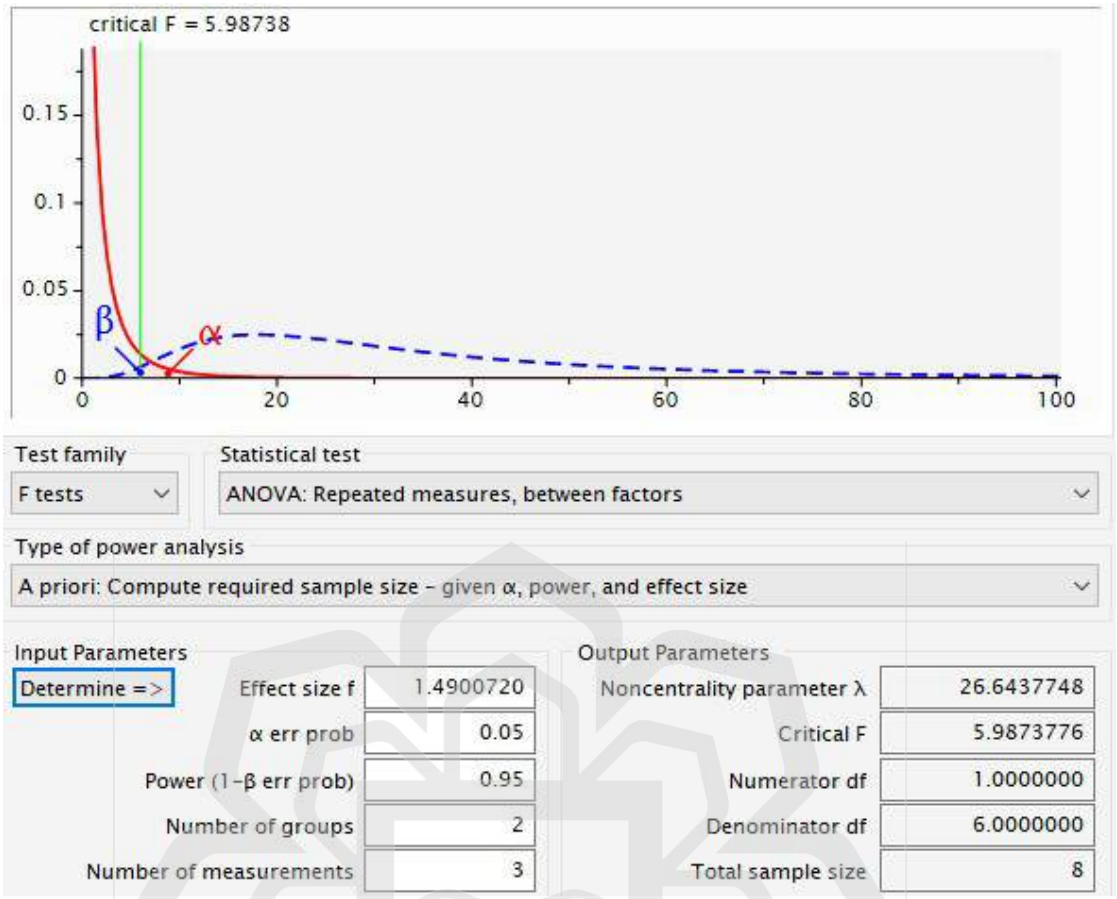

Figure 3.1 Sample Size Calculation Using G*Power Version 3.

3.4 ETHICAL APPROVAL

The animal handling, treatment and all experimental procedures were approved by the International Islamic University Malaysia, Institutional Animal Care and Use Committee, Kuantan campus (No. of IACUC Approval: IIUM /IACUC-2019 (14). The study was confined to the Malaysian guidelines for the care and use of animals for scientific purposes (Animal Welfare Board, 2020).

3.5 EXPERIMENTAL ANIMALS

Animals used in this study were 6-7 weeks old male Sprague–Dawley rats, weighing 200-300 grams. Animals were obtained from A-Sapphire Enterprise, Seri Kembangan. Each rat was kept in a clean single rat per cage (Figure 3.2). Under controlled conditions: temperature 20±2 ºC, relative humidity at 60±5%, and a 12-hour light/ dark cycle. Rats were allowed free access to food and water. Animals were maintained on a standard commercial dry pellet diet (Gold Coin Feed Mill Sdn. Bhd, Kuala Lumpur, Malaysia) containing 23% crude protein content, 13% moisture, 5% crude fibre, 3% crude fat, 8% ash, 0.8%, calcium, and 0.6% phosphorus. Animals were acclimatised to the laboratory conditions for two weeks. The animals were treated according to the guidelines of the IIUM Institutional Animal Care and Use Committee (IACUC) and to the standards and regulations of the Care and Use of Laboratory Animals.

Figure 3.2 The Image Representing Single Rat in Cage with Free Access to Food and Water.

3.5.1 Experimental Design

The research was conducted in two phases. The first phase is the pilot study. The second phase is the main study (Figure 3.3). Phase 1 (pilot study), which was conducted to determine the duration of exposure to HCD required to develop NAFLD and Phase 2 (main experiment), conducted under the same controlled laboratory conditions, with animals randomly divided into five groups.

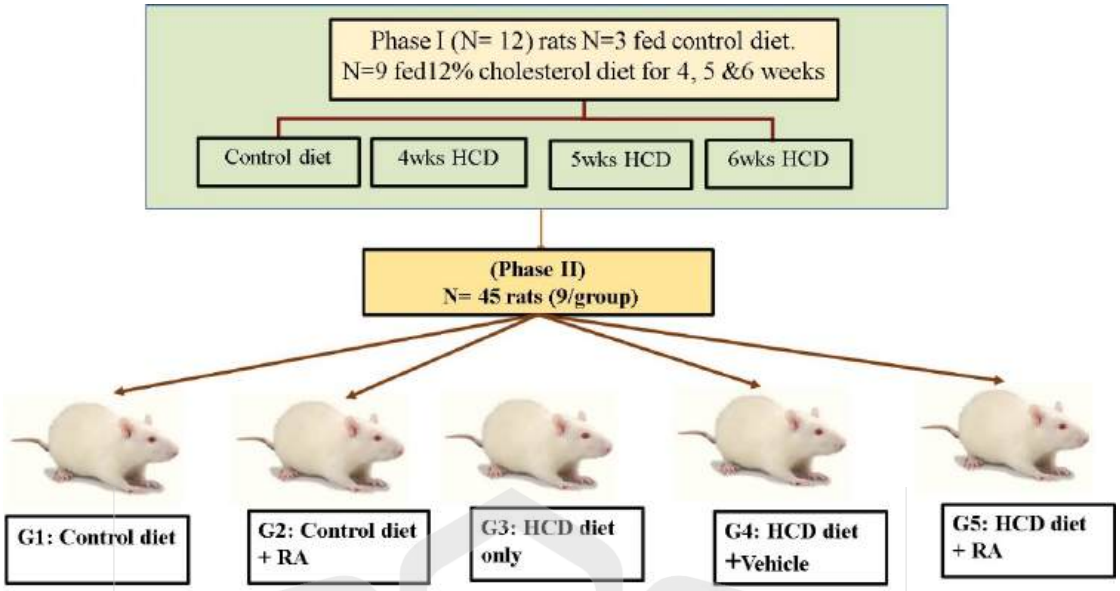

Figure 3.3 Animal Grouping and Experimental Research Design.

3.5.2 Phase 1 Establishment of Simple Hepatic Steatosis in Sprague Dawley Male Rats.

Before conducting the main research experiment, a pilot study was conducted to determine the time required for exposure to HCD to develop simple hepatic steatosis, in order to start the animal treatment at this stage of disease. Twelve animals were randomly divided into two groups. Both groups were fed a control diet for two weeks of acclimatisation. Then, the first group received a control diet (n=3), while the other nine rats received a high-cholesterol diet (refer to Section 3.5.1). The HCD-fed rats were randomly divided into three groups and sacrificed at 4, 5, and 6 weeks to determine the duration needed to develop simple hepatic steatosis. Animals were maintained in a controlled light and temperature conditions with free access to food and water. Body weight was measured at the beginning and end of the experiment.

At the end of the experiment, animals from each group were fasted for 12 hours before being anesthetised with 1 mL of ketamine intraperitoneally using a 26G needle. After the animals were assessed for deep anaesthesia, they were placed in a supine position (Figure 3.4). The blood samples were collected from orbital sinuses through

capillary tubes and kept in plain and citrate test tubes for liver enzymes (Section 3.9.3) and lipid profile (Section 3.9.1). The abdomen was opened, and the liver was harvested. The weight of the liver was measured using the Sartorius BT 2245 scale. Harvested liver tissue was processed for H&E staining (Section 3.10.2.3), and the percentage of steatosis was calculated in ten fields of H&E-stained sections for each animal, semi-quantitative image analysis was determined using ImageJ-NIH software (Section 3.10.2.4).

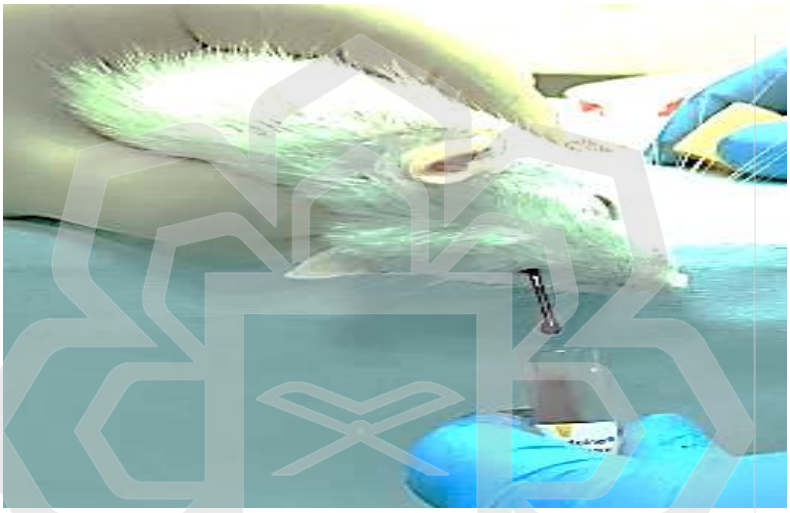

Figure 3.4 Blood Sample Collection from Orbital Sinus into Test Tube.

3.5.3 Phase 2 (Main Study).

According to pilot study results, a four-week duration was sufficient time for the development of the steatosis stage in NAFLD. Consequently, in this phase, animals were started to be treated with either RA or vehicle (DMSO) after 4 weeks of a high cholesterol diet and continued for another four weeks. Animals were randomly divided into five groups as shown in Figure 3.5. The workflow of the laboratory procedures conducted in Phase 2 is summarised in Figure 3.6.

The experimental animals were randomly divided into the following groups:

a. Group 1: The animals were fed a normal control diet for eight weeks.
b. Group 2: The animals were fed a normal control diet for four weeks and then received a subcutaneous injection of RA twice weekly for another four weeks.
c. Group 3: The animals were fed on a high-cholesterol diet for eight weeks.
d. Group 4: The animals were fed high-cholesterol diet for four weeks then, rats were injected with vehicle (DMSO) subcutaneously for an additional four weeks.
e. Group 5: The animals were fed a high-cholesterol diet similarly for four weeks, followed by another four weeks injection of RA subcutaneously twice weekly.

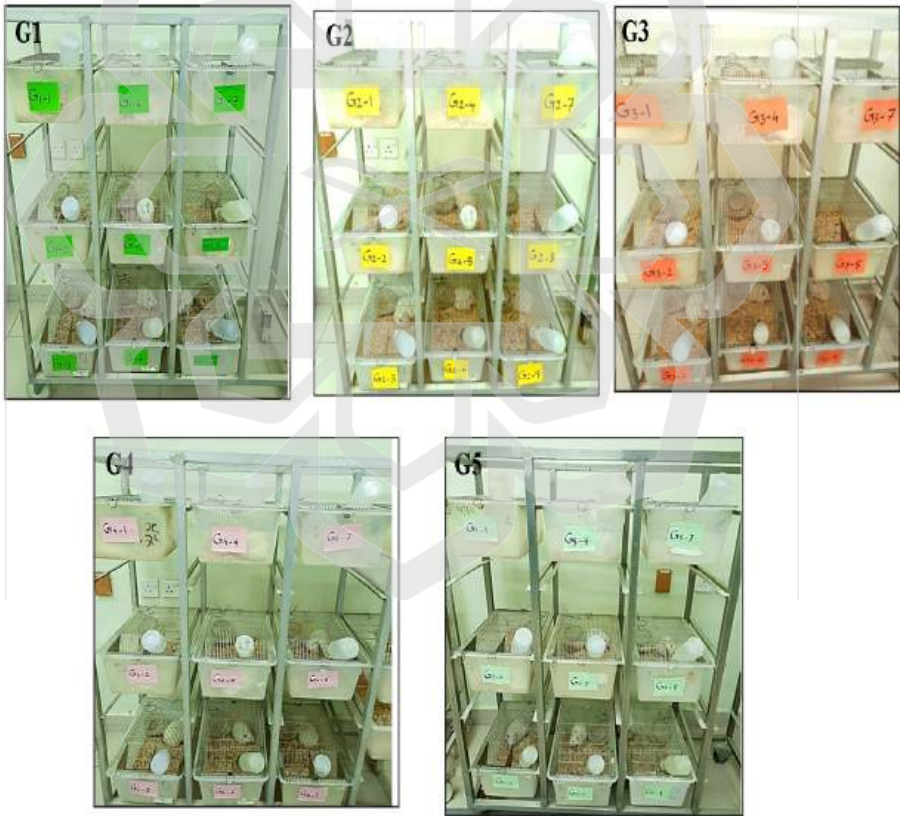

Figure 3.5 Actual Images of the Five Experimental Animal Groups Used in the Study. G1: Control diet animals, G2: Control diet animals received RA injection. G3: HCD-fed animals, G4: HCD animal received vehicle injection, G5: HCD-fed animals treated with RA.

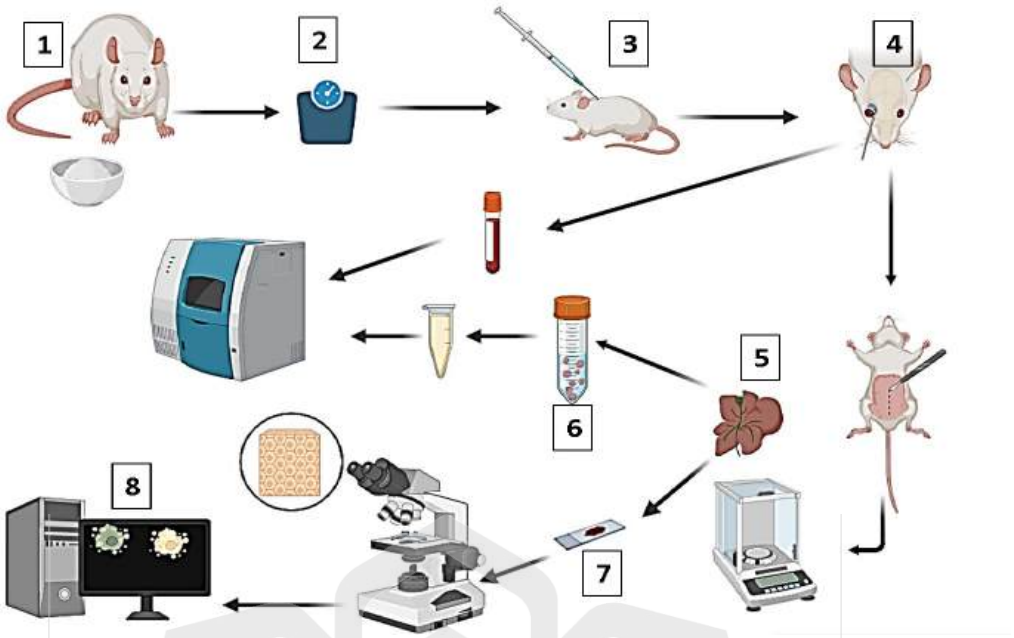

Figure 3.6 The Summary of The Experimental Workflow Is Illustrated in the Diagram Throughout the Experiment. (1) Animals Fed with CD or HCD; (2) Body Weight Measurement; (3) Initiation of Specific Treatment After 4 Weeks; (4) Blood Sample Collection; (5) Animal Anaesthesia And Liver Harvesting;(6) Part of Liver Tissue for Triglyceride (TG) Content; (7) Liver Tissue Prepared for Histopathology and Scanning Electron Microscopy (SEM).

3.6 CHOLESTEROL DIET

According to the animal model developed by Abdul Rahim et al., (2019), rats fed a 12% cholesterol and 3% cholic acid diet developed NASH at 6 weeks. In the present study, the focus was on the steatosis phase of NAFLD. Analytical-grade cholesterol powder and cholic acid (Nacalai-Tesque, Kyoto, Japan) were mixed with ground commercial rat pellets. The preparation of food was performed daily to prevent the oxidation effect. A total of 880 g of ground rat pellets was mixed with 120 g of cholesterol and 3 grams cholic acid to yield 12% cholesterol and 3% of cholic acid diet. The food was given to the rat in a clean glassware container to prevent a chemical reaction with other metal containers. The rat received freshly prepared food with 12% cholesterol daily.

3.7 RETINOIC ACID TREATMENT

Retinoic acid was obtained from Tokyo Chemical Industry/Japan (CAS RN 302-79-4). Retinoic acid powder was dissolved in dimethyl sulfoxide (DMSO, CAS: 67-68-5, R&M chemicals) at a concentration of 2 mg in 1 mL from R&M chemicals (Geng et al., 2017; Melis et al., 2019). Rats in Group 2 and Group 5 received 1.25 mL to 1.75 mL of the above-mentioned prepared retinoic acid via subcutaneous injection using 26 G needles twice weekly for 4 weeks (Figure 3.7). The rats in Group 4 received 1.25-1.75 mL of DMSO subcutaneously twice weekly for four weeks. The subcutaneous route was selected to ensure consistent systemic delivery of RA and to minimise variability related to oral absorption and food intake.

Figure 3.7 Administration of Retinoic Acid (RA) Via Subcutaneous Injection in a Rat.

3.8 BODY WEIGHT MEASUREMENTS

Body weight was measured at the beginning and end of the experiment. A plastic box was used to keep the animal on the scale. First, the scale is turned on and then tared to zero. Later, the rat was placed in the container, and the measurement was taken after the rat remained still briefly.

3.9 ANIMAL ANAESTHESIA

Animals were fasted for 12 hours prior to euthanasia. Anaesthesia was induced with xylazine (5 mg/kg) and ketamine (50 mg/kg) given through a 26 Gauge needle intraperitoneally. Deep anaesthesia was confirmed by the absence of the pedal withdrawal reflex, indicated by no limb withdrawal in response to pressure applied to the foot pad (Figure 3.8).

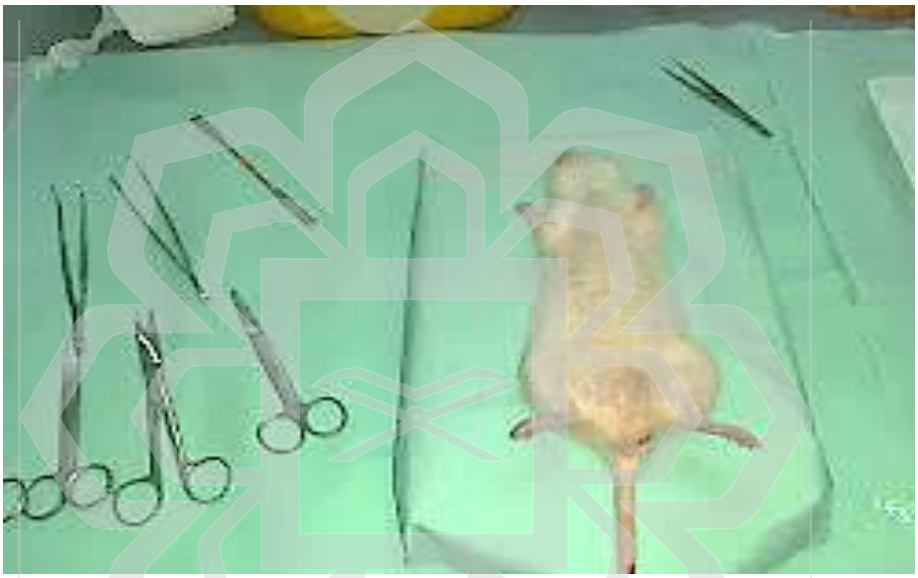

Figure 3.8 Anaesthetised Animal.

3.10 BLOOD COLLECTION AND ANALYSIS

Blood samples were collected through orbital sinus puncture (Figure 3.9) for the determination of liver enzymes (Section 3.9.3) and lipid profile (Section 3.9.1) (Kim et al.,2014). Three millilitres of blood were collected from the orbital sinus through capillary tubes, transferred into citrate test tubes and centrifuged at 1000 rpm for 10 min. Beckman Coulter® (AU 680, U.S) auto-analyser was used to quantify serum liver enzyme and lipid profile.

Figure 3.9 Blood Sample Collection from the Orbital Sinus into a Test Tube.

3.10.1 Serum Triglyceride (TG)

Serum triglyceride level is most commonly used to assess the degree of metabolic disturbance and dyslipidaemia status associated with NAFLD. An enzymatic method for the determination of serum TG is based on a couple of enzymatic reactions. First reaction, TG is hydrolysed by lipase to release glycerol. Second reaction, the resulting glycerol is phosphorylated by adenosine triphosphate (ATP) in the presence of glycerol kinase (GK). In the third reaction, the produced glycerol-3-phosphate is oxidised by oxygen in the presence of glycerol phosphate oxidase (GPO) and produces hydrogen peroxide (H2O2) and dihydroxyacetone phosphate. The fourth reaction, which yielded H2O2 reacts with 4-aminophenazone and N, N, 4-sulphobutyl-3,5-dimethylanine disodium (MADB) in the presence of peroxidase enzyme (POD) to produce chromophore, which is read spectrophotometrically at 660/800 nm and is proportional to TG content of the sample (Fossati & Prencipe, 1982).

(1) $\text{Triglyceride} + 3H_2O \xrightarrow{\text{Lipase}} \text{Glycerol} + 3\ \text{Fatty acids}$

(2) $\text{Glycerol} + \text{ATP} \xrightarrow{\text{GK}} \text{Glycerol} - 3 - \text{phosphate} + \text{ADP}$

(3) $\text{Glycerol} - 3 - \text{phosphate} + O_2 \xrightarrow{\text{GPO}} \text{Dihydroxyacetone phosphate} + H_2O_2$

(4) $H_2O_2 + 4 - \text{AAP} + \text{MADB} \xrightarrow{\text{POD}} \text{Blue dye} + 3\ H_2O$

3.10.2 Serum Cholesterol

Determination of serum total cholesterol is based on the enzymatic method. In this method, cholesterol ester in the sample is hydrolysed by cholesterol esterase (CHE) [Equ (1)]. Then the free cholesterol is oxidised by cholesterol oxidase (CHO) into cholestane-3-one and hydrogen peroxide (H2O2) [Equ (2)]. The latter reacts with 4-aminoantipyrine and phenol in the presence of peroxidase enzyme (POD) to produce a chromophore namely red quinonimine dye [Equ (3)], which is measured spectrophotometrically at 540 nm (Allain et al., 1974).

(1) $2\ \text{Cholesterol ester} + 2\ H_2O \xrightarrow{\text{CHE}} 2\ \text{Cholesterol} + 2\ \text{Fatty acid}$

(2) $2\ \text{Cholesterol} + 2O_2 \xrightarrow{\text{CHO}} 2\ \text{cholestene} - 3 - \text{one} + 2H_2O_2$

(3) $2H_2O_2 + 4 - \text{Aminoantipyrine} + \text{Phenol} \xrightarrow{\text{POD}} \text{Quinonimine} + 4\ H_2O_2$

3.10.3 Liver Enzyme

Plasma liver enzyme activity was used to examine the hepatocellular integrity. Aminotransaminases are only distributed intracellularly. Therefore, they are released from damaged hepatocytes due to increased cell membrane permeability (Walker, Hall, & Hurst, 1999). Elevated serum transaminase levels are considered an early evidence of hepatocyte injury even prior to the onset of clinical symptoms and signs (Walker et al., 1999).

3.10.3.1 Determination of Alanine Aminotransferase (ALT) Enzyme

The principle of ALT enzyme determination is that ALT enzyme transfers the amino group from alanine to 2-oxyoglutrate to form pyruvate and glutamate. Then pyruvate is catalysed by a Lactate Dehydrogenase (LDH) with NADH to produce lactate and NAD+ [Equ (3) and (4)]. The decrease in the absorbance due to consumption of NADH is measured at 340nm and is proportional to ALT enzyme activity in the sample (X. Huang et al., 2006).

(1) $\text{Oxoglutarate} + \text{L} - \text{Alanine} \xrightarrow{\text{ALT}} \text{L} - \text{Glutamate} + \text{Pyruvate}$

(2) $\text{Pyruvate} + \text{NADH} \xrightarrow{\text{LDH}} \text{L} - \text{Lactate} + \text{NAD}$

3.11 LIVER TISSUE COLLECTION AND ANALYSIS

After the blood sample was collected, the abdomen was opened along the linea alba with extension of the incision laterally to expose the whole abdominal organs (Figure 3.10). The intestines were pushed to one side, after the liver was removed gently, colour was observed and the wet weight of the liver was also determined immediately using a Sartorius BT electronic scale (Figure 3.11). Harvested liver tissue was washed with ice-cold PBS properly to remove the remaining blood. The left lobe was fixed in 10% NBF for 48 hours for paraffin sections, the middle lobe of the liver was fixed in McDowell's fixative at 4 ˚C for 2 weeks for further SEM processing, the right lobe was preserved for cryosection at 4 ˚C, while the caudate was kept in -80 ˚C in a glass container for 4 weeks for measurement of tissue TG.

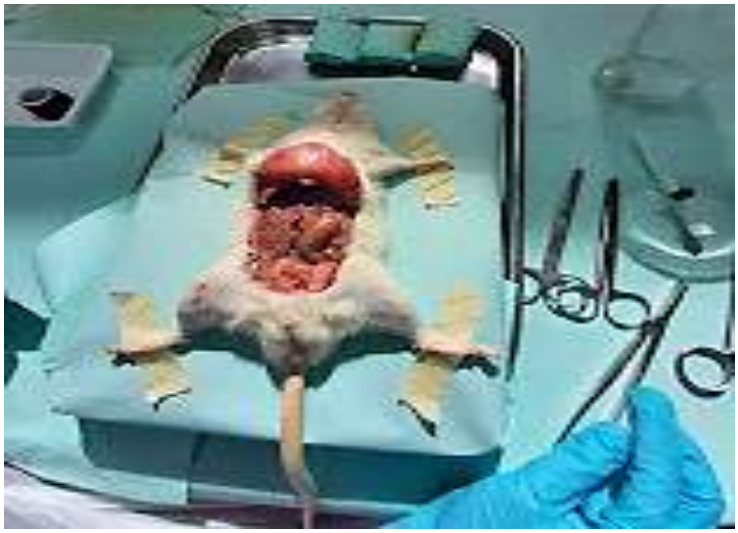

Figure 3.10 Opened Abdomen of Anaesthetised Rat Prepared for the Liver Harvesting.

Figure 3.11 Harvested Liver from Anaesthetised Animal and Wet Weight Measured Before Being Processed.

3.11.1 Lipid Extraction and Analysis

The quantification of hepatic fat is crucial for assessing the degree of fatty liver disease and relies on an efficient extraction method, specifically the Folch method (1957), which serves as the traditional gold-standard technique for separating lipids from liver tissue. Different solvents have been used to overcome the strong connection between tissue lipids and other cellular components, such as proteins and polysaccharides. Any lipids lacking polar groups (non-polar), for example triacylglycerols or cholesterol esters, are very soluble in hydrocarbons such as hexane, toluene or cyclohexane and also in diethyl ether or chloroform. Therefore, a polar solvent mixture such as methanol is not an ideal solvent for non-polar lipids such as triglyceride, because they do not dissolve in it and keep sticking to the tissues (Christie, 1993).

Lipid extraction from tissues is consistently performed with volatile organic solvents, which require the use of well-ventilated laboratories. The most widely used, and generally effective solvent for the extraction of all types of lipids is a mixture of chloroform and methanol. The main method used is a mixture of chloroform and methanol in a volume ratio (2:1), which extracts lipids more thoroughly than any other solvent combination (Christie, 1993). The standard method was described by (Folch, Lees, & Sloane Stanley, 1956). Moreover, these solvents are capable of removing contaminant materials simply by shaking one-fourth volume of water, a dilute solution of salt, such as potassium chloride (0.88%) or sulphuric acid (0.05%). Then these solvents are divided into two layers; the purified lipid is in the lower phase, which forms 60% of the total volume. In contrast, the upper phase contains non-lipid contaminants. One of the significant points in this method is that the proportion of chloroform, methanol, and water in the combined phase should be close to 8:4:3 by volume (Christie, 1993).

The most specific component of glycerides is glycerol. Based on this, two conventional methods are used to determine the TG level, either chemical or enzymatic; The chemical method includes solvent extraction of the TG, chemical hydrolysis to produce glycerol, followed by oxidation and production of formaldehyde, and then creation of coloured or fluorescent material. However, this method is not widely used in laboratories (Fossati & Prencipe, 1982). The other direct colourimetric method

involves quantification of glycerides based on the determination of the amount of glycerol which is released by alkaline hydrolysis. Kreutz (1962) determined the glyceride content without extraction or isolation from other types of lipids either in serum or tissue homogenate. In the enzymatic method, TG is hydrolysed by lipase to release glycerol; the resulting glycerol is monitored spectrophotometrically in the ultraviolet range by measuring the production or disappearance of coupled NADH (Fossati & Prencipe, 1982).

3.11.1.1 Folch Method for Extraction of Tissue Lipid and Analysis

Immediately after the whole rat liver was weighed, part of the central lobe of the liver was gently cut to avoid *in vivo* lipolysis (Christie, 1993), washed with cold saline and kept in a sealed glass container at -80 ˚C. Then the tissues were homogenised by Heidolph Brinkmann Silent crusher M to produce higher output of diacylglycerols (Abe & Kogure, 1986). Lipid extraction procedure was done under a fume hood, about 100 mg of the liver was homogenised using a Heidolph homogeniser (Germany) in a glass container with 5 mL of a mixture of chloroform and methanol (2:1). The mixture was vortexed briefly, kept overnight at 4 ˚C and then filtered. Subsequently, 1 mL of (0.05%) sulphuric acid was added, vortexed again, and centrifuged at 1500 × g for 15 min, resulting in a two-layer separation of the mixture (Figure 3.12). Consequently, the upper aqueous layer was pipetted out and the lower phase containing lipid was dried in an oven at 60 ˚C. Subsequently, the dried lipid was redissolved in a 1:2 mixture of chloroform and 2% Triton X-100 and kept in an oven at 45 ˚C until dry. Later, the lipid was dissolved in 2 mL of distilled water, vortexed and kept at 60 ˚C for 5 min. Later, triglyceride and cholesterol were determined in the sample using a Beckman Coulter Autoanalyser (Beckman Coulter Autoanalyser AU 680, Inc., California, USA).

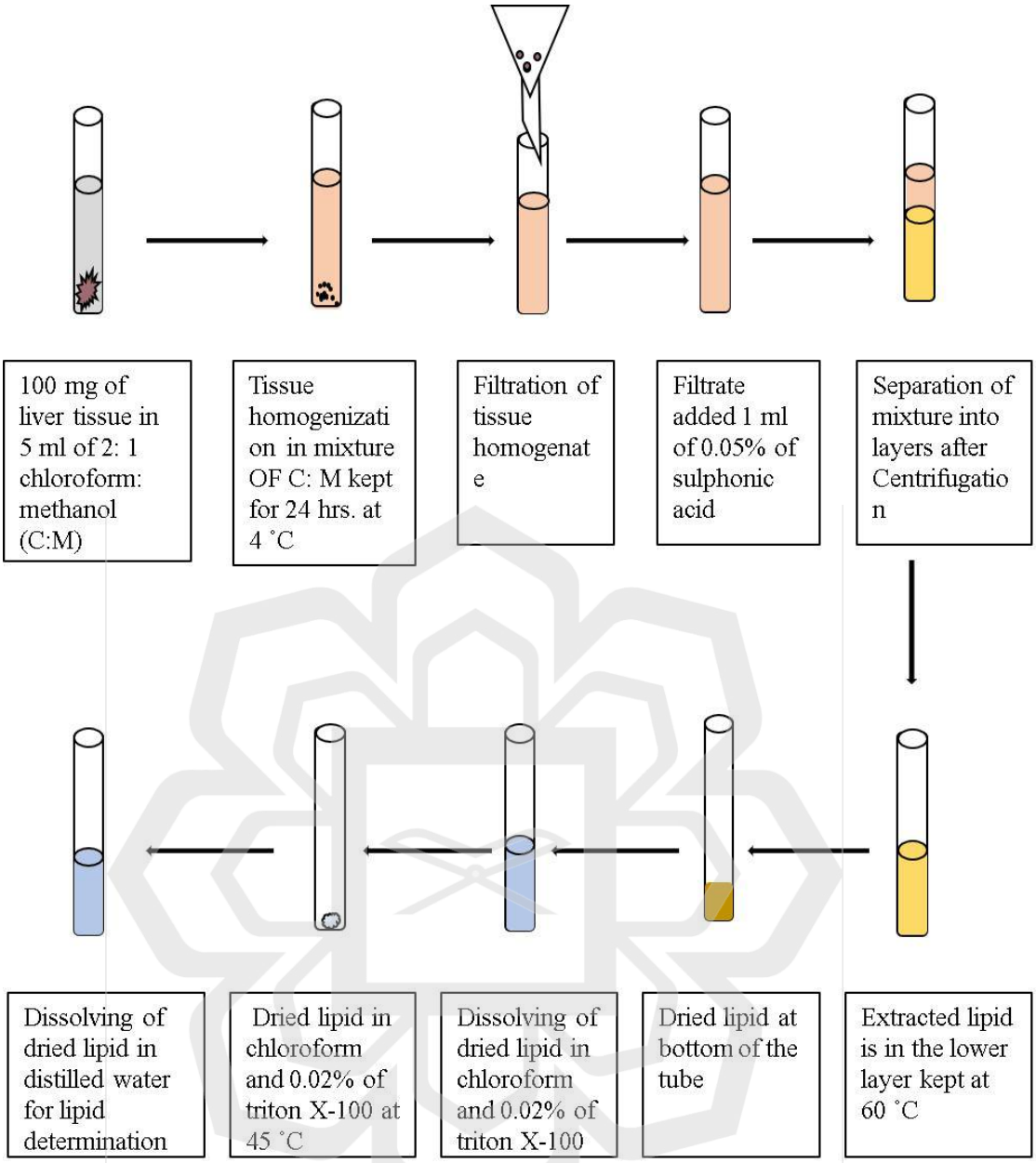

Figure 3.12 Illustration of Tissue Lipid Extraction Using Folch Method.

3.11.2 Histopathological Examination

3.11.2.1 Tissue Processing and Paraffin Embedding for H&E and MT staining

Tissues were fixed in appropriate fixatives paraffin-embedded section and cryosections (fixed and embedded in OCT medium) were prepared and sectioned three slides per each animal for all five groups, and stained for H&E, MT stains, and Oil O Red stain and subsequently examined under a light microscope. Below is the equipment used for tissue processing and paraffin embedding:

a. Automated benchtop tissue processing (Leica TP 1020, Germany)
b. Paraffin embedding machine (Leica EG 1160, Germany)
c. Tissue sectioning machine (Leica RM 2245, Germany)
d. Water bath (Leica HI 1210, Germany)
e. Hot plate (Leica HI 1220, Germany)

After fixation in 10% neutral buffered formalin (NBF), specimens were placed in labelled cassettes and processed in an automated tissue processor (Leica TP 1020, Germany) according to the protocol described in Appendix III for 16 hours (Figure 3.13). The processed specimens were then embedded in paraffin wax (Figure 3.14), and the paraffin blocks were allowed to harden for 24 hours. The blocks were subsequently trimmed and sectioned using a rotary microtome (Leica RM 2245, Germany) at a thickness of 3 μm. Ribbon sections were floated on a water bath (Leica HI 1210, Germany) maintained at 45 °C, mounted on frosted-end glass slides (Sail Brand, Cat. No. 7105, China), and baked on a hot plate (Leica HI 1220, Germany) at 65 °C before staining. For each animal, three slides were prepared for haematoxylin and eosin (H&E) staining and three slides for Masson's trichrome (MT) staining. Therefore, 27 slides were prepared per group for each staining method, giving a total of 135 slides for H&E staining and 135 slides for MT staining across the five experimental groups.

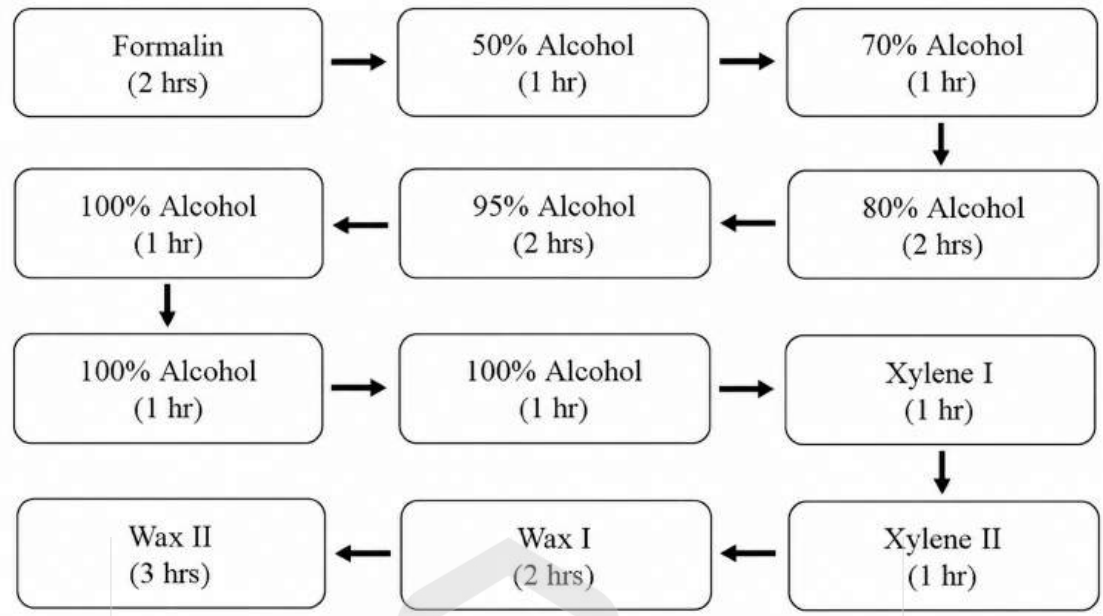

Figure 3.13 Tissue Processing Protocol.

Figure 3.14 Paraffin Embedding Machine and Paraffin Blocks

3.11.2.2 Haematoxylin and Eosin Staining (H&E)

Haematoxylin and eosin (H&E) are the most commonly utilised histological stain, because it is easy to use and determines structural tissue variances clearly. Haematoxylin stains the cell nuclei a dark blue colour, with obvious intranuclear detail. In contrast, eosin gives cell cytoplasm and connective tissue varying grade and intensity of pink, orange and red (Suvarna, Layton, & Bancroft, 2018). In hepatic tissue, haematoxylin is used to localise the nucleus in the hepatocyte either central or eccentric, while eosin stains the general morphology of hepatic cytoplasm. Thus, a stained section with H&E facilitates in the assessment of hepatic architecture and lipid deposition.

Tissues were stained according to Cardiff, Miller, and Munn (2014) protocol. Paraffin sections were dewaxed with xylene and rehydrated through descending grades of alcohol (70%, 80%, 90%, 100%). The section was washed with tap water for 5 minutes after each solution until the dehydration step. Following that, the section was stained by HistoCore SPECTRA H&E stain (Leica Biosystems, Richmond, IL, USA) according to the manufacturer's protocol, for 15 minutes. Next, differentiated with acid alcohol (1% HCL and 70% ethanol) for 2 seconds. Afterwards, sections were stained with blueing solution for 1 minute then stained with eosin Y (Surgipath, Leica Biosystems, Richmond, IL, USA) for 10 minutes. Later, sections were dehydrated through ascending alcohol concentration (70%, 80%, 90%, and 100%), then washed again with xylene and dried in a universal oven at 56 ˚C. Finally, sections were mounted with DPX-mounting solution and a cover slip and later viewed under an Olympus light microscope (Olympus BX51, Olympus Corporation, Tokyo, Japan) operated with Axio-Vision Software (Carl Zeiss Microscopy GmbH, Jena, Germany).

3.11.2.3 Quantification of Hepatic Steatosis Using ImageJ Software

Quantification of hepatic steatosis is still challenging due to a lack of consensus across studies. No clear optimal method has been approved yet. Computerised image analysis is significantly decreasing the quantification efforts. A number of stained sections are used to determine hepatic lipid deposition (Jamieson et al., 2011). Usually, the analysis of the stained sections requires an experienced histopathologist. Nevertheless, inter-observer discrepancy has been reported between pathologists. Therefore, some semiautomated, computer-assisted image analysis methods have been implicated, which shows more accuracy than human visual estimation (Fiorini et al., 2004; Marsman et al., 2004).

ImageJ software is a Java-based image program (Abràmoff et al., 2004) developed by Rasband in 1987 at the National Institutes of Health (Schneider, Rasband, & Eliceiri, 2012). It has been applied for the analysis of lipid droplet size and number (Le et al., 2012). The software also calculates the total fat content in digital images for different stained tissues by dividing the fat area by field area (Marsman et al., 2004; Yang et al., 2014).

In this study, ImageJ software was used to quantify hepatic steatosis following the protocol used by Levene et al. (2012), Mehlem (2013) ,Yang et al. (2019) and Wang et al. (2020). Quantification of hepatic steatosis was performed on ten non-overlapping fields from H&E-stained sections from each animal sample, viewed using an Olympus U-TV0.5XC-3 microscope of H&E-stained sections from each animal sample with 200x magnification. Areas with staining artefacts or large blood vessels were excluded (Kumar, Farrell, Fung, & George, 2002).

Images were captured using an Infinity Lite camera (Canada) and saved in TIFF format to enable image editing. Then the digital images were loaded into ImageJ (http://rsb.info.nih.gov/ij/index.html) for Windows. A computer-based image analysis was used to estimate the hepatic steatosis according to a previously used protocol. The image was converted into RGB with an eight-bit greyscale image. Then the threshold was adjusted by adapting the black colour to lipid droplets and white for the rest of the liver tissue (Figure 3.15) (Catta-preta et al., 2011). Subsequently, the percentage area

occupied by lipid vesicles was assessed and measured automatically using ImageJ software (Jamieson et al., 2011).

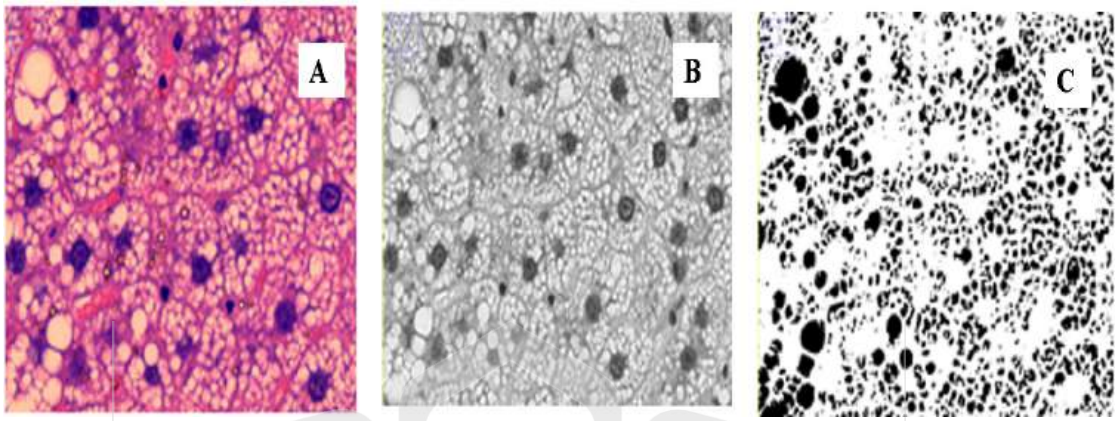

Figure 3.15 ImageJ Processing of Haematoxylin-Eosin Section (Original Magnification ×40) of Liver Tissue (A), Same Section After Conversion to Greyscale Using Image Analyser (B), and Selected Lipid Vesicles for Morphologic Quantification of Steatosis Are Outlined in Black (C).

3.11.2.4 Quantification of Inflammatory Foci Using H&E-Stained Sections

Hepatic inflammatory state was determined in each animal sample using an Olympus light microscope fitted with an Infinity Lite camera and operated with Axio-Vision Software. Inflammatory foci were counted in five randomly selected fields at 100x magnification power according to Sampey et al. (2011) and Schuck et al. (2014). Then, the number of foci was summed and the average was obtained for each rat sample.The slides were assessed blindly for the degree of hepatocyte ballooning in steatotic zones under high-power magnification (400×). The scoring was as follows: Score 0, normal hepatocyte; Score 1, few enlarged hepatocytes; and Score 2, many ballooned cells.

Histological scoring was performed semi-quantitatively using the NAFLD Activity Score (NAS) system established by the NASH Clinical Research Network (CRN) (Kleiner et al., 2005). To ensure objectivity, all slides were blindly evaluated by an expert pathologist who was unaware of the experimental group allocations. The total

NAS was calculated as the unweighted sum of three individual histological components: steatosis (0–3), lobular inflammation (0–3), and hepatocellular ballooning (0–2), yielding a composite score ranging from 0 to 8.

3.11.3 Masson's Trichrome Staining

Masson's Trichrome is a widely used histological staining technique that differentiates connective tissue from muscle and cytoplasm by staining them in three distinct colours: usually blue or green for collagen, red for muscle and cytoplasm, and black/blue for nuclei. It is particularly useful for assessing fibrosis and liver cirrhosis. Therefore, this study used Masson's trichrome staining to assess fibrotic changes occurring during the progression of NAFLD.

Sections of 3 µm thickness were dewaxed by immersion twice in xylene for 3 minutes. Then the sections were rehydrated by soaking in decreasing concentration (100%, 95% and 75%) for 3 minutes each. Later, the sections were washed with distilled water for 2 minutes. After rehydration, the sections were kept in Wiegert's haematoxylin (WHx) for 30 minutes and then washed with distilled water for 30 seconds until the brown colour of the fluid resolved. Afterwards, staining was performed using the MT kit Masson-Goldner staining kit (1.00485.0001) from Sigma-Aldrich, Germany. First, the sections were soaked with R1 for 20 minutes, then, washed with acetic acid for 30 seconds. Then, they were soaked in R_2 for another 20 minutes followed by acetic acid washing. Finally, the sections were flooded with R_3 for 20 minutes and rinsed with acetic acid. Afterwards, the sections were dehydrated by dipping in increasing concentrations of alcohol, followed by xylene, then dried in an oven, and mounted with DPX complex and coverslips.

3.11.4 Cryosectioning and Oil Red O Staining

Oil red O (ORO) staining is a fat-soluble diazo dye. The principle of the ORO stain is that it is minimally soluble in the solvent, and the solubility is further decreased by dilution of ORO in water before use. The hydrophobic dye will therefore move from the solvent to associate with the lipids within tissue sections. ORO stains only the most hydrophobic and neutral lipids such as triglycerides, diacylglycerols and cholesteryl esters. It has also been found to be a reliable method for detecting and quantifying hepatic steatosis both in mouse and human liver biopsies. Paraffin-embedded tissues and alcohol-based fixatives cannot be used for this staining procedure, as the deparaffinisation process and alcohol fixation remove most lipids from the tissue sections. The following protocol can be adapted to include an additional step of brief paraformaldehyde fixation. It is important to freeze the tissue sample as soon as possible, either in liquid nitrogen or, if not available, in a dry ice and isopropanol bath. Then, the tissue is stored at -80 °C, and frozen tissue should not be thawed either before sectioning or during embedding, as this can cause damage to tissue integrity. During sectioning, three sections should be taken at different depths of the tissue sample (Mehlem et al., 2013).

However, some researchers reported that it is often not practical to obtain ideal conditions for rapid freezing. Ice crystal formation due to slow freezing produces irreversible damage to the tissue architecture. In order to improve tissue morphology and reduce damage due to ice crystal formation, biopsies must first be fixed in formaldehyde, then cryoprotected, and then frozen quickly. In this sense, tissues must be frozen by using cooled isopentane at −80 °C (freezer) or−160 °C (liquid nitrogen). This procedure minimises ice crystal formation and allows the cutting of frozen sections of good quality, suitable for most lipid histochemical methods and other staining techniques (Rostron & Lawrence, 2017). Currently, determination of tissue lipids is done on fresh (unfixed) frozen specimen as tissue processing will dissolve the lipid-containing specimen using alcohol and other organic solvents (Rostron & Lawrence, 2017).

Below are the equipment and chemicals used for ORO staining:

a. Tissue-Tek® O.C.T. Compound from Sakura, (USA). O.C.T. is stand for Optimal Cutting Temperature, a clear high viscosity, water soluble compound formed of glycols and resin. Works as tissue embedding medium and enables the specimen to bound to the holder of the cryostat therefore sectioning at -20 ˚C.
b. Cryostat chamber Leica CM1850 cryostat, Germany.
c. Metallic holders

A cryomould was kept in the cryostat chamber at -20 ˚C and filled completely with freezing compound (Figure 3.16). Fresh liver tissue was immediately harvested, washed with PBS then fixed in 10% formalin for 24 hours, washed with distilled water and cryoprotected in 30% sucrose in 1M phosphate buffer at 4 ˚C until cryosectioned. Cryomould was prepared earlier, completely covered by freezing compound. Trimming the prepared cryomould by sectioning 10 µm thickness and then adjusting the section thickness to 5 µm. Once satisfactory sectioned ribbons were obtained, they were picked from the blade edge with an eyelash probe and attached to a glass slide. Then the slide with the section was fixed by immersion in 10% NBF at 65 ˚C for 1 min.

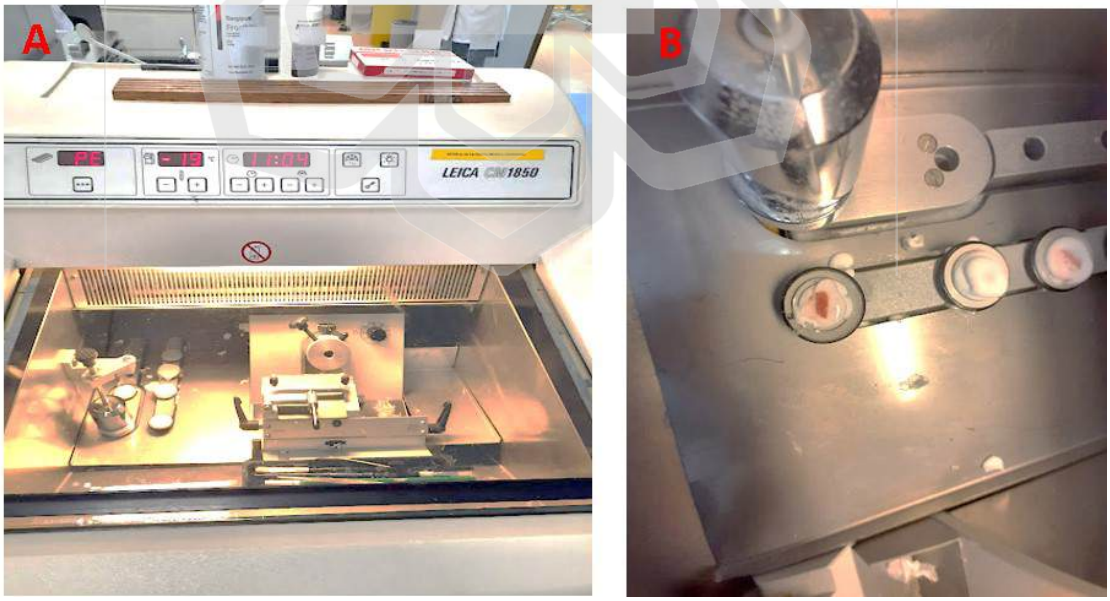

Figure 3.16 Cryostat Chamber with Cryomould Inside (A), Close-Up View Cryomoulds Inside the Cryostat Chamber (B).

Lipids in tissue were demonstrated with the Oil Red O staining ORO (Sigma-Aldrich, cat. no. 00625), which is harmless, but it leaves stains; wear necessary protective clothing and protect working areas. Rinsing the section in 60% isopropanol briefly and staining for 3 min in an Oil Red O solution, which is composed of 4 mL stock solution (i.e. 0.5% Oil Red O in 99% isopropanol) and 6 mL of distilled water. The staining solution was prepared and filtered just before use. Subsequently stained sections were differentiated in 60% isopropanol until a negative control section appeared colourless, washed in water, counterstained for 5 minutes with Mayer's haematoxylin (Histolab, cat. no. 01820, Sweden), and washed in running tap water for 3 to 5 min. The sections were mounted with glycerine-gelatine (Goor, Gerrits, & Grond, 1986).

3.11.5 Immunohistochemistry for DGAT2

Immunohistochemistry (IHC) is the method which allows the identification of certain and highly specific cellular epitopes in formalin-fixed, paraffin waxed processed tissues by selective antibodies and an appropriate labelling system. Previously formalin-fixed and processed tissues were believed not to be suitable for IHC, as it was thought that many epitopes, and some antigens could not be exhibited in paraffin wax sections. Later, with the initiation of heat-induced epitope retrieval techniques, which enabled the demonstration of many epitopes in formalin-fixed, paraffin wax-processed tissue. Therefore, many antibodies are now available to recognise epitopes which survive formalin fixed, processed and paraffin wax embedded tissue. Recently, advances in IHC have made it an important test in the diagnosis of cancer. Many other tests are now recommended to use as prognostic and predictive markers that permit the pathologist to make diagnosis evaluations which directly influence patient management (Suvarna et al., 2018).

In this study, liver tissue was fixed in 10% NBF for 48 hours at 4 ˚C and then washed with distilled water for 2 hours to remove residual fixative. The washed tissue was then kept in 70% alcohol at 4 ˚C until processing, followed by paraffin embedding, sectioning and staining according to the DGAT2 IHC kit (Cat. No. bs-12998R) protocol. The detailed method is provided in Appendix VII.

Sections of 5 µm were dewaxed in xylene for two changes of 10 minutes each, and rehydrated through a graded ethanol series (100%, 95%, 80% and 70%) then washed with distilled water for 10 minutes. Antigen retrieval was performed by heat-induced epitope retrieval (HIER) using EnVision FLEX Target Retrieval Solution at high pH (pH 9) in a Dako Omnis at 100 ˚C for 30 seconds and then at 90 ˚C for 20 minutes.

Next, the sections were incubated with 3% hydrogen peroxide for 30 minutes at room temperature to block endogenous peroxidase activity and then washed twice with PBS. Protein blocking was performed using 5% bovine serum albumin (BSA) from Calibiochem (Cat. No. 126593, USA) and incubated for 30 minutes at room temperature to block non-specific background staining. Later, the slides were incubated overnight at 4 °C with the primary antibody diluted 1:200 in a humidified chamber.

The slides were washed three times in buffer. The HRP conjugate was then applied and incubated for 15 minutes, followed by rinsing four times in buffer. The sections were then incubated with DAB for 5 minutes, followed by four washes with buffer. Finally, counterstain was applied.

For image analysis, DGAT2 immunostaining was assessed in representative liver parenchymal areas while avoiding tissue folds, artefacts, large blood vessels and poorly stained regions. Five non-overlapping representative fields from each animal were captured at the same magnification and exposure settings. DGAT2 immunostaining was quantified using ImageJ software, and the same threshold settings were applied to all images to minimise measurement bias.

3.11.6 Scanning Electron Microscope (SEM) Processing and Analysis

Scanning electron microscopy (SEM) enables detailed topographical examination of liver architecture by providing high-resolution, three-dimensional images of hepatic microstructure. It can also be used to assess collagen deposition associated with the progression of NAFLD to liver fibrosis. Additionally, SEM can evaluate changes in liver microcirculation, particularly the fenestration of hepatic sinusoids. Because liver tissue is delicate, specialised multi-step processing is required to preserve cellular architecture and minimise artefacts.

In this study, the liver sample was washed with cold PBS, then fixed in McDowell's fixative to arrest cellular metabolism, stabilise organelles and molecules *in situ*, and preserve tissue structure during subsequent processing (Collins et al., 1977; Glaumann, 1975). Wedge fixation was done using a part of the middle lobe measuring approximately 1x1x1cm^3, which was injected with McDowell's fixative containing 10% formalin and 1% glutaraldehyde in 0.1 M phosphate buffer (Speilberg, Evensen, & Skjerve, 1993).

Then, the liver tissue was kept in McDowell's fixative at 4 ˚C for 2 weeks before processing. The sample was washed in phosphate buffer three times to remove the remnant of glutaraldehyde before contact with osmium (White, Mazurkiewicz, & Barrnett, 1979). Afterwards, the tissue was post-fixed in 2% osmium tetroxide (Agar Scientific, UK) in phosphate buffer for 2 hours, washed again, then dehydrated in an increasing concentration of alcohol (30%, 50%, 70%, 90%, 95%, 100%) for 15 minutes.

Each specimen was held in a labelled metallic basket for critical point drying (Figure 3.17), where the water content of the sample was replaced by liquid carbon dioxide. The latter was then evaporated by heating above its critical point; then, the liquid became gas and was released from the specimen (Boyde & Wood, 1969).

The sample was then cut into two parts and mounted on metallic stubs with the fractured surface facing upward using carbon adhesive tape. Finally, the specimens were coated with gold using a sputter machine gold (SCD Cool Sputter Coater, Bal-Tec AG) and viewed using SEM (Carl Zeiss EVO 50, Germany) (Kashi et al., 2014). Lastly, five images were captured at 10k magnification. Fenestration and porosity of liver

sinusoidal endothelial cells were quantified according to the protocol of Cogger and colleagues (2015). Three images of 15,000 - 20,000 × magnification per animal is generally sufficient for the quantification of fenestrations using ImageJ [National Institutes of Health (NIH), Bethesda, MD]. (http://rsb.info.nih.gov/ij/index.html).

Once ImageJ was opened and the images were uploaded into the software, the polygon tool in ImageJ was used to trace around the entire flat area of the LSEC, including fenestrated and defenestrated areas. Any large debris on the cell surface that might obscure the fenestrations was excluded. The fenestration diameter was measured by tracing a line through the longest diameter of each fenestra by selecting the line tool, and press "m" to measure the line, and "d" (draw) to permanently draw the line on the image. All gaps, which are large holes in the LSEC cytoplasm over 250 nm, were measured, as they are often artefacts reflecting poor perfusion or fixation. However, gaps can also occur as a result of disease and toxicity. The data for gaps were excluded from the calculation of fenestration parameters later in the analysis. Data from the above measurements in the results box in ImageJ were pasted into an Excel spreadsheet for further analysis (Cogger et al., 2015). The calculations were done based on the resulting measurements according to the following formulas:

1. Fenestration area = πr^2, where r, the radius, is calculated from the individual fenestrations' diameter (r=d/2), not including gaps.
2. Porosity (%) = (Σ (πr^2)/total area analysed - Σ (area of gaps)) (μm^2)) × 100.
3. Fenestration frequency = total number of fenestrations/ (total area analysed-Σ (area of gaps) (μm^2).

Figure 3.17 SEM Stub Holding Coated Liver Tissue Samples Prepared for Viewing.

3.12 STATISTICAL ANALYSIS

Data were tested for normality and presented as mean ± standard deviation (SD). For normally distributed numerical variables, intergroup differences were analysed using one-way ANOVA followed by Scheffé's post hoc test. A P value < 0.05 was considered statistically significant. Descriptive statistics (Mean, SD) were used to summarise body weight, liver weight, and NAS scoring. All analyses were performed using SPSS 22.0 for Windows.

CHAPTER FOUR

RESULTS

4.1 GENERAL WELLBEING

At the end of the experimental procedures, all animals were closely observed daily with food and water supplements, and careful handling. Close monitoring of the signs of distress or compromised health, including assessment of food intake, body weight, and locomotor activity. At the beginning of the experiment, animals were acclimatised for two weeks to mitigate the stress and allow them to adapt to their new environment. All animals maintained normal coat appearance and normal behaviour throughout the experiment. Body weights were also recorded and no significant alterations were observed within the same group. Furthermore, no signs of drug toxicity were observed in the treated groups.

4.2 PHASE 1: PILOT STUDY RESULTS

The purpose of this pilot was to determine the duration required for HCD-fed animals to develop simple steatosis. This was achieved after 4 weeks of feeding with HCD. The detailed results of the pilot study are described below.

4.2.1 Body Weight and Liver Weight

At baseline, no differences were observed comparing the body weights of rats in control groups to those in HCD groups (Figure 4.1). Increased body weight gain in HCD groups occurred as early as two weeks after the treatment compared to controls. As expected, HCD rats (422.2 gm ±20.3) developed obesity and significantly higher final body weights compared to controls (342.7±11.3 gm) ($P< 0.05$). Liver weight and relative body weight were significantly increased ($P<0.05$) in HCD-fed rats after 5 weeks (17.5±1.2) gm (Figure 4.1 and Figure 4.2) when compared to control diet group

(9.6±0.8gm). However, the absolute liver weights were significantly increased at the earlier times at 4 weeks (15.6± 1.5gm).

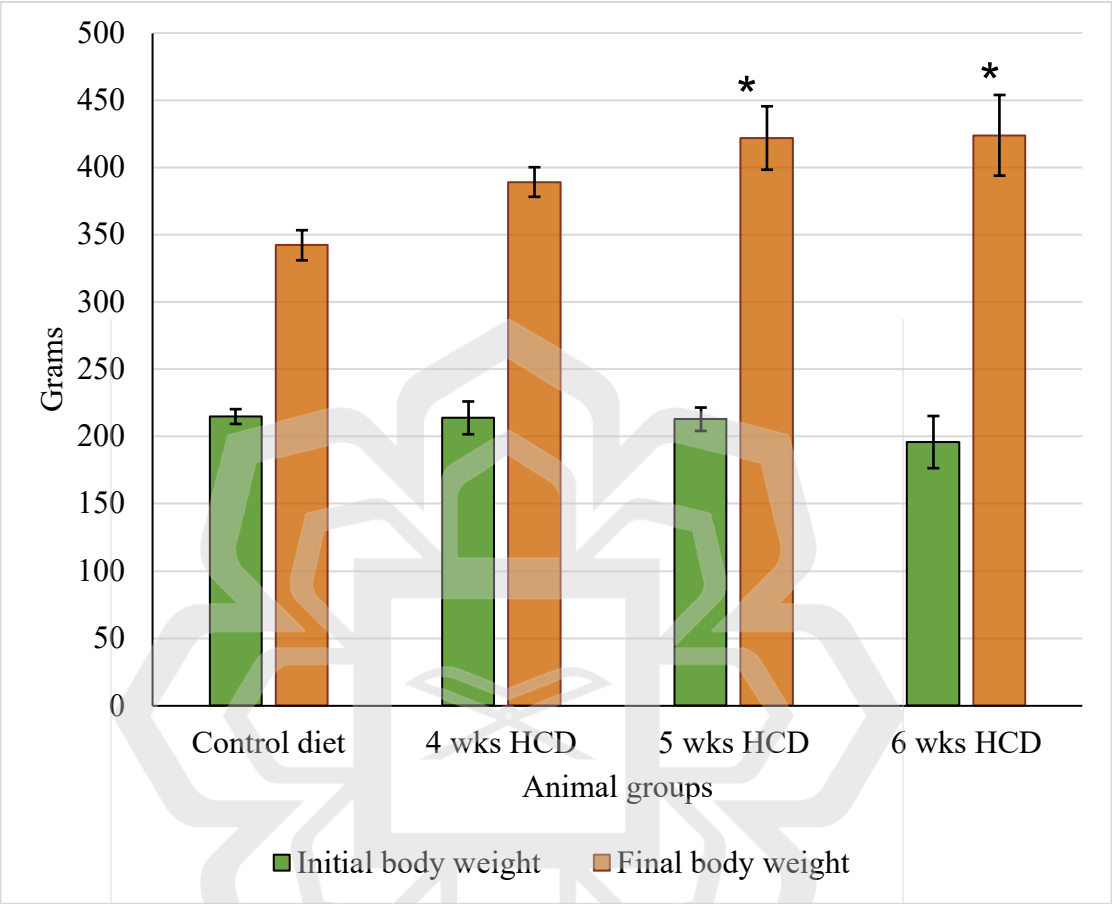

Figure 4.1 Comparison of Initial and Final Body Weights in Control and HCD-Fed Rats. N = 3 in Each Group. Data Are Expressed as Mean ± SD. *p < 0.05 Vs. Control.

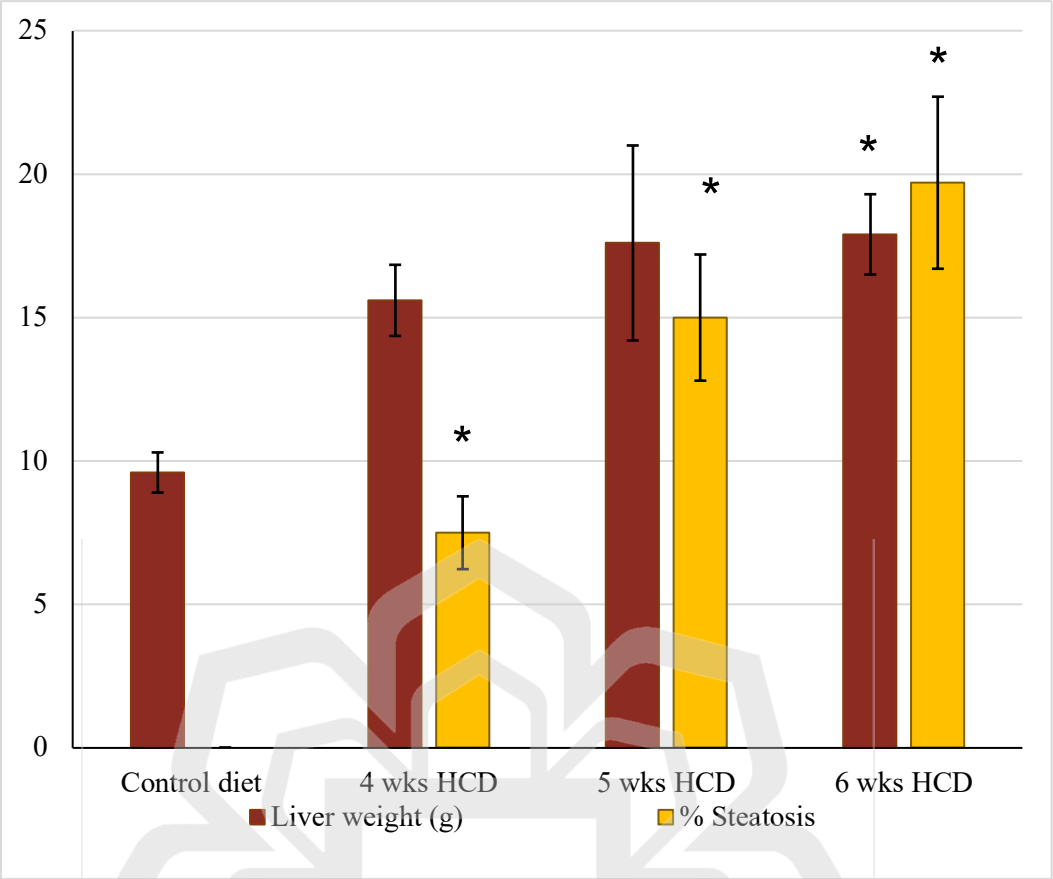

Figure 4.2 Liver Weight and Percentage of Steatosis in Control and HCD-Fed Rats from the Pilot Study. An Increase in Both Liver Weight and Steatosis Percentage Was Observed in the HCD Group Compared to the Control Group. N = 3 Per Group. Data Are Expressed as Mean ± SD. *$p < 0.05$ Vs. Control.

4.2.2 MACROSCOPIC AND MICROSCOPIC RESULTS

Grossly, the liver showed a notable change in colour and texture in the HCD groups compared to the control diet group (Figure 4.3a). This was most obvious in the 5-and 6-week HCD groups. The liver appeared greasy and yellow in colour. Histopathological examination in H&E-stained liver tissue showed normal liver architecture and well-arranged liver acini in the control diet group. In contrast, this arrangement was gradually lost due to hepatocyte swelling as it became laden with lipid (hepatic steatosis), as seen in the 4-weeks HCD group. Additionally, hepatocytes with degenerative changes, cytoplasmic rarefaction (hepatocyte ballooning) and a large number of fat vacuoles in the cytoplasm were seen in 5- and 6-week HCD groups.

Besides, signs of steatosis in these groups, lobular inflammatory infiltrates were also present (Figure 4.3b). Specifically, the percentage of steatosis was significantly different in all groups of HCD when calculated in H&E-stained images using ImageJ software. This confirms that the 4-week HCD group represents the steatosis stage of NAFLD in this animal model. In conclusion, the 12% high cholesterol and 3% cholic acid diet animal model demonstrated the histopathological progression of NAFLD, which progressed from a simple steatosis in the four-week groups to NASH in the 5- and 6-week groups. Therefore, this model could be an ideal model to study pathophysiology, disease progression and response to new therapeutic targets.

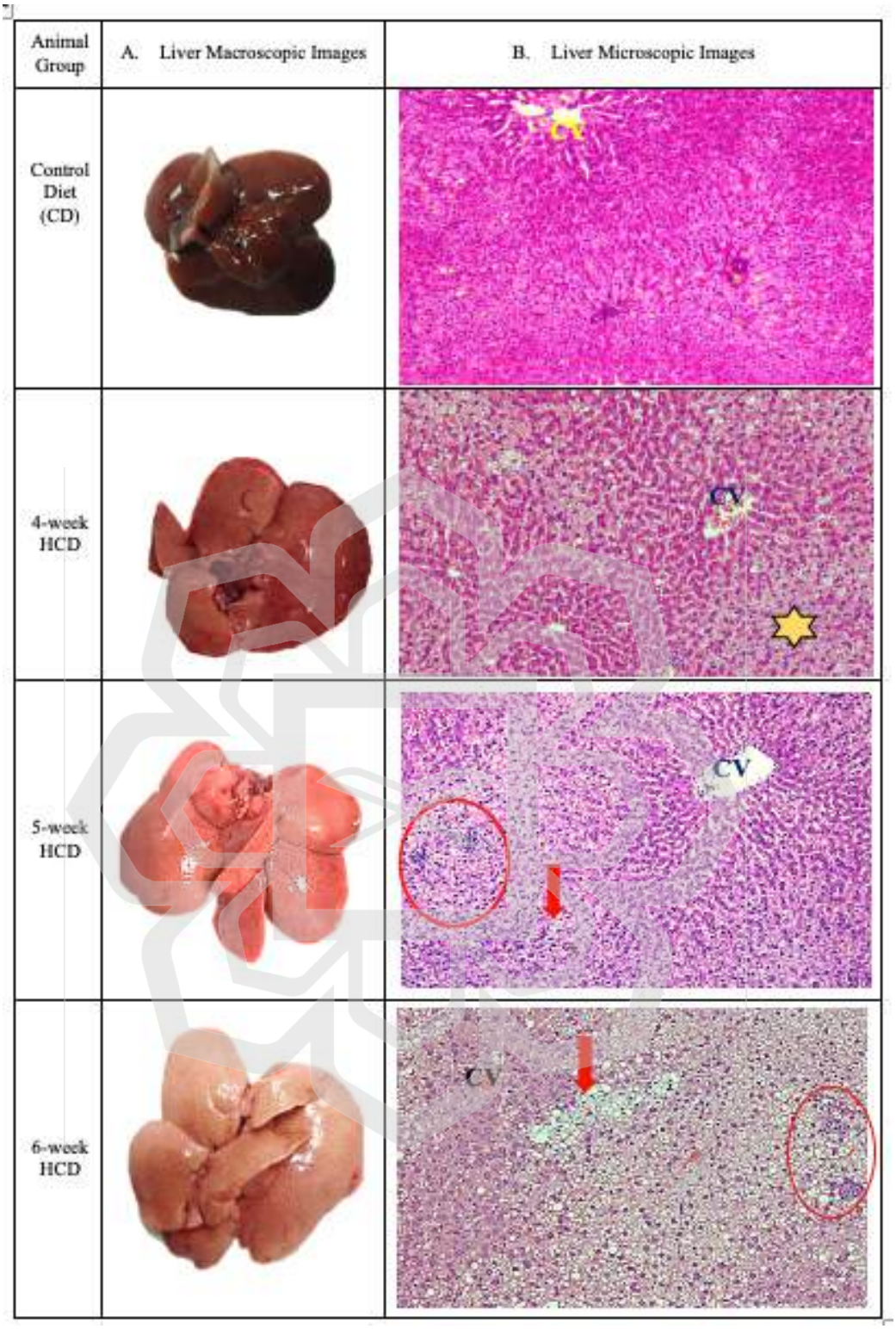

Figure 4.3 Gross Colour Changes of the Liver in Different Pilot Study Groups (A). The Microscopic Changes of H&E-Stained Liver Tissue Images at 100X (B). CV: Central Vein, PA: Portal Area. Inflammatory Foci (O), Ballooning Arrow (⇩) (B), Star: Simple Steatosis.

4.3 PHASE 2: MAIN RESEARCH RESULTS

Phase two was designed to evaluate the response of fatty liver in the rat model to RA treatment. This phase consisted of four weeks for inducing NAFLD in animals, particularly the steatosis stage, as determined in the earlier phase. Followed by, another four weeks of duration for RA treatment for the specific animal groups.

4.3.1 Body and Liver Weights

At baseline, there were no significant differences in body weight among all experimental animals. By the final weight measurement, rats gained more weight in the HCD compared to the control diet group (HCD: 439.2±20.3gm vs. CD: 393.7±41.3), ($p < 0.05$). Additionally, a significant decrease in body weight was observed in RA-treated animals (HCD+RA: 349.4±65.6 gm) compared with HCD-fed rats (439. 2±20.gm $p < 0.05$) and HCD-fed rats injected with vehicle (HCD=V: 426.2±24) (Table 4.1).

Moreover, liver weight was significantly increased in all HCD groups, namely G3, G4, and G5 (16.5±1.9, 16.5±1.5, and 13.5±3.2, respectively, $p < 0.001$) when compared with G1(10.7±1.2). Likewise, relative liver weight (calculated by dividing the liver weight by the body weight) was notably increased in all HCD groups when compared to the control diet group. Meanwhile, liver weight and relative liver weight were substantially decreased in HCD rats treated with retinoic acid (RA) compared to G3 ($p < 0.001$) (Table 4.2). In favour of the above results, a decrease in the body and liver weights was observed in HCD-treated rats with RA. This reduction in liver weight of G5 (HCD-fed animals treated with RA) corresponds with a reduction in the body weight of a similar animal group when compared to G3 (HCD-fed animals).

Table 4.1 Baseline and Final Body Weight.

Animal group	Intial body weight	*p*-value	Final body weight	*p*-value
G1	302.5±20.8	-	393.7±41.3	0.03
G2	307.7±24.5	0.8	378.4±27.0	0.02
G3	311.6±14.2	0.9	439.2±20.3	-
G4	302.5±13.8	1	426.2±24.6	0.90
G5	302.5±20.8	1	393.7±41.3	0.001

Data is expressed as mean ± SD. The difference between groups was determined using one-way ANOVA and post HOC Scheffé's post hoc test. A p-value < 0.05 was considered statistically significant at 95% confidence interval, (n= 9). For final body weight, G1, G2, G4 and G5 were compared with G3. G1, control diet (CD); G2, control diet with retinoic acid (CD + RA); G3, high-cholesterol diet (HCD); G4, high-cholesterol diet with vehicle (HCD + vehicle); G5, high-cholesterol diet with retinoic acid (HCD + RA).

4.3.2 Biochemical Results

4.3.2.1 Liver Tissue Triglyceride

The key parameter of this research is the triglyceride accumulation in the liver to demonstrate fatty liver disease in the animal model, which had been confirmed in next section by histopathological examination. The result revealed a substantial increase in tissue TG accumulation (Table 4.2) in the liver of HCD-fed animals, G3 (230.4±39.4; p = 0.0001), and G4 (212.7±48.1; p = 0.0001), except for the group treated with the RA (G5= 102.3±19.3), when compared with the control diet animal group (G1=76.4±21.3). In addition, tissue content of TG was significantly reduced in G5(102.3±19.3) when compared to G3 (230.4±39.4; p = 0.001). Interestingly, rats fed on control diet, administered with the RA diet (G2=59.1±21.7), led to a reduction in liver TG content compared to animals fed with a similar diet and did not receive any treatment (G1=76.4±21.3). However, this reduction did not reach statistically significance (p = 0.8).

Table 4.2 Liver Parameters (Weight, Relative Liver Weight, and TG Content)

Animal group	Liver weight (g)	Relative liver weight (%)	Liver TG (mg/g tissue)
G1	10.7 ± 1.2^{b}	2.7 ± 0.2^{b}	76.4 ± 21.3^{b}
G2	10.3 ± 0.6^{b}	2.7 ± 0.1^{b}	59.1 ± 21.7^{b}
G3	16.5 ± 1.9^{a}	3.8 ± 0.3^{a}	230.4 ± 39.4^{a}
G4	16.5 ± 1.5^{a}	3.8 ± 0.3^{a}	212.7 ± 48.1^{a}
G5	$13.4\pm3.2^{a, b}$	$3.6\pm0.3^{a, b}$	102.3 ± 19.3^{b}

Data are expressed as mean ± SD (n = 9). Differences among groups were analysed using one-way ANOVA followed by Scheffé's post hoc test. Different superscript letters indicate significant differences between groups at $p < 0.05$: superscript a indicates a significant difference compared with G1, while superscript b indicates a significant difference compared with G3. G1, control diet (CD); G2, control diet with retinoic acid (CD + RA); G3, high-cholesterol diet (HCD); G4, high-cholesterol diet with vehicle (HCD + vehicle); G5, high-cholesterol diet with retinoic acid (HCD + RA).

4.3.2.2 Blood parameters

The main manifestation of NAFLD is dyslipidaemia, including high serum cholesterol. This was evident in the present NAFLD model, as revealed by the significant increase in serum cholesterol of all HCD-fed animals (G3: 3.3±0.7, G4: 2.4±0.6, G5: 3.4±0.8) when compared with control diet-fed animals (G1: 1.4±0.3 ; $p < 0.05$) (Table 4.3). However, RA treatment did not significantly reduce serum total cholesterol in HCD-fed rats, as no significant difference was observed between G5 (3.4 ± 0.8 mmol/L) and G3 (3.3 ± 0.7 mmol/L). Similarly, RA treatment did not significantly increase serum total cholesterol in control diet-fed rats, as G2 (1.5 ± 0.3 mmol/L) did not differ significantly from G1 (1.4 ± 0.3 mmol/L). Therefore, RA had no significant effect on serum total cholesterol in either control diet-fed or HCD-fed rats.

On the other hand, serum TG did not show a significant change across all groups. Serum TG was not increased in HCD-fed animals, nor decreased in RA-treated

animals, when compared to HCD-fed animals (G3). Surprisingly, the serum TG was high in control diet animals treated with retinoic acid.

Among the conditions associated with NAFLD and involved in the pathogenesis of the disease is the disturbance in glucose metabolism that results from insulin resistance. In this study, serum glucose was measured to assess the efficacy of RA on glucose concentration. The result revealed that RA can restore serum glucose level in G5 (5.0±0.5) when compared to G3 (6.5±1.8); however, it did not reach statistical significance (Table 4.3).

Alanine aminotransferase (ALT) is the main enzyme specific for hepatocyte damage, and it is frequently raised in NAFLD. However, in this study despite clear metabolic changes and histopathological manifestation of NAFLD, serum ALT had not demonstrated a corresponding increase in serum of HCD-fed animals (G3, G4, G5). Serum ALT was not significantly different among all animal groups, even in the HCD group that received RA treatment.

Table 4.3 Serum Biochemical Parameters (Cholesterol, Triglyceride, Glucose, and Alanine Aminotransferase)

Animal groups	Serum Chol (mmol/L)	Serum TG (mmol/L)	Blood sugar (mmol/L)	ALT (U/L)
G1	1.4±0.3[b]	0.58±0.2	6.2±0.7	70.8±13.9
G2	1.5±0.3[b]	1.0± 0.4	6.1±0.6	71±15.4
G3	3.3±0.7[a]	0.7±0.3	6.5±1.8	72.8±1.2
G4	2.4±0.6[a]	0.6±0.3	6.5±1.7	73.5±2.1
G5	3.4±0.8[a]	0.5±0.2	5.0±0.5	85±2.4

Data are expressed as mean ± SD (n = 9). Differences among groups were analysed using one-way ANOVA followed by Scheffé's post hoc test. Different superscript letters within the same column indicate significant differences between groups at $p < 0.05$: superscript a indicates a significant difference compared with G1, while superscript b indicates a significant difference compared with G3. G1, control diet (CD); G2, control diet with retinoic acid (CD + RA); G3, high-cholesterol diet (HCD); G4, HCD + vehicle; G5, HCD + RA.

4.3.3 Macroscopic and Microscopic Histopathological Results

The gross appearance of the livers from HCD-fed rats (G3, G4) were pale yellow in colour. Additionally, livers from (G3, G4) were markedly enlarged compared with those of the rats from the control group (G1) and RA-treated HCD-fed animals (G5) which, appeared more brownish in colour (Figure 4.4A).

4.3.3.1 Haematoxylin and Eosin Staining

Histopathological examination of liver tissue demonstrated that HCD-fed animals induced hepatic lipid accumulation, which was more obvious at the portal areas in all groups of HCD-fed animals. In contrast, well-preserved liver architecture and hepatic acini in the control diet group were recognisable (Figure 4.4B). The main predictive sign of NASH in HCD-fed rats was also apparent in H&E staining. Hepatocyte ballooning and inflammatory infiltration were evident. A notable decrease in lipid accumulation was observed in HCD-fed rats treated with RA (G5) when compared to non-treated HCD-fed animals. This was confirmed by semi-quantification of hepatic steatosis using ImageJ software in 10 fields of 200x magnification (Table 4.4). A significant decrease in the percentage of steatosis in HCD-fed animals treated with RA (22.1±12.4) compared with untreated HCD-fed animals (48.6±9.8 ; p = 0.001). Moreover, the inflammatory infiltration and hepatic ballooning were also decreased in G5 when compared with G3.

Table 4.4 Histopathological assessment and scoring of hepatic steatosis

Animal group	Steatosis (%) (mean ± SD)	*p*-value
G1 (CD)	0±0	NA
G2 (CD+RA)	0±0	NA
G3 (HCD)	48.6±9.8	1
G4 (HCD+V)	54.4±6.9	0.7
G5 (HCD+RA)	22.1±12.4	0.001

Data are expressed as mean ± SD. Differences among groups were analysed using one-way ANOVA followed by Scheffé's post hoc test. The *p*-values represent comparisons with G3. A *p*-value < 0.05 was considered statistically significant. G1, control diet (CD); G2, control diet with retinoic acid (CD + RA); G3, high-cholesterol diet (HCD); G4, high-cholesterol diet with vehicle (HCD + vehicle); G5, high-cholesterol diet with retinoic acid (HCD + RA); NA, not applicable.

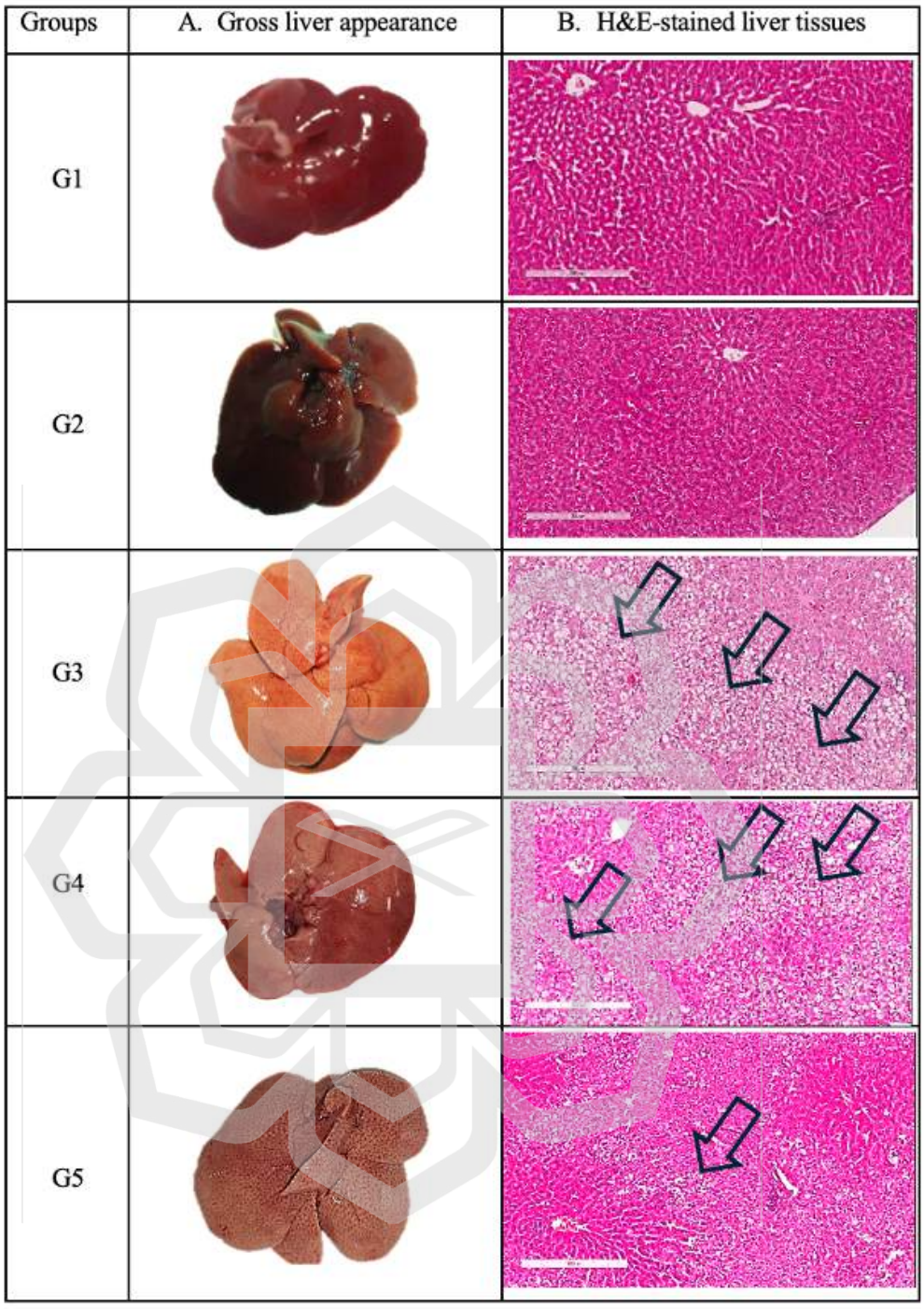

Figure 4.4 Gross and Microscopic Feature of the Liver in All Animal Groups. (A) Gross appearance of the liver. (B) Representative haematoxylin and eosin-stained liver sections. G1, control diet (CD), and G2, control diet with retinoic acid (CD + RA), show preserved liver architecture. G3, high-cholesterol diet (HCD), and G4, high-cholesterol diet with vehicle (HCD + vehicle), show extensive hepatic steatosis, while G5, high-cholesterol diet with retinoic acid (HCD + RA), shows reduced hepatic steatosis. Arrows indicate areas of steatosis. Scale bar = 300 µm.

Inflammatory infiltration of hepatic tissue was observed in the lobular zones. Foci of inflammation were seen in all animal groups. fed on HCD (G3, G4 and G5) but were absent in the control diet groups (G1 and G2). The number of inflammatory foci per field was also markedly reduced in HCD-fed animals administered RA. This result was confirmed by quantitative analysis, with the highest score of the inflammation was found in G3(1.7±0.6), and G4(1.6±0.5). A significant difference in semi-quantitative scoring of NAFLD was seen in HCD-treated with RA when compared to HCD-fed animals (G3) (1.3±0.6 vs. 1.7±0.6, *p*-value = 0.028). In both control diet animal groups with and without vehicle injection (G1 and G2) showed zero score. In contrast, there was no statistically significant difference between G3 and G4.

Hepatocyte ballooning is a characteristic manifestation of steatohepatitis. It appeared as distended, swollen, pale, and rarefied cytoplasm. This feature was prominent and widely distributed in HCD-fed animals (G3 and G4) in the liver tissue, but was less frequently seen in G5, and absent in control diet animals (G1 and G2). More precisely, semi-quantitative analysis for scoring of ballooned hepatocyte according to NASH Clinical Research Network (NASH CRN) system revealed a statistically significant increased ballooning score in G3 compared to HCD-fed animal treated with RA (G5) (1.6±0.5 vs. 0.57±0.6, $p < 0.001$) (Table 4.5). The result highlights the protective effect of RA against hepatocyte damage caused by a high cholesterol diet and prevents the progression of NAFLD. However, there was no significant difference observed between G4 (1.7±0.4) and G3 (1.6±0.5).

The NAS scoring system demonstrated that HCD induced NAFLD rats in G3, and G4 (5.3±0.9 and 5.2±0.8, respectively) developed the histopathological features of NASH. RA treatment significantly reduced the NAFLD Activity Score in HCD-fed rats compared with untreated HCD-fed rats (3±0.9 vs. 5.3±0.9, respectively; $p < 0.001$). This decline in NAS displayed an improvement in the main histological parameters of NAFLD, including diminished steatosis, inflammation, and hepatocyte ballooning**.** These NAS components in HCD treated with RA, compared to HCD-fed animals, contributed to a reduction in the total score of NAFLD. This finding supports the potential efficacy of RA in regressing the progression of NAFLD to NASH.

Table 4.5 Assessment of NAFLD Severity Using the NAS System in All Animal Groups.

Animal groups	Steatosis scoring (*p*-value)	Inflammatory scoring (*p*-value)	Ballooning score (*p*-value)	NAS scoring (*p*-value)
G1	0±0 (<0.0001)	0±0 (<0.001)	0±0 (<0.0001)	0±0 (<0.0001)
G2	0±0 (<0.0001)	0±0 (<0.001)	0±0 (<0.0001)	0±0 (<0.0001)
G3	1.9±0.3	1.7±0.6	1.6±0.5	5.3±0.9
G4	2±0.2 (1)	1.6±0.5 (1)	1.7±0.4 (1)	5.2±0.8 (1)
G5	1.1±0.9 (<0.001)	1.3±0.6 (0.028)	0.57±0.6 (<0.001)	3±0.9 (<0.001)

Data are expressed as mean ± SD. Non-parametric data were analysed using the Kruskal–Wallis test, with G3 used as the reference group. G1, control diet (CD); G2, control diet with retinoic acid (CD + RA); G3, high-cholesterol diet (HCD); G4, high-cholesterol diet with vehicle (HCD + vehicle); G5, high-cholesterol diet with retinoic acid (HCD + RA).

4.3.3.2 Oil Red O Staining

Oil Red O staining is a specific stain demonstrating intracellular red coloured lipid deposition on frozen liver sections. Sections from control diet groups showed no detectable red colour staining, indicating the absence of increased lipid in the liver of these animal groups (G1, G2). In contrast, extensive red colour staining was observed in liver sections of HCD-fed rats (G3, G4), confirming lipid accumulation in NAFLD animal models. Whereas, less extensive red coloured lipid droplets were seen in the liver sections from the HCD-fed animals treated with RA (G5) (Figure 4.5A). A notable decrease in the red staining of the liver section treated with RA, demonstrating a reduction in lipid accumulation in the liver, and the main reduction was around the central vein consistent with the findings from H&E staining and ImageJ semi-quantification.

4.3.3.3 Masson's Trichrome Staining

Masson's trichrome-stained liver sections were used for the evaluation of hepatic fibrosis. No significant increase in fibril deposition was recognised in control diet groups (G1, G2). While noticeable fibrils deposition was demonstrated in liver sections by intense blue staining, mainly seen in perisinusoidal and peri-portal areas in HCD-fed rats (G3, G4). In contrast, the fibrous tissue was significantly reduced, with minimal blue staining detected in liver sections of HCD-rats treated with RA when compared to HCD-fed animals (G3, G4). These results suggest the effect of RA in diminishing fibrotic changes and preventing the progression of NAFLD, meaning that collagen deposition was suppressed by RA treatment (Figure 4.5B).

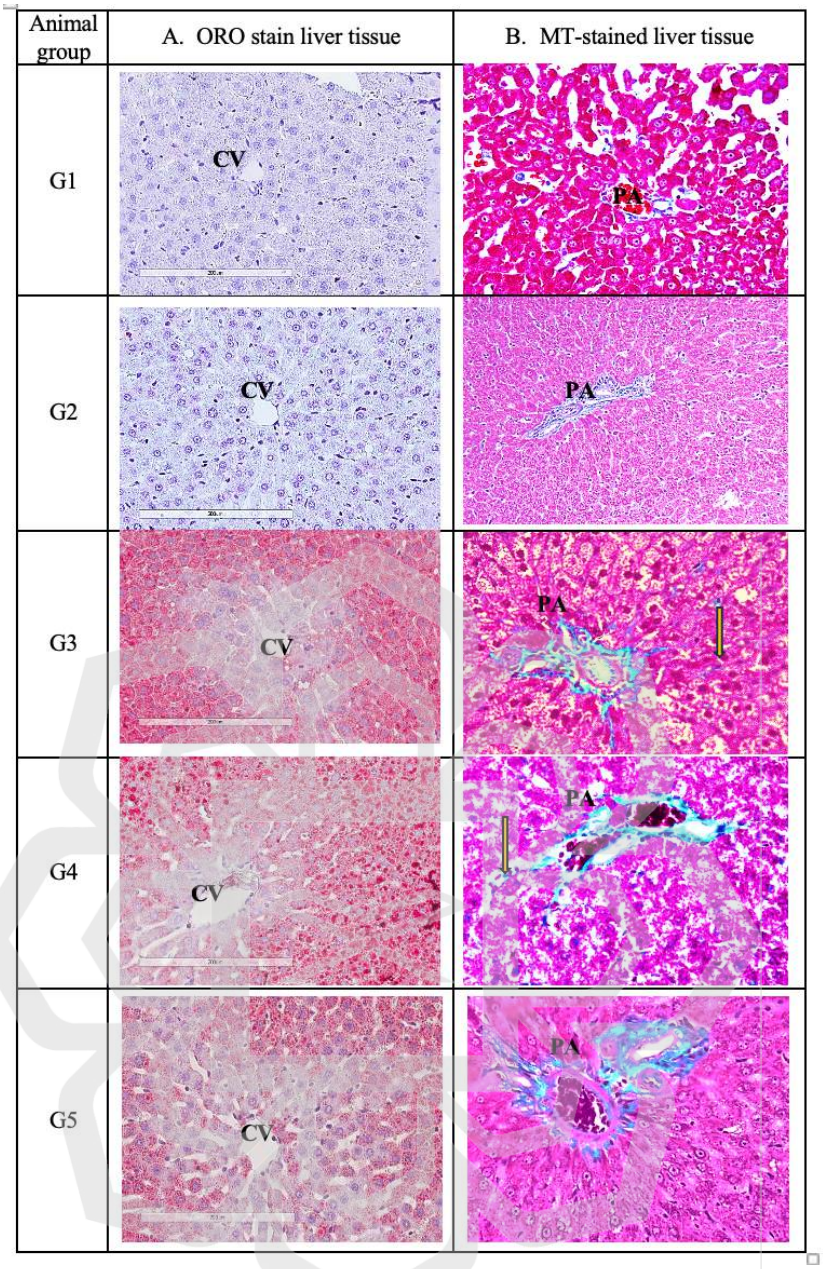

Figure 4.5 Photomicrographs of Liver Sections Stained with Oil Red O (ORO) and Masson's trichrome (MT). Representative photomicrographs of liver sections stained with ORO and MT. A. Oil Red O staining highlights lipid droplets in red. Scale bar = 200 µm . 200x magnification. B. Masson's Trichrome-staining highlights collagen fibres in blue. 400x magnification. CV = central vein; PA = portal area. Yellow arrows indicate perisinusoidal fibrosis. G1, control diet (CD); G2, control diet with retinoic acid (CD + RA); G3, high-cholesterol diet (HCD); G4, high-cholesterol diet with vehicle (HCD + vehicle); G5, high-cholesterol diet with retinoic acid (HCD + RA). The G2 Masson's trichrome image represents the portal area but was captured at a lower magnification than the corresponding images from the other groups.

4.4 DGAT2 IMMUNOHISTOCHEMISTRY STAINING

The DGAT2 expression in representative images of liver tissue for immunohistochemical staining was determined in all animal groups (Figure 4.6). Semi-quantitative analysis of DGAT2 expression was determined by ImageJ software (Table 4.8). The highest expression of the DGAT2 was observed in liver sections from HCD-fed rats G3 and G4 (G3 = 21.5 ± 1.9, and G4 = 21.7 ±1.8). Although DGAT2 is constitutively expressed in normal liver tissue, its expression was lower in the control diet-fed group, G1 (7.0 ± 1.4), than in the HCD-fed groups, G3 (21.5 ± 1.9) and G4 (21.7 ± 1.8). Interestingly, the expression of the DGAT2 was significantly higher in the control diet group injected with RA compared to only control diet fed animals (12.5 ± 1.7 vs.7.0 ± 1.4, $p < 0.05$). This result corresponds with the elevated level of serum TG in the same animal group, as DGAT2 is the main enzyme responsible for the synthesis of TG in the liver. A marked reduction in DGAT2 expression was observed in HCD fed rats treated with RA (G5) when compared to only HCD fed animal (G3) (12.1 ±1.8 vs. 21.5 ± 1.9. $p < 0.001$). Similarly, the result of DGAT2 expression in the liver of treated animals (G5) was in line with the result of reduction in tissue TG level in the same animal group. No significant difference in the expression of DGAT2 enzyme between HCD-fed animals only (G3) and HCD-fed animals treated with vehicle (G4).

Animal group	DGAT2 IHC
G1	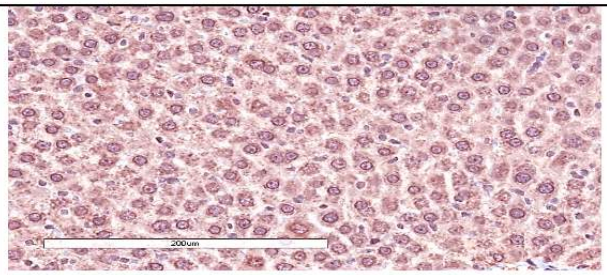
G2	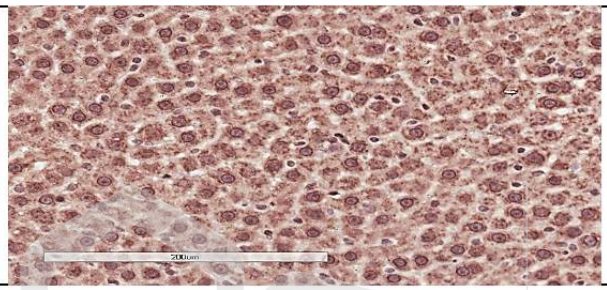
G3	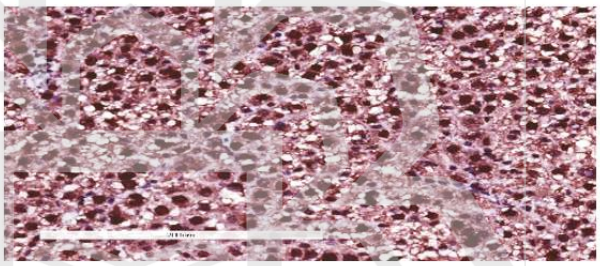
G4	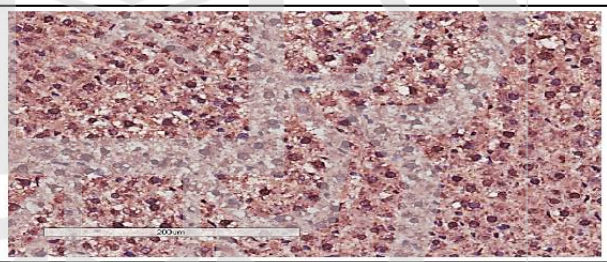
G5	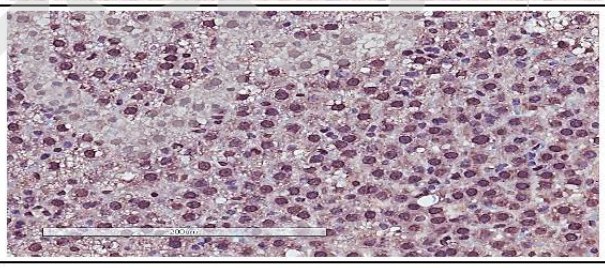

Figure 4.6 Representative Photomicrographs of Hepatic DGAT2 Expression. Representative liver sections showing DGAT2 immunohistochemistry (IHC) in G1, control diet (CD); G2, control diet with retinoic acid (CD + RA); G3, high-cholesterol diet (HCD); G4, high-cholesterol diet with vehicle (HCD + vehicle); and G5, high-cholesterol diet with retinoic acid (HCD + RA). Brown cytoplasmic staining indicates DGAT2 immunoreactivity. Images were selected from the central vein (CV) area. Scale bar = 200 μm. Magnification = 200×.

Table 4.6 DGAT2 Expression in Liver Tissue Using Immunohistochemistry (IHC)

Animal groups	DGAT2 expression (Mean ±SD)	*p*-value (Vs G3)
G1	7.0 ± 1.4	<0.0001
G2	12.5 ± 1.7	<0.0001
G3	21.5 ± 1.9	-
G4	21.7 ±1.8	>0.05
G5	12.1 ±1.8	<0.0001

Data are expressed as mean ± SD (n = 9). Data were analysed using one-way ANOVA followed by Scheffé's post hoc test. Comparisons were made against G3. A *p*-value < 0.05 was considered statistically significant. G1, control diet (CD); G2, control diet with retinoic acid (CD + RA); G3, high-cholesterol diet (HCD); G4, high-cholesterol diet with vehicle (HCD + vehicle); G5, high-cholesterol diet with retinoic acid (HCD + RA).

4.5 ULTRASTRUCTURAL CHANGES IN HEPATOCYTES AND LSECS

Scanning electron microscopy (SEM) provided evidence of surface morphological changes in hepatocytes and liver sinusoidal endothelial cells (LSECs) associated with NAFLD progression, as shown by increased fibril deposition, representing the manifestation of NASH.

In control diet groups (G1, G2), SEM revealed a distinctive polygonal shape of hepatocytes with well-defined boundaries. In contrast, hepatocytes of the NAFLD animal model (G3, G4) appeared swollen, rounded in shape, and lost their polygonal figure and well-defined edges (Figure 4.7A). Additionally, dense distribution of coarse fibril bundles deposition was observed in HCD-fed animals (G3, G4), suggesting the development of fibrotic changes associated with NASH. These ultrastructural changes were consistent with histopathological findings observed in MT-stained sections, further supported by increased NAS scoring in G3 and G4 animal groups. SEM result of HCD-fed animals treated with retinoic acid revealed improved hepatocyte morphology, preserved polygonal shape and more defined cellular boundaries,

indicating a protective effect of the treatment against HCD. Furthermore, HCD-fed animals that received RA treatment revealed a noticeable reduction in fibril accumulation together with improved liver histology, reflecting the antifibrotic effect of RA.

Liver sinusoidal endothelial cells (LSECs) play an important role in the development of NAFLD and are implicated in disease progression. They are essential in regulating exchange between hepatocytes and sinusoidal blood, and disruption of this function contributes to NAFLD progression. SEM enabled detailed visualisation of LSEC fenestrations, which are critical for endothelial permeability. Also, impaired liver function in NAFLD was attributed to the loss of LSECs' fenestration. In this study, SEM for liver tissue from control diet-fed animals (G1 and G2) revealed well-preserved endothelial cells with normal fenestration, distributed in sieve plates. In contrast, SEM for liver tissue obtained from NAFLD groups (G3, G4 and G5) demonstrated a notable reduction of LSECs fenestra, indicating disrupted endothelial permeability and resulting in capillarization of LSECs (Figure 4.7B).

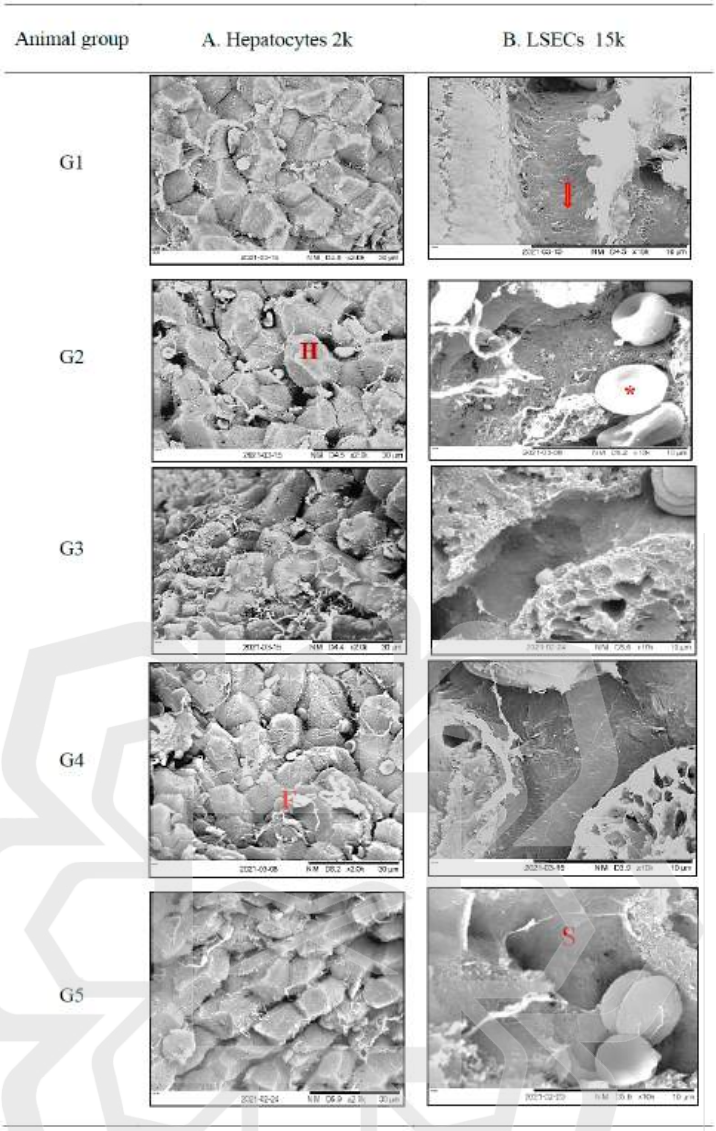

Figure 4.7 Scanning Electron Micrographs of Liver Tissue Showing Hepatocytes and LSECS. (A) Low magnification SEM micrographs (2,000x), showing parenchymal cells and sinusoids openings with scattered erythrocytes. Hepatocytes exhibit preserved polygonal shape and distinct cell borders in G1, G2, and G5, whereas G3 and G4 show loss of characteristic architecture, with swollen and crowded hepatocytes. Scale bar = 30µm (B) Higher magnification SEM micrographs (10,000x) demonstrating sinusoidal endothelial fenestrations, which are clearly visible in G1 and G2 but markedly reduced in G3, G4 and G5. Scale bar = 10µm. H, hepatocyte; S, sinusoid; asterisk, erythrocytes; arrow, fenestrae; F, fibril deposition. G1, control diet (CD); G2, control diet with retinoic acid (CD + RA); G3, high-cholesterol diet (HCD); G4, high-cholesterol diet with vehicle (HCD + vehicle); G5, high-cholesterol diet with retinoic acid (HCD + RA).

In the context of evaluating the liver microarchitecture changes, especially the sinusoidal endothelial fenestrae and their distribution in the sinusoids. A detailed semi-quantitative assessment of LSEC fenestrae was used to determine the degree of liver injury, enabling estimation of the difference in LSEC fenestrae between the groups. Herein, the semi-quantitative result for porosity and fenestrae frequency revealed uniformly distributed and abundant fenestrae in the sinusoid of the control diet groups (G1 and G2). Average sinusoidal porosity was 2.3 ± 0.3% in G1 and 2.1 ± 0.4% in G2. In contrast, the frequency of fenestrae was estimated to be more than three fenestrae per one square micrometre of sinusoid (G1=3.6 ± 1, G2= 3.7 ± 0.7). Both sinusoidal porosity and fenestrae frequency were significantly higher in control diet-fed animals (G1 and G2) when compared to HCD-fed animals ($p < 0.05$) (G3: porosity 0.3 %± 0.2, fenestrae frequency 0.6 ± 0.2), representing preserved LSEC ultrastructure and function in the absence of HCD-induced defenestration (Table 4.7).

In contrast, to the control diet-fed groups, the NAFLD groups, G3 and G4, showed significantly reduced sinusoidal porosity (0.3 ± 0.2% and 0.3 ± 0.1%, respectively) and fenestrae frequency (0.6 ± 0.2 and 0.5 ± 0.1 per μm², respectively) (both $p < 0.05$), indicating HCD-induced LSEC defenestration (Table 4.7).. These results showed a marked reduction in both LSEC parameters, reflecting disrupted sieve plates, decreased fenestrae density and partial or complete defenestration of the endothelial surface. The changes also indicate impaired hepatic microvascular exchange associated with the progression of NAFLD.

In RA-treated NAFLD animals (G5), unexpectedly, no significant improvement in sinusoidal porosity (G5: 0.2 ± 0.1 vs G3: 0.3 ± 0.2) and fenestrae frequency (G5: 0.4 ± 0.1 vs. G3: 0.6 ± 0.2) was observed following treatment with RA when compared with the HCD group. The result suggests that RA treatment did not effectively repair or preserve the microvasculature of the liver sinusoids in this NAFLD model, despite the beneficial effect of RA in improving other parameters of NAFLD, such as histopathological reduction in tissue TG content and partial preservation of hepatocyte morphology, as shown in the SEM result.

Table 4.7 Quantitative Analysis of LSECs Porosity and Fenestrae Frequency

Animal groups	Porosity % (pores area/sinusoidal area) X 100	Fenestra frequency (number/μm^2)
G1	2.3 ± 0.3*	3.6 ± 1.0*
G2	2.1 ± 0.4*	3.7 ± 0.7*
G3	0.3 ± 0.2	0.6 ± 0.2
G4	0.3 ± 0.1	0.5 ± 0.1
G5	0.2 ± 0.1	0.4 ± 0.1

All data presented as mean ± SD (n=3).). Data were analysed using one-way ANOVA followed by Scheffé's post hoc test. *A *p*-value < 0.05 was considered statistically significant compared with G3. G1, control diet (CD); G2, control diet with retinoic acid (CD + RA); G3, high-cholesterol diet (HCD); G4, high-cholesterol diet with vehicle (HCD + vehicle); G5, high-cholesterol diet with retinoic acid (HCD + RA).

CHAPTER FIVE

DISCUSSION

5.1 INTRODUCTION

Great advances have been made in understanding the mechanisms involved in the development of NAFLD, which opens new avenues for therapeutic interventions. Recent research has highlighted novel strategies targeting lipid metabolism, inflammation, oxidative stress, gut microbiota, and fibrogenic pathways. Experimental studies and clinical trials are now evaluating agents such as FXR agonists, PPAR modulators, GLP-1 receptor agonists, antioxidants, and agents modulating lipid synthesis enzymes. In March 2024, the first FDA-approved drug called resmetirom was used for NASH patients in clinical trials, and early data have shown promising results, with reported side effects including diarrhoea, nausea, itching, stomach pain, vomiting, dizziness, and constipation. Meanwhile, long-term safety studies to identify the potential adverse effects that are not apparent in the initial stages are yet to be determined. Moreover, the rising prevalence of disease worldwide has increased the demand for effective treatment strategies to address the increasing burden of NAFLD.

Additionally, the incidence of vitamin A deficiency globally was estimated to be 489 million cases in 2019 (Liang et al., 2025), further supporting the rationale for exploring the retinoid-based intervention. Therefore, this study was designed to demonstrate the therapeutic role of retinoic acid on the NAFLD animal model through the DGAT2 enzyme. The aim was to prevent the progression of NAFLD by reducing the triglyceride deposition in the liver. As shown in this study, retinoic acid reduced the body weight and liver weight in HCD animals treated with retinoic acid compared to untreated HCD animals. More importantly, in this study, the liver content of triglyceride was reduced and histopathological features also supported this finding.

The prevalence of NAFLD varies worldwide; however, it is particularly high among obese individuals. A recent meta-analysis reported that 80-90% of patients with NAFLD are obese (Targher et al., 2024). Therefore, obesity is a major risk factor for

the development of NAFLD. In this study, a 12% cholesterol diet resulted in an increase in body weight and liver weight as early as 4 weeks of feeding, whereas the body weight of mice fed on 1% cholesterol diet was not increased compared to the control diet even after 30 weeks of feeding (Savard et al., 2013). In the same study, the 1% cholesterol diet only produced a slight increase in liver weight (1.6 ± 0.5 g) compared to controls (1.2 ± 0.1 g). By contrast, the animal model developed by Abdul Rahim et al., (2019) revealed a significant increase in relative liver weight when fed Sprague-Dawley (SD) rats with 1% cholesterol diet for 14 weeks.

5.2 PHASE 1 – ESTABLISHMENT OF NAFLD ANIMAL MODEL

The present pilot study using a 12% cholesterol diet successfully produced obesity in SD rats in a shorter time compared to 1% cholesterol diet. Moreover, the healthy liver in control diet animals is characteristically deep reddish-brown, while the 12% HCD model induces a progressive colour change; with the liver shifting to a mottled, light yellow appearance. This is consistent with histological evaluation of liver tissue, as all rats fed on HCD for 4 weeks developed grade I steatosis (5-33%). The addition of 3 g of cholic acid per kilogram of diet may have accelerated hepatic cholesterol accumulation and inflammation, thereby promoting the rapid progression from simple steatosis to NASH. In line with our result, SD rats fed on HCD and 2% cholic acid developed NASH after 9 weeks, along with increased body weight and liver weight (Ichimura-shimizu, Watanabe, Kashirajima, Nagatomo, & Wada, 2022).

Additionally, another rat model of NAFLD developed stage one steatosis at 4 weeks when animals were fed on a diet containing 15% fat and 1% cholesterol (Maciejewska et al., 2019), which corresponds with the result of this research. Meanwhile, NASH developed later, after 12 weeks of feeding the rats with HFD-HCD (15% fat and 1% cholesterol). These findings suggest that a 12% HCD diet can drive non-alcoholic steatohepatitis (NASH) earlier than a high-fat diet (HFD) because it rapidly triggers the hepatic inflammation. Moreover, our pilot study demonstrated an even earlier progression of NAFLD from simple steatosis at 4 weeks to NASH at 5 and 6 weeks.

Remarkably, a cohort study including 4013 patients with NAFLD demonstrated that 77% of patients developed rapid progression to end-stage liver disease within 0.5 to 3 years (Schattenberg et al., 2024). Consequently, the rapid progression of NAFLD in our animal model may reflect the rapid disease progression observed in a subgroup of patients with NAFLD. However, human disease progression is more variable and generally occurs over a longer period than in experimental animal models.

5.3 THE EFFECTS OF RA TREATMENT ON NAFLD

5.3.1 Body and Liver Weights

The pandemic of obesity worldwide has made NAFLD one of the leading causes of chronic liver disease. Weight loss through diet and exercise remains the cornerstone of therapy for NAFLD, and a recent study reported that weight reduction induces significant remission in patients with NASH (Fukuda, Okamoto, & Fukaishi, 2024).

In the present study, the HCD successfully induced obesity. Previous animal studies have demonstrated the effectiveness of oral, intraperitoneal and subcutaneous routes of RA administration, although differences in absorption and bioavailability may influence the therapeutic response. Oral administration is convenient but may be affected by gastrointestinal absorption and first-pass metabolism, whereas intraperitoneal administration may produce relatively rapid systemic exposure. Subcutaneous administration was selected in the present study because it enabled accurate and consistent dosing, avoided gastrointestinal and first-pass effects, and was suitable for repeated administration throughout the treatment period.

RA treatment significantly decreased body weight gain, with G5 showing 20% lower body weight compared with the other HCD groups (G3 and G4). A similar finding has been reported recently. The synthetic retinoid, fenretinide reduced body weight gain and adiposity in mice fed a high-fat, high-cholesterol diet (Thompson et al., 2023).

Likewise, RA treatment at 15 mg/kg/day prevented and even reversed obesity in mice fed a high-fat, high-cholesterol, and high-fructose diet for 16 weeks (Bawa et al., 2022).

Consistent with these findings, Mori et al. (2024) also reported 10% reduction in body weight in mice fed a control diet and treated with 10 mg/kg of RA for 4 weeks. These findings support the effect of RA on weight loss. Furthermore, the possible mechanism underlying the effect of RA in mitigating the body and liver weights may be related to its effect on lipid metabolism at the cellular level by increasing lipid burning through enhancing hepatic lipid oxidation and decreasing TG synthesis (Bawa & Zhang, 2023).

Notably, the present study showed that treatment with RA decreased liver weight and relative liver weight in HCD rats. In addition, oral administration of RA (50 mg RA per kilogram of diet) to high-fat diet rats for 8 weeks also demonstrated weight loss (Zhu et al., 2022).

Triglyceride accumulation in the cytoplasm of hepatocytes is a hallmark of NAFLD. As expected, TG levels were elevated in the HCD group and the HCD plus vehicle group but were attenuated by RA treatment in G5, as confirmed by histological examination. These results suggest that the reduction in liver triglyceride content might also contribute to the lower body weight observed in RA-treated rats. Furthermore, RA could exert its therapeutic effect on NAFLD not only by reducing hepatic TG accumulation but also by influencing systemic lipid metabolism. In line with our results, other studies have reported diminished liver TG content in NAFLD animals treated with RA. Bawa et al., (2022) reported a 67% reduction in hepatic TG levels in mice fed a high-fat, high-cholesterol diet and treated with RA (15 mg/kg) for 16 weeks. Consistent with these findings, Zhu et al. (2022) reported reduced hepatic TG content, and the synthetic retinoid (fenretinide) also decreased hepatic TG levels in NAFLD mice (Thompson et al., 2023).

5.3.2 Liver Enzymes

Alanine transaminase (ALT/SGPT) and aspartate transaminase (AST/SGOT) are two dependable biomarkers for hepatocellular injury (Chalasani et al., 2012); AST is also found in extrahepatic tissues such as skeletal muscle, kidney, cardiac muscle, brain, pancreas, lungs, leukocytes, and erythrocytes, whereas ALT is predominantly found in the liver and is therefore more liver-specific (Jastrzebski, Zychowska, Radziminski, Konieczna, & Kortas, 2015). Elevated serum levels of ALT and AST are the most common biochemical abnormalities in liver function tests and are considered a hallmark of non-alcoholic fatty liver disease. Another enzyme marker for liver disease is alkaline phosphatase (ALP), which is found in the serum and on the cell surface of the liver, bone, intestine and placenta tissue. A human study reported that an elevated ALP levels were associated with metabolic syndrome and NAFLD (Sohrabi et al., 2023). However, because AST and ALP are not liver-specific, the present study focused on ALT as a more specific marker of hepatocellular injury.

Unexpectedly, serum ALT was not raised in all HCD-fed animals when compared to controls, despite noticeable histopathological and other biochemical changes observed in the NAFLD groups. One possible explanation, as suggested by Zhu et al. (2022), is that intracellular hepatic enzyme levels may increase in NAFLD animals without a corresponding elevation in serum liver enzymes and may subsequently decrease following RA treatment. In the present study, serum ALT was measured rather than the intracellular hepatic enzyme levels. Serum ALT concentrations may also be influenced by the timing of blood collection relative to hepatocellular injury and enzyme clearance. As ALT is a lagging biomarker whose circulating concentration reflects both enzyme release and plasma clearance, a single measurement may not fully represent the extent or timing of ongoing hepatocellular injury (Sherman & Goessling, 2024**)**. A human study reported that the level of ALT is an imperfect biomarker for identifying histological inflammation and can be normal in patients with cirrhosis (Lominadze & Kallwitz, 2018). This may explain the normal ALT level despite advanced histopathological changes in the NAFLD animals that did not receive RA treatment. Moreover, differences in the animal model, timing of sample collection, disease severity and grade of NAFLD may have contributed to this finding.

On the other hand, it's been reported that treatment with synthetic retinoids leads to a number of biochemical and pathological changes in the liver due to their tendency to concentrate in it. One of its adverse effects reported in rats is the elevation of serum liver enzymes (Abass & Al-Harbi, 2022). However, it is important to note that the RA dose used in our study was far below the reported LD_{50} for mice (2200 mg/kg). Nevertheless, all animals treated with RA survived the whole duration of the experiment and did not report any signs of distress. Signs of RA toxicity, such as bone fracture, subcutaneous, internal haemorrhage, dry scaly skin and no hair thinning, were not observed (Howard and Willhite 1986).

5.3.3 Serum Lipid Profile

Non-alcoholic fatty liver disease (NAFLD) has recently been proposed to be renamed as metabolic-associated fatty liver disease (MAFLD), reflecting its strong association with the metabolic dysregulation, which includes impaired glucose metabolism or type 2 diabetes, dyslipidaemia, high blood pressure and obesity (Heida, 2023). Early diagnosis and treatment of NAFLD would prevent the progression of the disease into complicated conditions such as NASH. Dyslipidaemia is a central feature of the disease and one of the key manifestations of NAFLD. Dyslipidaemia includes high serum levels of triglycerides, total cholesterol, low-density lipoprotein (LDL), and reduced high-density lipoprotein (HDL). Therefore, investigation of serum lipid profile is an important parameter to determine the therapeutic efficacy of potential drugs used in treating NAFLD.

Our research results showed RA improved TG concentration in the blood, although this did not reach a statistically significant level. In contrast, no change in serum total cholesterol was observed. In contrast to our finding, Zhu et al. (2022) observed a decrease in serum cholesterol without changes in serum TG of NAFLD mice treated with RA. This discrepancy might be attributed to differences in the animal models or species, RA dosage, treatment duration, route of administration, baseline lipid levels and severity of NAFLD. Similarly, Zareia et al. (2020) reported a decrease in serum cholesterol only, without changes in serum TG, which may also be attributable to differences mentioned earlier.

In comparison, our findings were in agreement with those reported by Thompson et al. (2023) and Mori et al. (2024). Thompson et al. (2023) reported that serum cholesterol did not significantly change in HFD-HCD fed mice treated with fenretinide, a synthetic derivative of RA, whereas serum TG was significantly reduced. The greater reduction in serum TG reported in that study may be related to the use of fenretinide, which may differ from RA in its pharmacological activity, bioavailability and effects on lipid metabolism. This was also consistent with Mori. et al. (2024), who treated mice with RA at 10mg/kg body weight for 4 weeks. Differences in species, dietary composition, dose and treatment response may explain why the reduction in serum TG reached statistical significance in those studies but not in the present study. This suggests that RA or its derivative selectively reduce serum triglyceride, but not serum cholesterol. Specifically, this supports that RA controls hepatic fatty acid and TG metabolism but has a less direct effect on circulating cholesterol.

Despite no significant difference in serum TG among all animal groups, serum total cholesterol was significantly higher in all animal groups fed the HCD diet (G3, G4 and G5) compared to the control diet groups (G1 and G2). A high-cholesterol diet was successfully effective in inducing hypercholesterolaemia in all NAFLD rat models.

5.3.4 Gross and Microscopic Hepatic Changes

The gross hepatic changes in this research were in line with the report by Zhu et al. (2022), who demonstrated the beneficial effect of RA in reducing fat accumulation in the liver, as confirmed by tissue TG levels.

Currently, liver biopsy is considered the gold standard for the direct measurement of liver fat and the only reliable method for diagnosing fatty liver disease. Consistent with this, the histology of NAFLD liver tissue revealed fatty liver changes which resulted in increased liver mass. Moreover, prominent fatty deposition was observed in the centrilobular region (zone 3), as demonstrated by H&E staining and confirmed by ORO staining in all HCD-fed animals. Additionally, fibrotic changes were prominent around the portal area, corresponding to zone 1, as demonstrated by MT

staining. Meanwhile, this fat deposition within hepatocytes was reduced by about half in response to RA in G5, as quantified by image analysis software. This reduction was supported by findings from steatosis image scoring and tissue TG measurements in G5, both of which showed nearly a 50% decrease compared with the HCD group. The reduced steatosis was also accompanied by a lower NAS score and decreased hepatic DGAT2 expression, indicating improvements in overall histological severity and triglyceride synthesis. These findings confirm that the main effect of RA was the reduction of hepatic TG content. Our results align with those of the recent study by Thompson et al. (2023), who descriptively reported a decrease in hepatic lipid droplet formation and intracellular hepatic TG content in response to fenretinide, a retinoid derivative, in NAFLD mice. Another semi-quantitative study by Zareia et al. (2020) reported hepatic steatosis decreased by 62% (92.7 ±1.4 vs 32.5 ± 7.7) in an NAFLD rabbit model treated with RA compared with untreated animals. Differences in the percentage of steatosis reduction in response to RA treatment may be explained by variations in animal models, RA dosages and routes of administration.

5.3.5 Non-Alcoholic Activiy Score (NAS)

Although many studies have focused on various aspects of NAFLD and vitamin A, few have assessed the histopathological changes semi-quantitatively by applying the grading system of NAFLD in response to RA treatment. Zarei et al. (2020) treated a rabbit model of NAFLD with RA, describing a considerable decrease in the steatosis score from 3 in HCD rabbits to 1 in RA-treated NAFLD rabbits, although the other categories of the NAS score were not reported. Similarly, a study by Lim et al. (2019) demonstrated that oral administration of provitamin A (xanthophyll carotenoid) to NAFLD mice reduced the steatosis score to 2 in the supplemented group, compared to a score of 3 in untreated NAFLD mice. However, the authors did not describe the inflammatory and cell ballooning scores in this study. The differences in the reported reduction of NAS steatosis scores across studies could be attributed to differences in the animal model, dosage, administration route, treatment form, and duration of treatment.

5.3.6 Oil Red O Staining

Oil Red O (ORO) stain is a specific stain used widely to detect neutral lipids, mainly triglycerides, within tissue. In NAFLD, ORO staining provides visual evidence of hepatic steatosis. It can also be used to estimate the extent of lipid accumulation in liver tissue. In this study, ORO staining was used to indicate the presence of hepatic steatosis in HCD-fed animal groups. RA treatment reduced lipid deposition in liver tissue, as evidenced by decreased staining intensity, indicating fewer lipid droplets within hepatocytes. This finding reflects the effectiveness of RA in ameliorating hepatic steatosis. Our results are in agreement with those reported by Thompson et al. (2023) and Bawa et al. (2022). Similarly, Oil Red O staining and Azan staining showed a substantial increase in the areas of steatosis and fibrosis in the liver of peretinoin-treated NAFLD mice (Okada et al., 2017).

5.3.7 Masson's Trichrome (MT) Staining

Masson's Trichrome staining is a specialised histological stain used to assess the collagen deposition in tissue. As NAFLD has a wide disease spectrum, it includes simple steatosis, which, if left untreated, progresses to steatohepatitis, fibrosis and eventually cirrhosis. Vitamin A is closely related to NAFLD as the liver is the main storage site of vitamin A, and quiescent hepatic stellate cells become activated into cells responsible for fibrogenesis. Hepatic stellate cells become profibrogenic when they lose their vitamin A content. Serum RA levels have been shown to be the lowest in NASH patients with fibrosis compared to simple steatosis patients. Therefore, the degree of fibrosis inversely correlated with serum retinoic acid (Allam et al., 2020).

In the present study, MT staining was used to assess fibrotic changes in NAFLD liver tissue and to evaluate the therapeutic efficacy of RA. Collagen deposition was evident in all HCD-fed animals, whereas RA treatment resulted in noticeable reductions in fibrotic changes. These findings were in agreement with the findings of a molecular study from the NASH model, where an RA receptor agonist demonstrated anti-fibrotic effects (Tang et al., 2021). Similarly, a human study reported a negative association between serum retinol and fibrosis (Niu et al., 2023).

5.3.8 Immunohistochemistry for DGAT2 Enzyme

Diacylglycerol O-acyltransferase 2 (DGAT2) is a key regulatory enzyme for triglyceride synthesis in the liver. As triglyceride accumulation in hepatocytes represents the main pathological feature of NAFLD, and effective pharmacological treatments remain limited, DGAT2 has been proposed as an attractive therapeutic target. Therefore, many studies have investigated this enzyme as a target for treating NAFLD (Badi, Mostafa, Khaleel, & Satti, 2019). In an animal study, a specific DGAT2 inhibitor was investigated for its potential to reverse NAFLD (Amin et al., 2019).

In the present study, the expression of DGAT2 was markedly elevated in the NAFLD rat model. RA treatment significantly reduced hepatic DGAT2 expression, which was in line with the decrease in hepatic triglyceride content and serum TG. This was also consistent with the reduction in hepatic steatosis, which is mainly due to TG accumulation and the improvement in the NAS score in the RA-treated animal group. These parallel changes suggest that RA may reduce hepatic triglyceride synthesis, at least partly, through reduced DGAT2 expression. Reduced DGAT2 activity would be expected to limit the final step of triglyceride synthesis, thereby decreasing lipid accumulation within hepatocytes and consequently improving steatosis, hepatocyte ballooning and inflammation. However, as DGAT2 activity and its upstream regulatory pathways were not directly measured, the present findings demonstrate an association rather than confirm a causal mechanism. These findings are noteworthy in light of recent clinical data, where pharmacological inhibition of DGAT2 using ervogastat was shown to reduce hepatic steatosis in NAFLD patients (Amin. et al., 2023). Future studies should therefore assess DGAT2 mRNA and protein expression, enzymatic activity and relevant upstream pathways, such as RAR/RXR-mediated transcription, fatty acid oxidation and de novo lipogenesis, to confirm the mechanism by which RA regulates hepatic triglyceride metabolism.

5.3.9 Scanning Electron Microscopy of Hepatocytes and LSECs

A scanning electron microscope was used to assess ultrastructural changes in the morphology of hepatocytes and LSECs in NAFLD models and the treated group. Hepatic endothelial cells are specialised cells because they lack a basement membrane and have fenestrae arranged in sieve plates that control the transport of macromolecules, including lipids and lipoproteins, between the sinusoid and hepatocytes (Erhaegh et al., 2021). LSECs play an important role in the immune system and in the clearance of bioactive substances produced by bacteria and viruses through recognition and phagocytosis (Zhou, Wang, Zhang, & Zhang, 2025).

LSEC defenestration reduces the permeability of hepatic sinusoids, leading to increased portal vein pressure. Defenestration of LSECs in NAFLD has been explained by oxidative stress, which drives disruption of the fenestration structure through the overproduction of reactive oxygen species, leading to inflammatory responses and fibrosis. ultimately resulting in LSEC defenestration (Zhou et al., 2025). The regulation of LSEC fenestrations was investigated, and the nitric oxide (NO) pathway was found to be the most important mediator of hepatic fenestration (Szafranska et al., 2021). Elevated levels of reactive oxygen species, which are products of oxidative stress, react with NO to generate reactive nitrogen species, thereby decreasing the bioavailability of NO and simultaneously impairing its function (Zhou et al., 2025).

Recently, LESCs have gained increasing attention in NAFLD research, with some evidence suggesting that defenestration may represent one of the initial pathological manifestations. Besides that, RA has shown histopathological improvement in NAFLD models, and different mechanisms have been suggested. Nevertheless, changes in sinusoidal porosity and fenestration frequency in response to RA in NAFLD models have not been clearly established. Therefore, this study aimed to determine the effect of RA on LSEC porosity anf fenestration.

In the control diet groups, the fenestrae were clearly seen in the sinusoids, with an estimated density of more than three fenestrae per square micron of sinusoidal surface. This was comparable to a previous report in mice, where fenestration frequencies in rat hepatic sinusoids closely matched those in mice (4.55 ± 0.34) (Hunt

et al., 2019). Similarly, the porosity percentage in the control group was 2.3% ± 0.3, corresponding to the reported range in rats, which is 2.5% to 4.1% (Couteur et al., 2008). In contrast, HCD-fed animals showed a marked reduction in fenestrae frequency and porosity compared with the control diet groups, consistent with defenestration of hepatic sinusoids (Jung et al., 2024; Moon, 2019). However, no improvement in sinusoidal porosity or fenestration frequency was observed in response to RA-treated HCD-fed animals. Despite the beneficial effect of retinoic acid on histopathological features and partial preservation of hepatocyte polygonal shape, defenestration of the endothelium was not restored.. This could be attributed to the insufficient duration of RA exposure, or to the possibility that defenestration in hepatic endothelial cells at this stage of NAFLD was irreversible.

5.4 LIMITATIONS OF THE STUDY

While the findings of this research contributed valuable insights into the role of retinoic acid in the NAFLD animal model, certain experimental limitations should be considered. One of the study limitations is the use of a cholesterol diet to induce NAFLD, which might not fully mimic the complex metabolic characteristics of human NAFLD. This animal model did not reveal increased ALT enzyme levels in all HCD models of NAFLD despite progressive histopathological changes. Therefore, the use of other animal models that have correlated biochemical and histopathological findings should be considered.

Another limitation is the subjective variability due to differences in researchers' techniques, optimisation of tissue processing protocols, interpretation of histological assessment based on the researcher's skills, and maintaining standardised sampling. Recognising the reliance on researcher expertise, strict protocols and comprehensive training were implemented to reduce bias and improve the reliability of histological data. These acknowledged limitations should be taken into account when interpreting and extrapolating the results. Future research efforts should focus on overcoming these challenges to provide a deeper and more comprehensive understanding of the complexity of NAFLD.

CHAPTER SIX

CONCLUSION

This study evaluated the therapeutic effects of retinoic acid (RA) on triglyceride metabolism, DGAT2 expression and hepatic changes in a high-cholesterol diet (HCD)-induced NAFLD rat model. Phase 1 confirmed that four weeks of HCD feeding was sufficient to induce simple hepatic steatosis, providing a suitable model for evaluating RA treatment.

In Phase 2, RA treatment limited body weight gain and reduced liver weight compared with untreated HCD-fed animals, suggesting a protective effect against diet-induced metabolic alterations. Hepatic TG content was significantly reduced with RA, although serum TG and cholesterol level did not show significant improvement, suggesting that RA acts mainly at the hepatic level rather than through systemic lipid clearance.

Histopathological analyses demonstrated that RA improved liver architecture by reducing steatosis, inflammation, ballooning degeneration, and fibrosis, as reflected by H&E, Oil Red O, Masson's trichrome staining, together with lower NAFLD activity scores. Importantly, immunohistochemical staining revealed that RA reduced hepatic DGAT2 expression in HCD-fed animals. This suggests a link between RA and triglyceride regulation at the tissue level, although more detailed molecular studies would be required to confirm the underlying mechanism. This result provides a new understanding of how RA works and indicates that DGAT2 may serve as an important therapeutic target.

At the ultrastructural level, RA improved hepatocyte morphology and reduced fibril deposition, consistent with histological findings. Despite these improvements, RA did not significantly improve liver sinusoidal endothelial cell (LSEC) fenestration or porosity. Although porosity was consistently lower in HCD-fed animals compared to controls, RA did not reverse this effect, indicating that its hepatoprotective action is

more likely mediated through changes in hepatocellular lipid handling rather than through sinusoidal clearance.

Taken together, these findings suggest that RA may prevent disease progression from steatosis to steatohepatitis (NASH) by mitigating TG accumulation, inflammation, and fibrosis, supported by its effect on DGAT2 expression.

These findings provide a basis for future studies investigating the molecular mechanisms underlying the effects of RA on DGAT2 expression. Further research should evaluate longer treatment durations, combination therapies and different RA doses to determine the minimum effective dose that achieves the optimal therapeutic response. Additional molecular studies are also required to clarify why RA showed limited efficacy in reversing LSEC defenestration. Although the present findings are promising, clinical studies are needed to determine the safety and therapeutic potential of RA in patients with NAFLD.

REFERENCES

Abass, Z. M., & Al-Harbi, H. J. (2022). Estimation of Some Biomarkers of Liver Damage And Its Tissue In Male Albino Rats Treated With Isotretinoin At Different Periods. *International Journal of Health Sciences*, *6*(April), 9328–9334. https://doi.org/doi.org/10.53730/ijhs.v6nS5.11942

Abbott, N. J., Abdelhadi, S. I., Abraham, D. J., Abraham, M. H., Abrahamsson, B., Acher, F. C., Avery, M. A. (2007). *Comprehensive Medicinal Chemistry II*. (J. B. Taylor & D. J. Triggle, Eds.) (2nd Editio). Buffalo, USA: Elsevier.

Abdul Rahim, R., Ghani, A. S. A., Muhammad, N., Abdullah, N. Z., & Ramli, N. (2019). Non alcoholic Steatohepatitis Animal Model Induction. *World Journal of Pharmcy and Pharmaceutical Sciences*, *8*(4), 1523–1538. https://doi.org/10.20959/wjpps20194-13542

Abe, K., & Kogure, K. (1986). Accurate Evaluation of 1, 2-Diacylglycerol in Gerbil Forebrain Using HPLC and In Situ Freezing Technique. *Journal of Neurochemistry*, *47*(2), 577–582. https://doi.org/https://doi.org/10.1111/j.1471-4159.1986.tb04538.x

Abràmoff, M. D., Magalhães, P. J., & Ram, S. J. (2004). Image Processing with ImageJ. *Biophotonics Interntional*, *11*(7), 36–42. https://doi.org/ISSN: 1081-8693

Abu-Freha, N., Cohen, B., Gordon, M., Weissmann, S., Fich, A., Munteanu, D., Etzion, O. (2023). Comorbidities and Malignancy among NAFLD Patients Compared to the General Population , A Nation-Based Study. *Biomedicines*, *11*(1110), 1–11. https://doi.org/https://doi.org/ 10.3390/biomedicines11041110

Adamantidi, T., Lafara, M., Venetikidou, M., Likartsi, E., Toganidou, I., & Tsoupras, A. (2025). Utilization and Bio-Efficacy of Carotenoids , Vitamin A and Its Vitaminoids in Nutricosmetics , Cosmeceuticals , and Cosmetics' Applications with Skin-Health Promoting Properties. *Applied Sciences*, *15*(1657). https://doi.org/https://doi.org/10.3390/app15031657

Allain, C. C., Poon, L. S., Chan, C. S. G., Richmond, W., & Fu, P. C. (1974). Enzymatic Determination of Total Serum Cholesterol. *Cenical Chemistry*, *20*(4), 470–475. https://doi.org/https://doi.org/10.1093/clinchem/20.4.470

Allam, A. S., Salama, M. M., Nasser, H. M., Kabiel, W. A. Y., & Elsayed, E. H. (2020). Comparison between NAFLD fibrosis score and retinoic acid serum level in NAFLD. *Egyptian Liver Journal*, *10*(2), 1–7. https://doi.org/10.1186/s43066-019-0014-7

Amengual, J., Ribot, J., Bonet, M. L., & Palou, A. (2010). Retinoic acid treatment enhances lipid oxidation and inhibits lipid biosynthesis capacities in the liver of mice. *Cellular Physiology and Biochemistry*, *25*(6), 657–666. https://doi.org/10.1159/000315085

Amin, N. B., Carvajal-Gonzalez, S., Purkal, J., Zhu, T., Crowley, C., Perez, S., Goodwin, B. (2019). Targeting diacylglycerol acyltransferase 2 for the treatment of nonalcoholic steatohepatitis. *Science Translational Medicine*, *11*(520), 1–13. https://doi.org/10.1126/scitranslmed.aav9701

Amin, N. B., Darekar, A., Anstee, Q. M., Wong, V. W.-S., Tacke, F., Vourvahis, M., Yunis, C. (2022). Efficacy and safety of an orally administered DGAT2 inhibitor alone or targeted ACC coadministered with inhibitor in adults with non-alcoholic steatohepatitis (NASH): Rationale and design of the phase II , dose controlled . *British Medical Journal*, *12*, 1–11. https://doi.org/10.1136/bmjopen-2021-056159

Amin, N. B., Saxena, A. R., Somayaji, V., & Dullea, R. (2023). Inhibition of Diacylglycerol Acyltransferase 2 Versus Diacylglycerol Acyltransferase 1 : Potential Therapeutic Implications of Pharmacology. *Clinical Therapeutics*, *45*(1), 55–70. https://doi.org/10.1016/j.clinthera.2022.12.008

Animal Welfare Board. (2020). *Malaysian code of practice for the care and use of animals for scientific purposes (MYCODE)* (2nd ed.). Department of Veterinary Services Malaysia.

Babboni, S.; Vacca, P.G.; Simonini, L.; Pezzati, D.; Martinelli, C.; Frongillo, F.; Bianco, G.; Marciano, E.; Basta, G.; Ghinolfi, D.; et al. Cholangiocyte Organoids: The New Frontier in Regenerative Medicine for the Study and

Treatment of Cholangiopathies. J. Clin. Med. 2024, 13, 1804. https://doi.org/10.3390/ jcm13061804 Academic

Badi, R. M., Mostafa, D. G., Khaleel, E. F., & Satti, H. H. (2019). Resveratrol protects against hepatic insulin resistance in a rat's model of non - alcoholic fatty liver disease by down - regulation of GPAT - 1 and DGAT2 expression and inhibition of PKC membranous translocation. *Clinical and Experimental Pharmacology and Physiology*, *46*, 545–555. https://doi.org/10.1111/1440-1681.13074

Banales, J. M., Huebert, R. C., Karlsen, T., Strazzabosco, M., LaRusso, N. F., & Gores, G. J. (2019). Cholangiocyte pathobiology. *Nature Reviews Gastroenterology & Hepatology*, *16*, 269–281. https://doi.org/10.1038/s41575-019-0125-y

Bawa, F. N. C., Xu, Y., Gopoju, R., Plonski, N.-M., Shiyab, A., Hu, S., Zhang, Y. (2022). Hepatic retinoic acid receptor alpha mediates all- - trans retinoic acid 's effect on diet- induced hepatosteatosis. *Hepatology Communications*, *6*(February), 2665–2675. https://doi.org/10.1002/hep4.2049

Bawa, F. N. C., & Zhang, Y. (2023). Retinoic Acid Signaling in Fatty Liver Disease *Liver Research*, *7*(3), 189–195. https://doi.org/10.1016/j.livres.2023.07.002

Benedict, M., & Zhang, X. (2017). Non-alcoholic fatty liver disease: An expanded Review. *World Journal of Hepatology*, *9*(16), 715–732. https://doi.org/DOI: 10.4254/wjh.v9.i16.715

Bieghs, V., Gorp, P. J. Van, Wouters, K., Hendrikx, T., Gijbels, M. J., Van, M., Lutjohann, D. (2012). LDL Receptor Knock-Out Mice Are a Physiological Model Particularly Vulnerable to Study the Onset of Inflammation in Non-Alcoholic Fatty Liver Disease. *PLOS ONE*, *7*(1), 1–11. https://doi.org/10.1371/journal.pone.0030668

Blaner, W. S., Byrne, S. M. O., Wongsiriroj, N., Kluwe, J., Ambrosio, D. M. D., Jiang, H., Libien, J. (2009). Hepatic Stellate Cell Lipid Droplets : A Specialized Lipid Droplet For Retinoid Storage. *Molecular and Cell Biology of Lipids*, *1791*(6), 467–473. https://doi.org/10.1016/j.bbalip.2008.11.001

Borén, J., & Taskinen, M.-R. (2021). *Prevention and Treatment of Atherosclerosis*. (A.

von Eckardstein & C. J. Binder, Eds.) (270th ed.). Cham, Switzerland: Springer.

Boyde, A., & Wood, C. (1969). Preparation of Animal Tissues for Surface-Scanning Electron Microscopy. *Journal of Microscopy*, *90*(December), 221–249.

Brown, G. T., & Kleiner, D. E. (2015). Histopathology of Nonalcoholic Fatty Liver Disease and Nonalcoholic Steatohepatitis. *Metabolism Clinical and Experimental*, *65*(8), 2–23. https://doi.org/10.1016/j.metabol.2015.11.008

Brunt, E. M., Janney, C. G., Bisceglie, A. M. Di, Neuschwander-Tetri, B. A., & Bacon, B. R. (1999). Nonalcoholic Steatohepatitis : A Proposal for Grading and Staging the Histological Lesions, *94*(9).

Brunt, E. M., Kleiner, D. E., Carpenter, D. H., Rinella, M., Harrison, S. A., Loomba, R., J., S. A. (2021). NAFLD : Reporting Histologic Findings in Clinical Practice. *Hepatology*, *73*(5), 2028–2038. https://doi.org/10.1002/hep.31599

Buzzetti, E., Pinzani, M., & Tsochatzis, E. A. (2016). The multiple-hit pathogenesis of non-alcoholic fatty liver disease (NAFLD). *Metabolism: Clinical and Experimental*, *65*(8), 1038–1048. https://doi.org/10.1016/j.metabol.2015.12.012

Caballero, F., Colell, A., Morales, A., Caballeria, J., Fernandez, A., Enrich, C., Garcı´a-Ruiz, C. (2006). Mitochondrial free cholesterol loading sensitizes to TNF- and Fas-mediated steatohepatitis. *Cell Metabolism*, *4*(September), 185–198. https://doi.org/10.1016/j.cmet.2006.07.006

Cain, O. L., & H€ubscher, S. G. (2019). Histological assessment of the liver Key points. *Medicine*, *47*(11), 707–712. https://doi.org/10.1016/j.mpmed.2019.08.006

Cao, Y., Deng, Y., Wang, J., Zhao, H., Zhang, J., & Xie, W. (2021). The Association Between NAFLD And Risk Of Chronic Kidney Disease : A Cross-Sectional Study. *Therapeutic Advances in Chronic Disease*, *12*, 1–15. https://doi.org/https://doi.org/10.1177/20406223211048649 20406223211048649

Cardiff, R. D., Miller, C. H., & Munn, R. J. (2014). Manual Hematoxylin and Eosin Staining of Mouse Tissue Sections. *Cold Spring Harbor Laboratory Press*,

2020(2), 655–658. https://doi.org/10.1101/pdb.prot073411

Carriel, V., Campos, F., Aneiros-Fernández, J., & Kiernan, J. A. (2017). Tissue Fixation and Processing for the Histological Identification of Lipids. In C. Pellicciari, M. Biggiogera, & M. Šahinović (Eds.), *Histochemistry of Single Molecules: Methods and protocols* (First Eidt, Vol. 1560, pp. 219–229). Switzerland: Humana Press. https://doi.org/10.1007/978-1-4939-6788-9

Catta-preta, M., Mendonca, L. S., Fraulob-aquino, J., Aguila, M. B., & Mandarim-de-lacerda, C. A. (2011). A Critical Analysis of Three Quantitative Methods Of Assessment Of Hepatic Steatosis In Liver Biopsies. *Virchows Arch*, *459*, 477–485. https://doi.org/10.1007/s00428-011-1147-1

Chalasani, N., & Szabo, G. (Eds.). (2015). *Alcoholic and Non-Alcoholic Fatty Liver Disease, Bench to Bedside*. Switzerland: Springer International Publishing. https://doi.org/10.1007/978-3-319-20538-0

Chan, A. W. H., Quaglia, A., Haugk, B., & Burt, A. (2014). *Atlas of Liver Pathology*. (L. Cheng, Ed.) (First Edit). New York, USA: Springer-Verlag New York Inc. https://doi.org/10.1007/978-1-4614-9114-9

Chaves, G. V., Pereira, S. E., Saboya, C. J., & Ramalho, A. (2008). Non-alcoholic Fatty Liver Disease and Its Relationship with the Nutritional Status of Vitamin A in Individuals with Class III Obesity. *Obesity Surgery*, *18*, 378–385. https://doi.org/10.1007/s11695-007-9361-2

Chaves, G. V., Pereira, S. E., Saboya, C. J., Spitz, D., Rodrigues, C. S., & Ramalho, A. (2014). Association Between Liver Vitamin A Reserves and Severity of Nonalcoholic Fatty Liver Disease in the Class III Obese Following Bariatric Surgery. *Obesity Surgery*, *24*, 219–224. https://doi.org/10.1007/s11695-013-1087-8

Chen, W., & Chen, G. (2014). The Roles of Vitamin A in the Regulation of Carbohydrate , Lipid , and Protein Metabolism. *Journal of Clinical Medicine*, *3*(2014), 453–479. https://doi.org/10.3390/jcm3020453

Chen, Z., Liu, J., Zhou, F., Li, H., Zhang, X., She, Z., Li, H. (2021). Nonalcoholic Fatty

Liver Disease: An Emerging Driver of Cardiac Arrhythmia. *Circulation Research Review*, *128*, 1747–1765. https://doi.org/10.1161/CIRCRESAHA.121.319059

Christie, W. W. (1993). Preparation Of Lipid Extracts From Tissues. *Advances in Lipid Methodology*, *4*, 195–213.

Cogger, V.C., Hunt, N. J., & Le. Couteur, D. G. (2020). Fenestrations in The Liver Sinusoidal Endothelial Cell (2020). *The Liver: Biology and Pathobiology*. https://doi.org/DOI:10.1002/9781119436812

Cogger, V. C., Mohamad, M., Solon-Biet, S. M., Senior, A. M., Warren, A., Reilly, J. N. O., Dg, L. C. (2016). Macronutrients and The Aging Liver Sinusoidal Endothelial Cell. *American Journal of Physiology-Gastrointestinal and Liver Physiology*, *310*(26), 1064–1070. https://doi.org/10.1152/ajpheart.00949.2015

Cogger, V. C., Reilly, J. N. O., Warren, A., & Couteur, D. G. Le. (2015). A Standardized Method for the Analysis of Liver Sinusoidal Endothelial Cells and Their Fenestrations by Scanning Electron Microscopy. *Journal of Vesualized Experiments*, *98*(April), 1–9. https://doi.org/10.3791/52698

Collins, V. P., Arborgh, B., & Brunk, U. (1977). A comparison of the effects of three widely used glutaraldehyde fixatives on cellular volume and structure: A TEM, SEM, volumetric and cytochemical study. *Acta Pathologica et Microbiologica Scandinavica. Section A*, *85*, 157–168.

Cotoi, C. G., & Quaglia, A. (2016). *Normal Liver Anatomy and Introduction to Liver Histology*. (D. B. Stefano Guandalini, Anil Dhawan, Ed.) (First Edit). Berlin, Germany: Springer Nature Link. https://doi.org/10.1007/978-3-319-17169-2

Couteur, D., Warren, A., Cogger, V. C., Smedsrød, R. D., Sørensen, K. K., Cabo, R. D. E., Mccuskey, R. S. (2008). Old Age and the Hepatic Sinusoid. *The Anatomical Record*, *683*(December 2007), 672–683. https://doi.org/10.1002/ar.20661

Dawson, M. I., & Okamura, W. H. (1990). *Chemistry and Biology of Synthetic Retinoids*. (M. I. Dawson & W. H. Okamura, Eds.) (First Edit). Taylorand Francis: CRC Press.

Day, C. P., & James, O. F. W. (1998). Steatohepatitis: A Tale of Two "'Hits"'? *Gastroenterology*, *114*(4), 842–845.

Dunnington, K. (2021). *Drug Metabolism*. (Katherine Dunnington, Ed.) (20th ed.). Celerion, United States: IntechOpen. https://doi.org/10.5772/intechopen.91543

Duong, V., & Rochette-Egly, C. (2011). The molecular physiology of nuclear retinoic acid receptors . From health to disease. *Biochimica et Biophysica Acta*, *1812*(8), 1023–1031. https://doi.org/10.1016/j.bbadis.2010.10.007

Erhaegh, Pav. Isse, Edw, Unck, Toondem., Reve, J.anwig., Erheij, Jov, Iedl, R. Oek, Gerk. (2021). Electron microscopic observations in perfusion-fixed human non-alcoholic fatty liver disease biopsies. *Anatomical Pathology*, *53*(February), 220–228. https://doi.org/10.1016/j.pathol.2020.07.018

Esteban-pretel, G., Marı, M. P., Cabezuelo, F., Renau-piqueras, J., Timoneda, J., & Barber, T. (2010). Vitamin A Deficiency Increases Protein Catabolism and Induces Urea Cycle Enzymes in Rats. *The Journal of Nutrition and Disease*, *140*(4), 792–798. https://doi.org/10.3945/jn.109.119388.Recently

Estes, C., Chan, H. L. Y., Chien, R. N., Fung, J., Goh, G. B., Hu, T. H., Razavi, H. (2020). Modelling NAFLD disease burden in four Asian regions — 2019-2030. *Alimentary Pharmacology & Therapeutics*, *51*(February), 801–811. https://doi.org/10.1111/apt.15673

Fiorini, R. N., Kirtz, J., Periyasamy, B., Evans, Z., Haines, J. K., Cheng, G., Chavin, K. D. (2004). Development of an unbiased method for the estimation of liver steatosis. *Clinical Transplantaion*, *18*, 700–706. https://doi.org/10.1111/j.1399-0012.2004.00282.x

Folch, J., Lees, M., & Sloane Stanley, G. H. (1956). A simple Method for the Isolation and Purification of Total Lipids from Animal Tissues. *Journal of Biological Chemistry*, *226*(1), 497–509.

Fossati, P., & Prencipe, L. (1982). Serum Triglycerides Determined Colorimetrically with an Enzyme That Produce Hydrogen Peroxide. *Clinical Chemistry*, *28*(10), 2077–2080.

Fukuda, T., Okamoto, T., & Fukaishi, T. (2024). Extent to which weight loss contributes to improving metabolic dysfunction- associated and metabolic and alcohol related/associated steatotic liver disease : a study on Japanese participants undergoing health checkups. *Frontiers in Endocrinology*, *15*(May), 1–11. https://doi.org/10.3389/fendo.2024.1392280

Geng, C., Xu, H., Zhang, Y., Gao, Y., Li, M., Liu, X., Gao, M., Wang, X., Liu, X., Fang, F.,& Chang, Y. (2017). Retinoic acid ameliorates high-fat diet-induced liver steatosis through sirt1. *Science China Life Sciences*, *60*(11), 1234–1241. https://doi.org/10.1007/s11427-016-9027-6

Glaumann, H. (1975). Ultrastructural Demonstration of Phosphatases by Perfusion Fixation Followed by Perfusion Incubation of Rat Liver. *Histochemistry*, *44*, 169–178.

Gluchowski, N. L., Gabriel, K. R., Chitraju, C., Roderick, T., Mejhert, N., Boland, S., Walther, T. C. (2019). Hepatocyte Deletion of Triglyceride-Synthesis Enzyme Acyl CoA:Diacylglycerol Acyltransferase 2 Reduces Steatosis Without Increasing Inflammation or Fibrosis in Mice. *Hepatology*, *70*(6), 1972–1985. https://doi.org/10.1002/hep.30765.Hepatocyte

Gong, J., Tu, W., Liu, J., & Tian, D. (2023). Hepatocytes : A key role in liver infl ammation. *Frontiers in Immunology*, *13*(January), 1–9. https://doi.org/10.3389/fimmu.2022.1083780

Goor, H. Van, Gerrits, P. O., & Grond, J. (1986). The application of lipid-soluble stains in plastic-embedded sections. *Histochemistry and Cell Biology*, *85*(3), 251–253. https://doi.org/https://doi.org/10.1007/BF00494811

Gowda, D., Shekhar, C., Gowda, S. G. B., Chen, Y., & Hui, S. (2023). Crosstalk between Lipids and Non-Alcoholic Fatty Liver Disease. *Livers*, *3*, 687–708.

Grander, C., Grabherr, F., & Tilg, H. (2023). Non-alcoholic fatty liver disease : pathophysiological concepts and treatment options. *Cardiovascular Research*, *119*(9), 1787–1798. https://doi.org/10.1093/cvr/cvad095

Gugliucci, A. (2024). The chylomicron saga : time to focus on postprandial metabolism.

Frontiers in Endocrinology, *14*(January), 5–7. https://doi.org/10.3389/fendo.2023.1322869

Gurr, M., Frayn, K. N., & Frayn, K. N. (2008). *Lipid Biochemistry* (5 th). Oxford, UK: Blackwell Publishing.

Haaker, M. W., Vaandrager, A. B., & Helms, J. B. (2020). Retinoids in health and disease: A role for hepatic stellate cells in affecting retinoid levels. *Molecular and Cell Biology of Lipids*, *1865*(6), 1–13. https://doi.org/10.1016/j.bbalip.2020.158674

Heida, A. H. (2023). Liver disease: Exploring the role of novel candidates in the initiation and progression of Non-Alcoholic Fatty Liver Disease. *Andries Hendrik Heida*. University of Groningen. https://doi.org/10.33612/diss.649941239

Heyens, L. J. M., Busschots, D., Koek, G. H., Robaeys, G., & Francque, S. (2021). Liver Fibrosis in Non-alcoholic Fatty Liver Disease: From Liver Biopsy to Non-invasive Biomarkers in Diagnosis and Treatment. *Frontiers in Medicine*, *8*(April), 1–20. https://doi.org/10.3389/fmed.2021.615978

Houten, S. M., & Wanders, R. J. A. (2010). A general introduction to the biochemistry of mitochondrial fatty acid β -oxidation. *Journal of Inherited Metabolic Disease*, *33*, 469–477. https://doi.org/10.1007/s10545-010-9061-2

Hu, R., Yang, X., He, X., & Song, G. (2023). The relationship between NAFLD and retinol - binding protein 4 - an updated systematic review and meta - analysis. *Lipids in Health and Disease*, *22*(8), 1–13. https://doi.org/10.1186/s12944-022-01771-2

Huang, X., Choi, Y., Im, H., Yarimaga, O., Yoon, E., & Kim, H.-S. (2006). Aspartate Aminotransferase (AST/GOT) and Alanine Aminotransferase (ALT/GPT) Detection Techniques. *Sensors*, *6*(7), 756–782. https://doi.org/https://doi.org/10.3390/s6070756

Huang, Y., & Mahley, R. W. (2014). Apolipoprotein E: Structure and Function in Lipid Metabolism, Neurobiology, and Alzheimer's Diseases. *Neurobiology of*

Disease, *3*(12), 1–25. https://doi.org/10.1016/j.nbd.2014.08.025

Hunt, X. N. J., Lockwood, G. P., Warren, A., Mao, H., Mccourt, P. A. G., Couteur, D. G. Le, & Cogger, X. V. C. (2019). Manipulating fenestrations in young and old liver sinusoidal endothelial cells. *American Journal of Physiology-Gastrointestinal and Liver Physiology*, *316*, 144–154. https://doi.org/10.1152/ajpgi.00179.2018

Ibrahim, S. H., Hirsova, P., Malhi, H., & Gores, G. J. (2016). Animal Model of Nan alcoholic Fattty Liver Disease: Eat, Delete, Inflame. *Digestive Diseases and Sciences Journal*, *61*(5), 1325–1336. https://doi.org/10.1007/s10620-015-3977-1

Ichimura-shimizu, M., Watanabe, S., Kashirajima, Y., Nagatomo, A., & Wada, H. (2022). Dietary Cholic Acid Exacerbates Liver Fibrosis in NASH Model of Sprague – Dawley Rats Fed a High-Fat and High-Cholesterol Diet. *International Journal of Molecular Sciences*, *23*(3390), 1–11.

Ioannou, G. N. (2015). The Role of Cholesterol in the Pathogenesis of NASH. *Trends in Endocrinology & Metabolism*, *11*, 1–12. https://doi.org/10.1016/j.tem.2015.11.008

Iqbal, U., Perumpail, B. J., Akhtar, D., Kim, D., & Ahmed, A. (2019). The Epidemiology , Risk Profiling and Diagnostic Challenges of Nonalcoholic Fatty Liver Disease. *Medicine*, *6*(41), 1–19. https://doi.org/10.3390/medicines6010041

Jahn, D., Kircher, S., Hermanns, H. M., & Geier, A. (2018). Animal Models of NAFLD from a Hepatologist's Point of View. *BBA - Molecular Basis of Disease*, *294*(18), 1–39. https://doi.org/10.1016/j.bbadis.2018.06.023

Jamieson, R. W., Zilvetti, M., Roy, D., Hughes, D., Morovat, A., Coussions, C. C., & Friend, P. J. (2011). Hepatic Steatosis and Normothermic Perfusion — Preliminary Experiments in a Porcine Model. *Basic and Expermintal Research*, *92*(3), 289–295. https://doi.org/10.1097/TP.0b013e318223d817

Johnson, B. C., & Wolf, G. (1961). The Function of Vitamin A in Carbohydrate

Metabolism: Its Role in Adrenocorticoid Production. *Vitamins and Hormones*, *18*, 457–482.

Jung, E., Baek, E. B., Hong, E., Kang, J. H., Park, S., & Park, S. (2024). TXNIP in liver sinusoidal endothelial cells ameliorates alcohol-associated liver disease via nitric oxide production. *International Journal of Biological Sciences*, *20*. https://doi.org/10.7150/ijbs.90781

Kang, H. W., Bhimidi, G. R., Odom, D. P., Brun, P., Fernandez, M., & Mcgrane, M. M. (2007). Altered lipid catabolism in the vitamin A deficient liver. *Molecular and Cellular Endocrinology*, *271*, 18–27. https://doi.org/10.1016/j.mce.2007.03.002

Kang, J.-S. (2025). *A Comprehensive Guide to Non-alcoholic Fatty Liver Disease*. (J.-S. Kang, Ed.) (First). London, United Kingdom: intechopen. https://doi.org/10.5772/intechopen.1010672

Kantartzis, K., Machicao, F., Machann, J., Schick, F., Fritsche, A., Häring, H., & Stefan, N. (2010). The DGAT2 Gene is a Candidate for Dissociation between Fatty Liver and Insulin Resistance in Humans. *Clinical Science*, *116*(6), 531–537. https://doi.org/10.1042/CS20080306ff. ffhal-00479444f

Kashi, A. M., Tahermanesh, K., Chaichian, S., Joghataei, M. T., Beyranvand, F., Tavangar, S. M., Abed, S. M. (2014). How to Prepare Biological Samples and Live Tissue for Scanning Electron Microscope (SEM). *Galen Medical Journal*, *3*(2), 63–80.

Khammas, A. S. A., Hassan, H. A., Salih, S. Q. M., Kadir, H., Ibrahim, R. M., Nasir, N. N. M., & Mahmud, R. (2019). Prevalence and risk factors of sonographically detected non-alcoholic fatty liver disease in a screening centre in Klang Valley, Malaysia: An observational cross-sectional study. *Porto Biomedical Journal, 4*(2), e31. https://doi.org/10.1016/j.pbj.0000000000000031

Kietzmann, T. (2017). Metabolic zonation of the liver : The oxygen gradient revisited. *Redox Biology*, *11*(January), 622–630. https://doi.org/10.1016/j.redox.2017.01.012

Kim, K., Hong, S., Han, K., Park, C., & Park, C. (2024). Association of non-alcoholic fatty liver disease with cardiovascular disease and all cause death in patients with type 2 diabetes mellitus: Nationwide population based study. *British Medical Journal.*, *384*(e076388), 1–12. https://doi.org/10.1136/bmj-2023-076388

Kim, S. C., Kim, C., Axe, D., Cook, A., Lee, M., Li, T., Lee, Y. K. (2014). All-trans-Retinoic Acid Ameliorates Hepatic Steatosis in Mice by a Novel Transcriptional Cascade. *Hepatology*, *59*(5), 1750–1760. https://doi.org/10.1002/hep.26699

Kirsch, R., Clarkson, V., Shephard, E. G., Marais, D. A., Jaffer, M. A., Woodburne, V. E., Hall, P. D. L. M. (2003). Rodent Nutritional Model of Non-Alcoholic Steatohepatitis: Species, Strain And Sex Difference Studies. *Journal of Gastroentrology and Hepatology*, *18*(March), 1272–1282. /https://doi.org/10.1046/j.1440-1746.2003.03198.x

Kleiner, D. E., Brunt, E. M., Natta, M. Van, Behling, C., Contos, M. J., Cummings, O. W., Ferrell, L. D., Liu, Y.-C., Torbenson, M. S., Unalp-Arida, A., Yeh, M., McCullough, A. J., & Sanyal, A. J. (2005). Design and Validation of a Histological Scoring System for Nonalcoholic Fatty Liver Disease. *Hepatolgyepatology*, *41*(6), 1313–1321. https://doi.org/10.1002/hep.20701

Kohjima, M., Enjoji, M., Higuchi, N., Kato, M., Kotoh, K., Yoshimoto, T., Fujino, T., Yada, M., Yada, R., Harada, N., Takayanagi, R., & Nakamuta, M. (2007). Re-evaluation of fatty acid metabolism-related gene expression in nonalcoholic fatty liver disease. *International Journal of Molecular Medicine20*, *20*, 351–358. https://doi.org/https://doi.org/10.3892/IJMM.20.3.351.

Kounatidis, D., Vallianou, N. G., Geladari, E., Panoilia, M. P., Daskou, A., Stratigou, T., & Dalamaga, M. (2024). NAFLD in the 21st Century : Current Knowledge Regarding Its Pathogenesis , Diagnosis and Therapeutics. *Biomedicines*, *12*(826), 1–16.

Kreutz, F.H. (1962). Enzymatic glycerin determination. *Klin Wochenschr*, *40*(1957), 362–363. https://doi.org/https://doi.org/10.1007/BF01732450

Kumar, D., Farrell, G. C., Fung, C., & George, J. (2002). Hepatitis C Virus Genotype 3 Is Cytopathic to Hepatocytes: Reversal of Hepatic Steatosis After Sustained

Therapeutic Response. *Hepatology*, *36*(5), 1266–1272. https://doi.org/10.1053/jhep.2002.36370

Lai, L.-L., Wan Yusoff, W. N. I., Vethakkan, S. R., Nik Mustapha, N. R., Mahadeva, S., & Chan, W.-K. (2019). Screening for non-alcoholic fatty liver disease in patients with type 2 diabetes mellitus using transient elastography. *Journal of Gastroenterology and Hepatology,* *34*(8), 1396–1403. https://doi.org/10.1111/jgh.14577

Lawitz, E. J., Li, K. W., Nyangau, E., Field, T. J., Chuang, J., Billin, A., Hellerstein, M. K. (2022). Elevated de novo lipogenesis, slow liver triglyceride turnover, and clinical correlations in nonalcoholic steatohepatitis patients. *Journal of Lipid Research*, *63*(9), 100250. https://doi.org/10.1016/j.jlr.2022.100250

Le, T. T., Ziemba, A., Urasaki, Y., Brotman, S., & Pizzorno, G. (2012). Label-free Evaluation of Hepatic Microvesicular Steatosis with Multimodal Coherent Anti-Stokes Raman Scattering Microscopy. *PLOS ONE*, *7*(November), 11. https://doi.org/10.1371/journal.pone.0051092

Leclercq, I. A., Farrell, G. C., Schriemer, R., & Robertson, G. R. (2002). Leptin is essential for the hepatic fibrogenic response to chronic liver injury. *Journal of Hepatology*, *37*(2002), 206–213. https://doi.org/10.1016/s0168-8278(02)00102-2

Lee, S., Yuen, J. J., Jiang, H., Kahn, B. B., Blaner, W.S., & Al, Le e. T.. (2016). Adipocyte-Specific Overexpression of Retinol-Binding Protein 4 Causes Hepatic Steatosis in Mice. *Hepatology*, *64*(5), 1534–1546. https://doi.org/10.1002/hep.28659

Lerner, U. H. (2024). Vitamin A Discovery , Metabolism , Receptor Signaling And Effects On Bone Mass And Fracture Susceptibility. *Frontiers in Endocrinology*, *15*(April), 1–18. https://doi.org/10.3389/fendo.2024.1298851

Levene, A. P., Kudo, H., Armstrong, M. J., Thursz, M. R., Gedroyc, W. M., Anstee, Q. M., & Goldin, R. D. (2012). Quantifying hepatic steatosis - more than meets the eye. *Histopathology*, *60*(6), 971–981. https://doi.org/10.1111/j.1365-2559.2012.04193.x

Liang, S., Xi, S., Liu, J., Tang, G., Zhang, W., Guo, X., … Zhang, C. (2025). Global burden and cross-country inequalities of nutritional deficiencies in adults aged 65 years and older, 1990 – 2021 : population-based study using the GBD 2021. *BioMed Central Geriatrics*, *25*(74), 1–15.

Liang, W., Menke, A. L., Driessen, A., Koek, G. H., Lindeman, J. H., Stoop, R., Van Den, A. M. (2014). Establishment of a General NAFLD Scoring System for Rodent Models and Comparison to Human Liver Pathology. *PLOS ONE*, *9*, 1–18. https://doi.org/10.1371/journal.pone.0115922

Liava, C., & Sinakos, E. (2021). Semaglutide for nonalcoholic steatohepatitis: Closer to a solution? *HepatoBiliary Surgery and Nutrition*, *10*(9), 541–544. https://doi.org/10.21037/hbsn-21-231

Liu, J., Wang, P., Ho, K. E. D. G. N. H. W., Rankin, M. M., Du, F., Hinke, S. A., Albarazanji, K. A. & Nawrocki, A. R. (2020). Foz Foz Mice with a Mutation in the Alms1 Gene Model the Metabolic Syndrome with Advanced Stages of Nonalcoholic Steatohepatitis and Fibrosis. *Diabetes*, *69*(1), 1821. https://doi.org/10.2337/db20-1821-P

Lominadze, Z., & Kallwitz, E. R. (2018). Misconception : You Can't Have Liver Disease With Normal Liver Chemistries. *Clinical Liver Disease*, *12*(4), 96–99. https://doi.org/10.1002/cld.742

Maciejewska, D., Agnieszka, Ł., Dec, K., Ż, K. S.-, Gutowska, I., Skórka-majewicz, M., Stachowska, E. (2019). Diet-Induced Rat Model of Gradual Development of Non-Alcoholic Fatty Liver Disease (NAFLD) with Lipopolysaccharides (LPS) Secretion.*Diagnostics*,*9*(205),1–10. https://doi.org/10.3390/diagnostics9040205

Mak, K. M., & Lieber, C. S. (1984). Alterations in Endothelial Fenestrations in Liver Sinusoids of Baboons Fed Alcohol : A Scanning Electron Microscopic Study. *Hepatology*, *4*(3), 386–391. https://doi.org/0270-9139/84/0403-0386$02.00/0

Makbol, R. M., Kadry, Z. M., Noaman, M. M., Abd, S., Kareem, E., & Othman, A. (2025). The effect of calcium and vitamin A in patients with metabolic - associated fatty liver diseases. *Beni-Suef University Journal of Basic and Applied Sciences*, *14*(24), 2–11. https://doi.org/10.1186/s43088-025-00612-2

Manikat, R., & Nguyen, M. H. (2023). Nonalcoholic fatty liver disease and non-liver co-morbidities. *Clinical and Molecular Hepatology*, *29*, 86-S102. https://doi.org/10.3350/cmh.2022.0442

Marsman, H., Matsushita, T., Dierkhising, R., Kremers, W., Rosen, C., Burgart, L., & Nyberg, S. L. (2004). Assessment of Donor Liver Steatosis : Pathologist or Automated Software? *Human Pathology*, *35*(4), 430–435. https://doi.org/10.1016/j.humpath.2003.10.029

Mehlem, A., Hagberg, C. E., Muhl, L., Eriksson, U., & Falkevall, A. (2013). Imaging of neutral lipids by oil red O for analyzing the metabolic status in health and disease. *Nature Protocol*, *8*(6), 1149–1154. https://doi.org/10.1038/nprot.2013.055

Melis, M., Tang, X., Trasino, S. E., Patel, V. M., Stummer, D. J., Jessurun, J., & Id, L. J. G. (2019). Effects of AM80 compared to AC261066 in a high-fat diet mouse model of liver disease. *PLOS ONE*, *14*(1), 1–18.

Mescher, A. L. (2016). *Junqueira's basic histology: Text and atlas* (14th edition). McGraw Hill.

Miyao, M., Kotani, H., Ishida, T., Kawai, C., Manabe, S., Abiru, H., & Tamaki, K. (2015). Pivotal role of liver sinusoidal endothelial cells in NAFLD / NASH progression. *Laboratory Investigation*, *95*(10), 1130–1144. https://doi.org/10.1038/labinvest.2015.95

Mönkemöller, V., Øie, C., Hübner, W., Huser, T., & Mccourt, P. (2015). Multimodal super-resolution optical microscopy visualizes the close connection between membrane and the cytoskeleton in liver sinusoidal endothelial cell fenestrations. *Scientific Reports*, *5*, 16279. https://doi.org/10.1038/srep16279

Moon, K. (2019). Upregulation of Nitric Oxide Synthase Activity by All- trans Retinoic Acid and 13-cis Retinoic Acid in Human Malignant Keratinocytes. *Biomedical Science Letters*, *25*(2). 196-202. https://doi.org /10.15616/BSL.2019.25.2.196

Mori, Y., Masuda, M., Yoshida-shimizu, R., Aoyagi, S., Adachi, Y., Nguyen, A. T., Ohminami, H. (2024). All- trans retinoic acid induces lipophagy through the activation of the AMPK-Beclin1 signaling pathway and reduces Rubicon

expression in adipocytes. *Journal of Nutritional Biochemistry*, *126*, 1–11. https://doi.org/10.1016/j.jnutbio.2024.109589

Nagral, A., Bangar, M., Menezes, S., Bhatia, S., Butt, N., Ghosh, J., Singh, S. P. (2022). Gender Differences in Nonalcoholic Fatty Liver Disease. *Euroasian Journal of Hepato-Gastroenterology*, *12*(1), 19–25.

Nakeep, S. El, Foda, E., Sheha, A. S., Abdelazeem, S. M., & Mohamed, G. A. (2024). Magnetic Resonance Spectroscopy As A Diagnostic Model For Assessment Of Liver Steatosis in Metabolic Dysfunction-Associated Steatotic Liver Disease In Non - Diabetic Patients. *Egyptian Journal of Radiology and Nuclear Medicine*, *55*(189), 1–12. https://doi.org/10.1186/s43055-024-01342-8

Niu, X., Liu, J., & Liu, K. (2023). Association of Nonalcoholic Fatty Liver Disease And Liver Fibrosis Detected By Transient Elastography With Serum Retinol In American Adults. *Frontiers in Nutrition*, *10*(March), 1–8. https://doi.org/10.3389/fnut.2023.1094161

Okada, H., Takabatake, R., Honda, M., Takegoshi, K., Yamashita, T., Nakamura, M., Kaneko, and S. (2017). Peretinoin , an acyclic retinoid , suppresses steatohepatitis and tumorigenesis by activating autophagy in mice fed an atherogenic high-fat diet. *Oncotarget*, *8*(25), 39978–39993.

Olivia, C., Jasirwan, M., Rinaldi, C., Lesmana, A., Hasan, I., Sulaiman, A. S., & Gani, R. A. (2019). The role of gut microbiota in non-alcoholic fatty liver disease : pathways of mechanisms. *Bioscience of Microbiota, Food and Health Vol.*, *38*(3), 81–88.

Paternostro, R., & Trauner, M. (2022). Current treatment of non-alcoholic fatty liver disease. *Journal of Internal Medicine*, *292*(2), 190–202. https://doi.org/10.1111/joim.13531

Pei, K., Gui, T., Kan, D., Feng, H., Jin, Y., Yang, Y., Li, Y. (2020). Review Article An Overview of Lipid Metabolism and Nonalcoholic Fatty Liver Disease. *BioMed Research International*, *10*, 1–12. https://doi.org/https://doi.org/10.1155/2020/4020249

Peng, Q., Zhang, Q., Xiao, W., Shao, M., Fan, Q., Zhang, H., Cai, H. (2014). Protective Effects of Sapindus Mukorossi Gaertn Against Fatty Liver Disease Induced by High-Fat Diet in Rats. *Biochemical and Biophysical Research Communications*, *450*(1), 685–691. https://doi.org/10.1016/j.bbrc.2014.06.035

Pouwels, S., Sakran, N., Graham, Y., Leal, A., Pintar, T., Yang, W., Ramnarain, D. (2022). Non-alcoholic fatty liver disease (NAFLD): A review of pathophysiology , clinical management and effects of weight loss. *BMC Endocrine Disorders*, *22*(63), 1–9. https://doi.org/10.1186/s12902-022-00980-1

Qi, X., Guo, J., Li, Y., Fang, C., Lin, J., Chen, X., & Jia, J. (2024). Vitamin E Intake Is Inversely Associated With NAFLD Measured By Liver Ultrasound Transient Elastography. *Scientific Reports*, *14*(12), 1–11. https://doi.org/10.1038/s41598-024-52482-w

Rappaport, A. M., Borowy, Z. J., Lougheed, W. M., & Lotto, N. W. (1952). Subdivision of Hexagonal Liver Lobules into A Structural and Functional Unit. *The Anatomical Record, Advances in Integrative Anatomy and Evolutionary Biology*, *119*(1), 11–33. https://doi.org/https://doi.org/10.1002/ar.1091190103

Rinella, M. E., & Green, R. M. (2004). The Methionine-Choline Deficient Dietary Model of Steatohepatitis Does Not Exhibit Insulin Resistance. *Journal of Hepatology*, *40*(2004), 47–51. https://doi.org/10.1016/j.jhep.2003.09.020

Rodés, J., & Benhamou, J.-P. (2007). *Textbook of Hepatology From Basic Science to Clinical Practice* (Third Edition). Oxford, UK: Blackwell Publishing.

Rong, S., Xia, M., Vale, G., Wang, S., Kim, C.-W., Li, S., Horton1, J. D. (2024). DGAT2 Inhibition Blocks SREBP-1 Cleavage And Improves Hepatic Steatosis By Increasing Phosphatidylethanolamine In The ER. *Cell Metabolism*, *36*(3), 617–629. https://doi.org/10.1016/j.cmet.2024.01.011.DGAT2

Rostron, K. A., & Lawrence, C. L. (2017). Histochemistry of Single Molecules. *Histochemistry of Single Molecules*, *1560*, 219–229. https://doi.org/10.1007/978-1-4939-6788-9

Rotbain, E. C., Hansen, D. L., Muckadell, O. S. De, Wibrand, F., Lund, A. M., &

Frederiksen, H. (2017). Splenomegaly Diagnostic validity, work-up, and underlying causes. *PLOS ONE*, *14*(10), 1–11. https://doi.org/https://doi.org/10.1371/journal.pone.0186674

Saeed, A., Dullaart, R. P. F., Schreuder, T. C. M. A., Blokzijl, H., & Faber, K. N. (2018). Disturbed Vitamin A Metabolism in Non-Alcoholic Fatty Liver Disease (NAFLD). *Nutrients*, *10*(29), 1–25. https://doi.org/10.3390/nu10010029

Salih, K. J. (2021). The major pathways of lipids (triglyceride and cholesterol) and lipoprotein metabolism. *ZANCO Journal of Pure and Applied Sciences*, *33*(4), 61–72. https://doi.org/DOI: http://dx.doi.org/10.21271/ZJPAS.33.4.6

Sampey, B. P., Vanhoose, A. M., Winfield, H. M., Freemerman, A. J., Muehlbauer, M. J., Fueger, P. T., Makowski, L. (2011). Cafeteria Diet Is a Robust Model of Human Metabolic Syndrome With Liver and Adipose Inflammation: Comparison to High-Fat Diet. *Obesity*, *19*(6), 1109–1117. https://doi.org/10.1038/oby.2011.18

Savard, C., Tartaglione, E. V., Kuver, R., Haigh, W. G., Farrell, G. C., Subramanian, S., N.George, I. (2013). Synergistic Interaction of Dietary Cholesterol and Dietary Fat in Inducing Experimental Steatohepatitis. *Hepatolgy*, *57*(1), 81–92. https://doi.org/10.1002/hep.25789.Synergistic

Schattenberg, J. M., Balp, M., Reinhart, B., Porwal, S., Tietz, A., Pedrosa, M. C., & Docherty, M. (2024). Identi fi cation of Fast Progressors Among Patients With Nonalcoholic Steatohepatitis Using Machine Learning. *Gastro Hepatic Advancesatic Advances*, *3*(1), 101–108. https://doi.org/10.1016/j.gastha.2023.09.004

Schneider, C. A., Rasband, W. S., & Eliceiri, K. W. (2012). NIH Image to ImageJ : 25 years of image analysis. *Nature Methods*, *9*(7), 671–675. https://doi.org/10.1038/nmeth.2089

Schuck, R. N., Zha, W., Edin, M. L., Gruzdev, A., Vendrov, K. C., Miller, T. M., Lee, C. R. (2014). The Cytochrome P450 Epoxygenase Pathway Regulates the Hepatic Inflammatory Response in Fatty Liver Disease. *PLOS ONE*, *9*(10), 1–12. https://doi.org/10.1371/journal.pone.0110162

Sherman, M. S., & Goessling, W. (2024). Discovery of biophysical rate laws from the electronic health record enables real-time liver injury estimation from transaminase dynamics. *Cell Reports Medicine, 5*(11), Article 101828. https://doi.org/10.1016/j.xcrm.2024.101828

Shirakami, Y., Lee, S.-A., Clugston, R. D., & Blaner, W. S. (2012). Hepatic Metabolism of Retinoids And Disease Associations. *Biochem Biophys Acta*, *1821*(1), 124–136. https://doi.org/10.1016/j.bbalip.2011.06.023.Hepatic

Sohrabi, M., Aghapour, S., Khoonsari, M., Ajdarkosh, H., Nobakht, H., & Zamani, F. (2023). Serum Alkaline Phosphate Level Associates with Metabolic Syndrome Components Regardless of Non-Alcoholic Fatty Liver: A Population-Based Study in Northern Iran. *Middle East Journal Digestive Diseases*, *15*(3), 175–179. https://doi.org/10.34172/mejdd.2023.340

Song, J., & Jiang, Z. G. (2023). Low vitamin A levels are associated with liver-related mortality : A nationally representative cohort study. *Hepatology Communications*, *7*(February), 1–14. https://doi.org/10.1097/HC9.0000000000000124

Song, S. J., & Wong, V. W. (2023). Implications of comorbidities in nonalcoholic fatty liver disease. *Clinical and Molecular Hepatology*, *29*(2), 384–389. https://doi.org/https://doi.org/10.3350/cmh.2023.0066

Sourianarayanane, A., & Nanchal, R. (2018). *Circulatory Physiology in Liver Disease* (Fifth). Camden, USA: Springer International Publishing. Retrieved from https://doi.org/10.1007/978-3-319-66432-3_2%0A21

Speilberg, L., Evensen, O., & Skjerve, E. (1993). Evaluation Of Five Different Immersion Fixatives For Light Microscopic Studies Of Liver Tissue In Atlantic salmon Salmo salar. *Diseases of Aquatic Organims*, *17*, 47–55.

Suvarna, K., Layton, C., & Bancroft, J. D. (2018). *Bancroft's Theory and Practice of Histological Techniques*. (8th ed.). Elsevier.

Szafranska, K., Kruse, L. D., Holte, C. F., Mccourt, P., Zapotoczny, B., & Harris, E. N. (2021). The whole Story About Fenestrations in LSEC. *Frontiers in Physiology*,

12(September), 1–25. https://doi.org/10.3389/fphys.2021.735573

Tang, X., Melis, M., Lu, C., Rappa, A., Zhang, T., Jessurun, J., Gudas, L. J. (2021). A Retinoic Acid Receptor B 2 Agonist Attenuates Transcriptome And Metabolome Changes Underlying Nonalcohol-Associated Fatty Liver Disease. *Journal of Biological Chemistry*, *297*(6), 1–13. https://doi.org/10.1016/j.jbc.2021.101331

Tang, Y., Fan, Y., Wang, Y., Wang, D., Huang, Q., Chen, T., You, Y. (2024). A Current Understanding of FXR in NAFLD : The multifaceted regulatory role of FXR and novel lead discovery for drug development. *Biomedicine & Pharmacotherapy*, *175*, 116658. https://doi.org/10.1016/j.biopha.2024.116658

Targher, G., Byrne, C. D., & Tilg, H. (2024). MASLD: A systemic Metabolic Disorder With Cardiovascular And Malignant Complications. *Recent Advances in Clinical Practice*, *73*, 691–702. https://doi.org/10.1136/gutjnl-2023-330595

Thompson, D., Mahmood, S., Morrice, N., Salino, S. K., Dekeryte, R., Hoffmann, P. A., Mody, N. (2023). Fenretinide Inhibits Obesity And Fatty Liver Disease But Induces Smpd3 To Increase Serum Ceramides And Worsen Atherosclerosis In LDLR-/-Mice. *Scientific Reports*, *13*(3937), 1–16. https://doi.org/10.1038/s41598-023-30759-w

Thompson, S. J., Sargsyan, A., Lee, S., Yuen, J. J., Cai, J., Ghyselinck, N., Graham, T. E. (2017). Hepatocytes are the principal source of circulating RBP4 in mice. *Diabetes*, *66*(1), 58–63. https://doi.org/https://doi.org/10.2337/db16-0286

Tricarico, P. M., Crovella, S., & Celsi, F. (2015). Mevalonate Pathway Blockade , Mitochondrial Dysfunction and Autophagy : A Possible Link. *International Journal of Molecular Sciences*, *16*, 16067–16084. https://doi.org/10.3390/ijms160716067

Walker, H. K., Hall, W. D., & Hurst, J. W. (1990). *Clinical Methods: The History, Physical, and Labratory Examination* (3rd ed.). Butterworths.

Wang, X., Walkey, C. J., Maretti-Mira, A. C., Johnson, D., Wang, L., & DeLeve, L. D. (2020). Susceptibility of rat steatotic liver to ischemia-reperfusion is treatable with liver-selective matrix metalloproteinase inhibition. *Hepatology, 72*(5),

1771–1785. https://doi.org/10.1002/hep.31179

Wang, Z., Du, H., Zhao, Y., Ren, Y., Ma, C., Long, G., Jiang, Y. (2023). Response to pioglitazone in non-alcoholic fatty liver disease patients with vs . without type 2 diabetes : A meta-analysis of randomized controlled trials. *Frontiers in Endocrinology*, *14*(March), 1–11. https://doi.org/10.3389/fendo.2023.1111430

White, D. L., Mazurkiewicz, J. E., & Barrnett, R. J. (1979). A chemical mechanism for tissue staining by osmium tetroxide-ferrocyanide-containing mixtures. *The Journal of Histochemistry and Cytochemistry*, *27*(7), 1084–1091. https://doi.org/https://doi.org/10.1177/27.7.89155

Wong, V. W., Ekstedt, M., Wong, G. L., & Hagström, H. (2023). Changing epidemiology, global trends and implications for outcomes of NAFLD. *Journal of Hepatology*, *79*(3), 842–852. https://doi.org/10.1016/j.jhep.2023.04.036

Yang, F., Jia, X., Lei, P., He, Y., Xiang, Y., Jiao, J., Duan, Q. (2019). Quantification of Hepatic Steatosis in Histologic Images by Deep Learning Method. *Journal of X-Ray Science and Technology*, *27*(6), 1033–1045. https://doi.org/10.3233/XST-190570

Yang, L., Rozenfeld, R., Wu, D., Devi, L. A., Zhang, Z., & Cederbaum, A. (2014). Cannabidiol protects the liver from binge alcohol-induced steatosis by mechanisms including inhibition of oxidative stress and increase in autophagy. *Free Radical Biology and Medicine*, *68*, 260–267. https://doi.org/10.1016/j.freeradbiomed.2013.12.026

Yen, C.-L. E., Stone, S. J., Koliwad, S., Farese, R. V., & Harris, C. (2008). Glycerolipids. DGAT enzymes and triacylglycerol biosynthesis. *Journal of Lipid Research*, *49*(11), 2283–2301. https://doi.org/10.1194/jlr.r800018-jlr200

Zarei, L., Farhad, N., & Abbasi, A. (2020). All-Trans Retinoic Acid (atRA) effectively improves liver steatosis in a rabbit model of high fat induced liver steatosis. *Archives of Physiology and Biochemistry*, *126*(2), 1–6. https://doi.org/10.1080/13813455.2020.1743725

Zhang, L., Shi, Y., Liang, B., & Li, X. (2024). An overview of the cholesterol

metabolism and its proinflammatory role in the development of MASLD. *Hepatology Communications*, *8*(0434), 1–24. https://doi.org/10.1097/HC9.0000000000000434

Zhong, F., Zhou, X., Xu, J., & Gao, L. (2020). Rodent Models of Nonalcoholic Fatty Liver Disease. *Digesion*, *101*(2020), 522–535. https://doi.org/10.1159/000501851

Zhong, H., Dong, J., Zhu, L., Mao, J., Dong, J., Zhao, Y., Ding, G. (2024). Non-alcoholic fatty liver disease : pathogenesis and models. *American Journal of Translational Research*, *16*(2), 387–399. https://doi.org/10.62347/KMSA5983.

Zhou, J., Wang, J., Zhang, L., & Zhang, C. (2025). Defenestration of Liver Sinusoidal Endothelial Cells: The Trigger of Liver Fibrosis. *Pharmaceuticals*, *18*(893). https://doi.org/10.3390/ ph18060893 Copyright:

Zhu, S., Zhang, J., Zhu, D., Jiang, X., Wei, L., & Chen, Y. Q. (2022). Adipose tissue plays a major role in retinoic acid-mediated metabolic homoeostasis. *Adipocyte*, *11*(1), 47–55. https://doi.org/10.1080/21623945.2021.2015864

APPENDIX I: RESEARCH APPROVAL LETTER

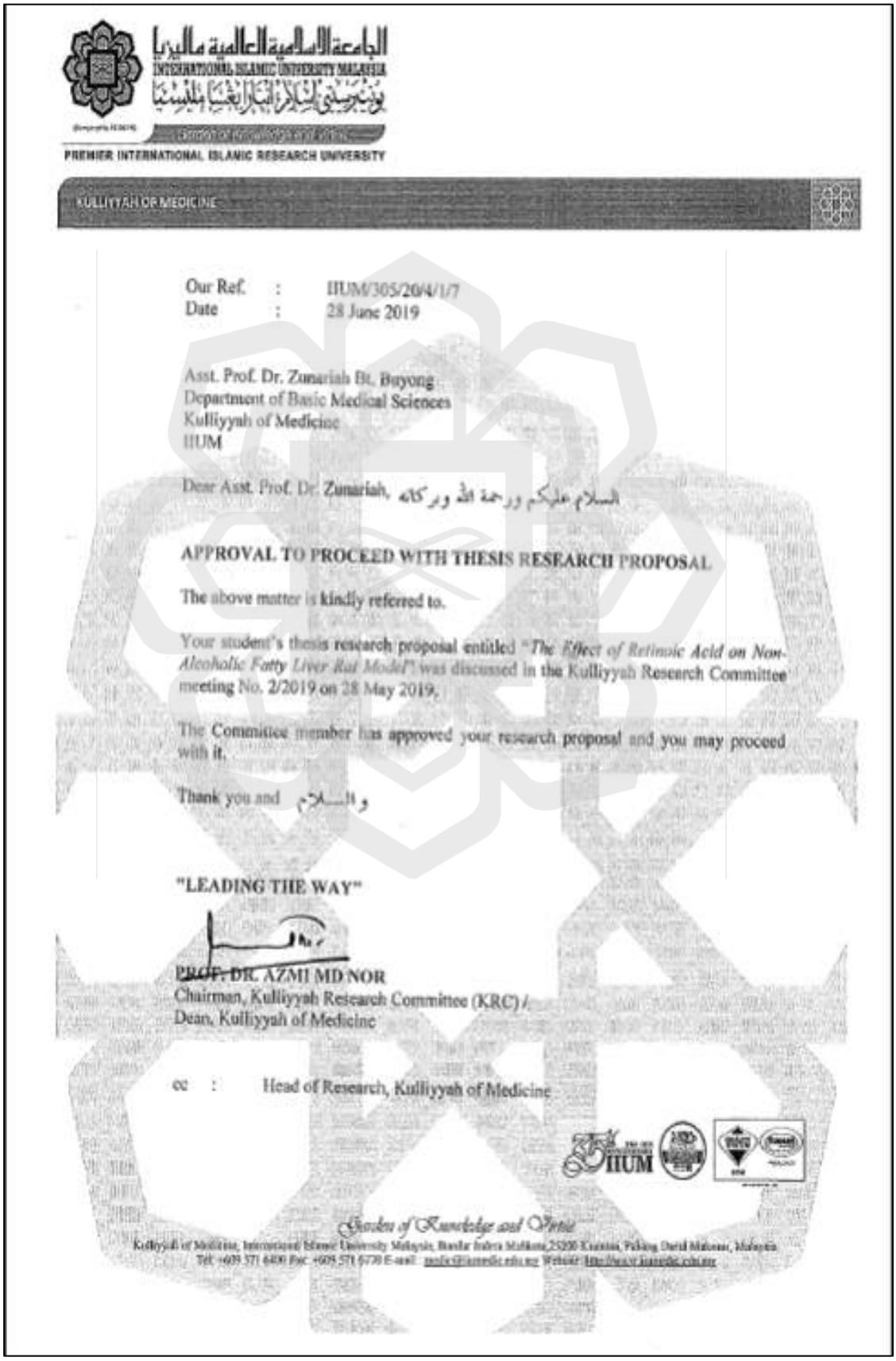

الجامعة الإسلامية العالمية ماليزيا
INTERNATIONAL ISLAMIC UNIVERSITY MALAYSIA
PREMIER INTERNATIONAL ISLAMIC RESEARCH UNIVERSITY

KULLIYYAH OF MEDICINE

Our Ref. : IIUM/305/20/4/1/7
Date : 28 June 2019

Asst. Prof. Dr. Zunariah Bt. Buyong
Department of Basic Medical Sciences
Kulliyyah of Medicine
IIUM

Dear Asst. Prof. Dr. Zunariah, السلام عليكم ورحمة الله وبركاته

APPROVAL TO PROCEED WITH THESIS RESEARCH PROPOSAL

The above matter is kindly referred to.

Your student's thesis research proposal entitled "*The Effect of Retinoic Acid on Non-Alcoholic Fatty Liver Rat Model*" was discussed in the Kulliyyah Research Committee meeting No. 2/2019 on 28 May 2019.

The Committee member has approved your research proposal and you may proceed with it.

Thank you and والسلام

"LEADING THE WAY"

PROF. DR. AZMI MD NOR
Chairman, Kulliyyah Research Committee (KRC) /
Dean, Kulliyyah of Medicine

cc : Head of Research, Kulliyyah of Medicine

IIUM

Garden of Knowledge and Virtue
Kulliyyah of Medicine, International Islamic University Malaysia, Bandar Indera Mahkota, 25200 Kuantan, Pahang Darul Makmur, Malaysia
Tel: +609 571 6400 Fax: +609 571 6720 E-mail: [illegible] Website: [illegible]

APPENDIX II: IACUC APPROVAL LETTER

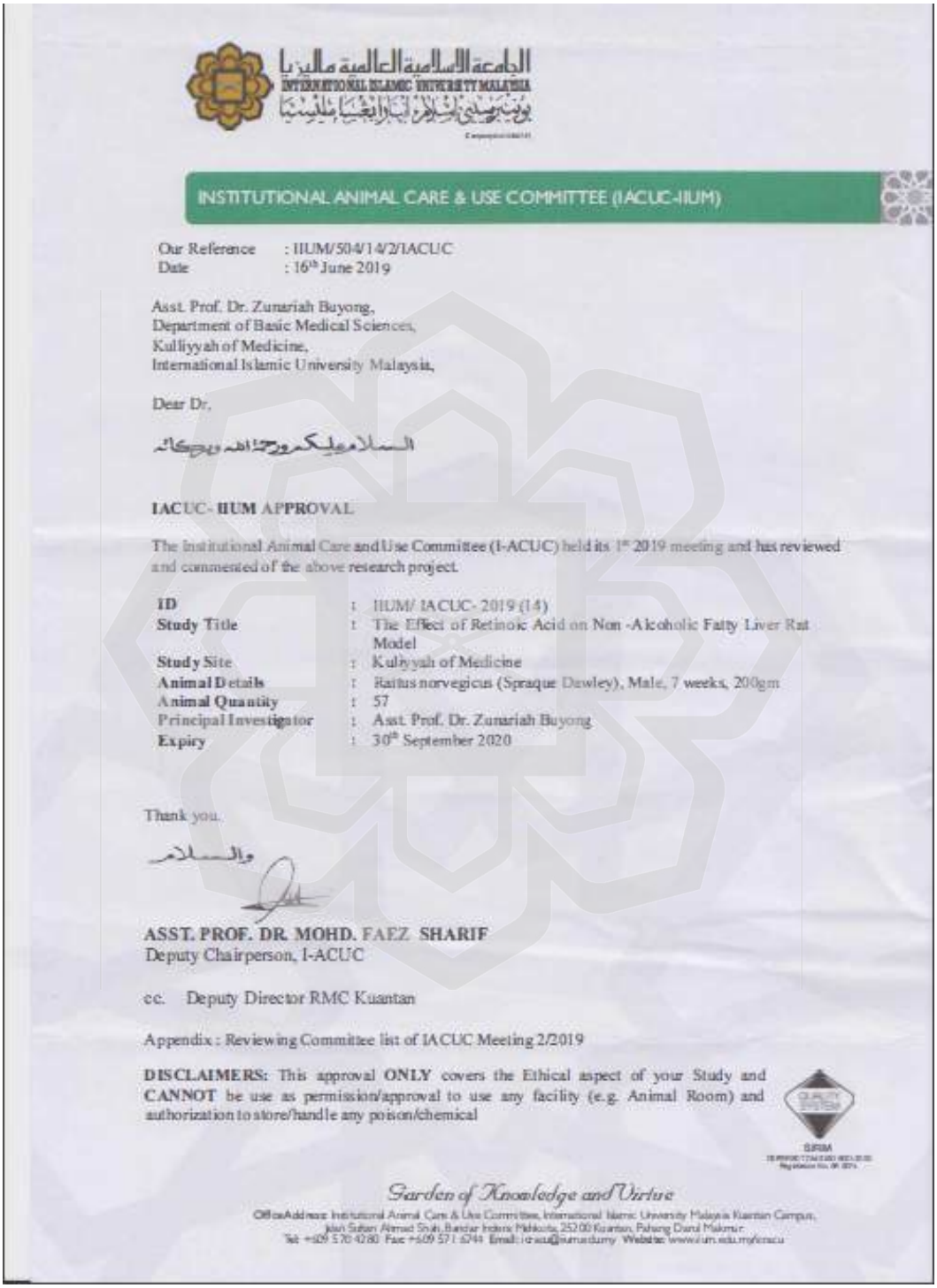

الجامعة الإسلامية العالمية ماليزيا
INTERNATIONAL ISLAMIC UNIVERSITY MALAYSIA

INSTITUTIONAL ANIMAL CARE & USE COMMITTEE (IACUC-IIUM)

Our Reference : IIUM/504/14/2/IACUC
Date : 16th June 2019

Asst. Prof. Dr. Zunariah Buyong,
Department of Basic Medical Sciences,
Kulliyyah of Medicine,
International Islamic University Malaysia,

Dear Dr,

السلام عليكم ورحمة الله وبركاته

IACUC- IIUM APPROVAL

The Institutional Animal Care and Use Committee (I-ACUC) held its 1st 2019 meeting and has reviewed and commented of the above research project.

ID	:	IIUM/ IACUC- 2019 (14)
Study Title	:	The Effect of Retinoic Acid on Non -Alcoholic Fatty Liver Rat Model
Study Site	:	Kulliyyah of Medicine
Animal Details	:	Rattus norvegicus (Spraque Dawley), Male, 7 weeks, 200gm
Animal Quantity	:	57
Principal Investigator	:	Asst. Prof. Dr. Zunariah Buyong
Expiry	:	30th September 2020

Thank you.

والسلام

ASST. PROF. DR. MOHD. FAEZ SHARIF
Deputy Chairperson, I-ACUC

cc. Deputy Director RMC Kuantan

Appendix : Reviewing Committee list of IACUC Meeting 2/2019

DISCLAIMERS: This approval **ONLY** covers the Ethical aspect of your Study and **CANNOT** be use as permission/approval to use any facility (e.g. Animal Room) and authorization to store/handle any poison/chemical

SIRIM

Garden of Knowledge and Virtue

Office Address: Institutional Animal Care & Use Committee, International Islamic University Malaysia Kuantan Campus,
Jalan Sultan Ahmad Shah, Bandar Indera Mahkota, 25200 Kuantan, Pahang Darul Makmur.
Tel: +609 570 4280 Fax: +609 571 6744 Email: iacuc@iium.edu.my Website: www.iium.edu.my/iacuc

APPENDIX III: TISSUE PROCESSING PROTOCOL

Overnight tissue processing protocol using automated tissue processing machine (Leica TP 1020 Semi-enclosed Benchtop Tissue Processor, Germany). Following protocol used by Carriel, Campos, Aneiros-Fernández, & Kiernan, (2017).for fatty tissue.

Chemical	**Concentration**	**Time**
Ethanol	50%	1 hour
Ethanol	70%	1 hour
Ethanol	80%	2 hours
Ethanol	95%	2 hours
Ethanol	100%	1 hour
Ethanol	100%	1 hour
Ethanol	100%	1 hour
Xylene I		1 hour
Xylene II		1 hour
Paraffin wax I		2 hours
Paraffin wax II		3 hours

APPENDIX IV: OIL RED O STAINING PROTOCOL

Chemicals and material

- ORO working solution 0.5% in isopropanol from Sigma-Aldrich (CAS# 1320-06-5)

  3:2 Diluted in distilled water then filtered through Whatman No. 1 filter paper.

- 60% isopropanol

  60ml isopropanol 100% + 40 ml distilled water

- Silane coated frosted 20 F (MuTo PURE, chemicaLs Co., LTD).
- Frozen section compound (FSC 22^{TM}) (Surgipath Canada)
- Cryostat chamber LEICA CM 1850

Procedure:

Formalin fixed and cryoprotected tissue in sucrose embedded in FSC at -20 ˚C. then sectioned at thickness 8 µm.

1. Let the section dry on the slide for 5 min at room temperature.
2. Section was washed with 60% isopropanol two times, stained with ORO solution for 15 min, later wash with 60% isopropanol.
3. Counterstained with Hematoxylin counterstain for 30 second.

APPENDIX V: MASSON'S TRICHROME STAINING PROTOCOL

According to Microscopy Masson-Goldner staining kit (1.00485.0001) from Sigma-Aldrich, Germany.

Chemical	**Time**
Xylene	3 min
Xylene	3 min
100% alcohol	3 min
100% alcohol	3 min
90% alcohol	3 min
Tape water	2 min
Weigerts Iron Hx	30 min
Tape water	30 sec
R1, Azophloxine	20 min
Acetic acid 1%	30 sec
R2 (phosphoric acid)	20 min
Acetic acid 1%	30 sec
R3 (light green SF)	20 min
Acetic acid 1%	30 sec
Alcohol 70%	30 sec
Alcohol 96%	30 sec
Alcohol 100%	30 sec
Alcohol 100%	30 sec
Alcohol 100%	2 min
Xylene twice	2 min

APPENDIX VI: OPTIMIZATION TRIALS FOR DGAT2 IHC

Protocol	AR PH	H202 time	Protein Block	1ry Ab dilution	Pry AB	HRP time	DAB	Result
P1	6	5 min	0	1:200	1hr	30min	10 min	-ve cytoplasm, +ve Nucleus
P2	6	5 min	0	1:100	1hr	30min	10 min	±ve cytoplasm, +ve Nucleus
P3	6	5 min	0	1:200	18hr	30min	10 min	-ve cytoplasm, +ve Nucleus
P4	6	5 min	0	1:100	18hr	30min	10 min	+ve cytoplasm, +ve Nucleus
P5	6	10 min	10 min	1:10	1hr	15min	10 min	+ve cytoplasm, +ve Nucleus
P6	9	10 min	10 min	1:100	1hr	15min	10 min	+ve cytoplasm, +ve Nucleus
P7	9	10 min	10 min	1:200	1hr	15min	10 min	+ve cytoplasm, +ve Nucleus
P8	9	30 min	1hr	0	0	10 min	2 min	Negative staining
P9	9	30 min	1hr	1:100	1hr	10 min	2 min	Prominent cytoplasm and nucleus stain
P10	9	30 min	18hr	1:100	1hr	10 min	2 min	Faint cytoplasm &++ nucleus
P11	9	30 min	2hrs	1:200	1hr	5 min	1 min	Faint cytoplasm &++ nucleus
P12	9	30 min	2hrs	1:300	1hr	5 min	1 min	Faint cytoplasm &++ nucleus
P13	9	30 min	2hrs	1:400	1hr	5 min	1 min	Faint cytoplasm &++ nucleus
P14	9	30 min	5% BSA for 30min	1:200	1hr	15 min	5 min	+ve cytoplasm, -ve Nucleus
P15	9	30 min	5% BSA for 1hr	1:200	1 hr	15 min	5 min	+ve cytoplasm, -ve Nucleus
P16	9	30 min	5% BSA for 30min	1:200	30 min	15 min	5 min	+ve cytoplasm, -ve Nucleus
P17	9	30 min	5% BSA for 30hr	1:200	15min	15 min	5 min	+ve cytoplasm, -ve Nucleus

APPENDIX VII: DGAT2 IMMUNOHISTOCHEMISTRY PROTOCOL

Primary antibody from Bioss Antibodies (bs-12998R) (size: 100µl, Concentration 1µg/µl). Host is Rabbit, Polyclonal, IgG antibody. Source from KLH conjugated synthetic peptide derived from human DGAT2.Purification by protein A. staining was done using DAKO auto-stainer at IIUM medical Center Pathology Laboratory. According to the bellow steps.

Detection kit steps:

1. Deparaffinized and rehydrated formalin fixed paraffin embedded tissue section.
2. Preformed pretreatment for antigen retrieval using EnVision FLEX target retrieval solution high PH (9) from Dako Omnis at 100 ˚C for 30 seconds then at 90 ˚C for 20 min. then let it cooled down at room temperature then washed 3 times in TBS buffer.
3. Added enough drops of Hydrogen peroxide Block to cover the sections. Incubate for 30 mins. Wash 2 times in buffer.
4. Protein block was applied by 5% Albumin, Bovine Serum (BSA) from CALIBIOCHEM (Cat# 126593) (U.S) and incubate for 30 mins at room temperature to block nonspecific background staining. Wash 1 time in buffer. (Zhao et al., Block for 30 min).
5. Section was then incubated in Primary antibody at concentration of 1:200 for 30 min. [Zhao et al., 2015 used anti-DGAT2 antibodies at (dilution 1:200 at 4°C overnight]
6. Wash 3 times in buffer. Apply HRP-conjugate and incubate for 15 min. rinse 4 times in buffer.
7. Then section was incubated in DAB for 5 min followed by 4 times wash by buffer.
8. Apply counter stain according to manufacturer instruction.

APPENDIX VIII: ACHIEVEMENTS

Medical Research Symposium 2018

APPENDIX IX: ACHIEVEMENTS

Kuantan Research Day 2019

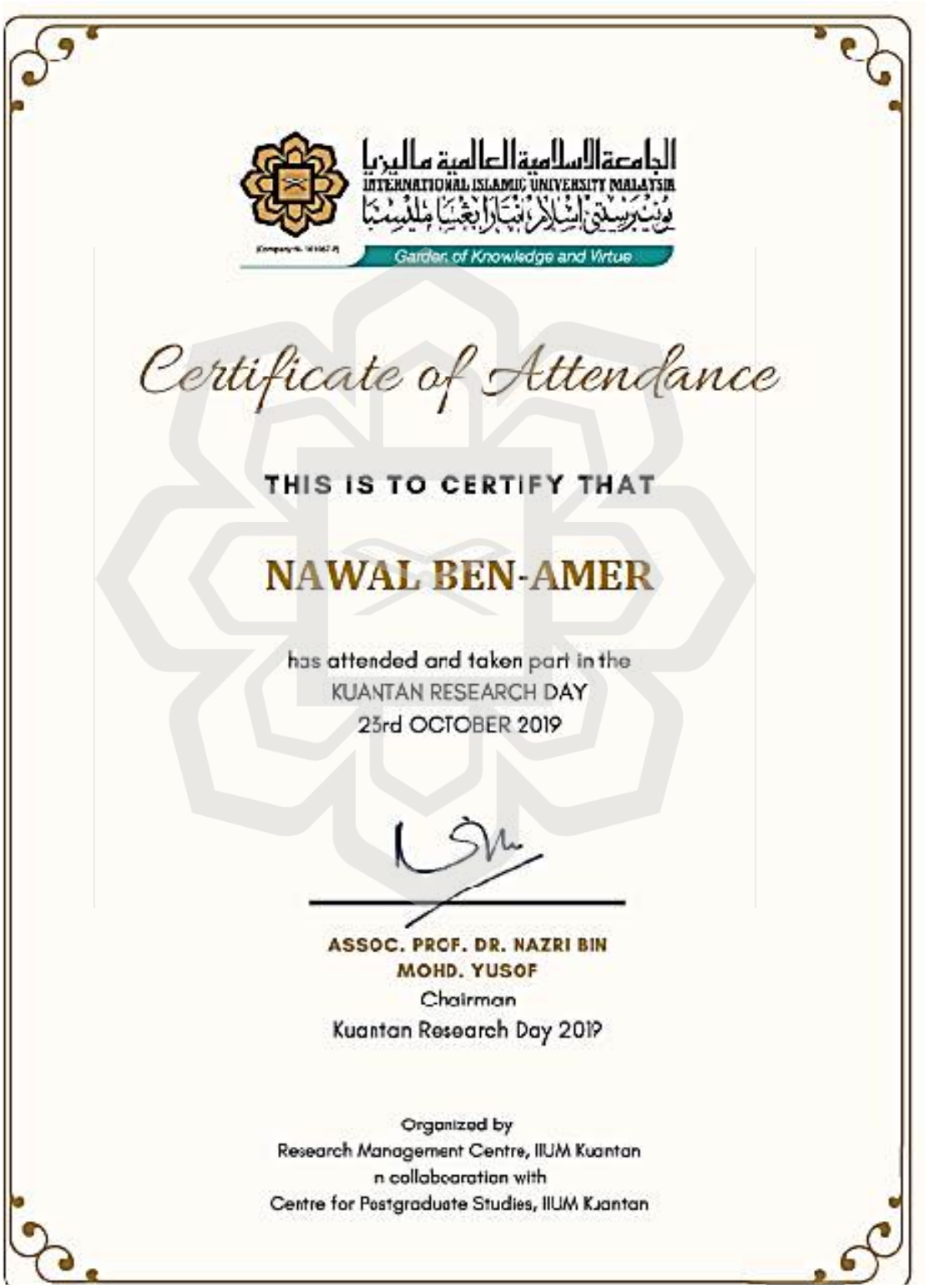

الجامعة الإسلامية العالمية ماليزيا
INTERNATIONAL ISLAMIC UNIVERSITY MALAYSIA
Gardan of Knowledge and Virtue

Certificate of Attendance

THIS IS TO CERTIFY THAT

NAWAL BEN-AMER

has attended and taken part in the
KUANTAN RESEARCH DAY
23rd OCTOBER 2019

ASSOC. PROF. DR. NAZRI BIN
MOHD. YUSOF
Chairman
Kuantan Research Day 2019

Organized by
Research Management Centre, IIUM Kuantan
n collabcaration with
Centre for Postgraduate Studies, IIUM Kuantan

APPENDIX X: ACHIEVEMENTS

Kuantan Research Day 2020

APPENDIX XI: ACHIEVEMENTS

IIUM Research Day 2021

APPENDIX XII: ACHIEVEMENTS

Postgraduate Colloquium 2021

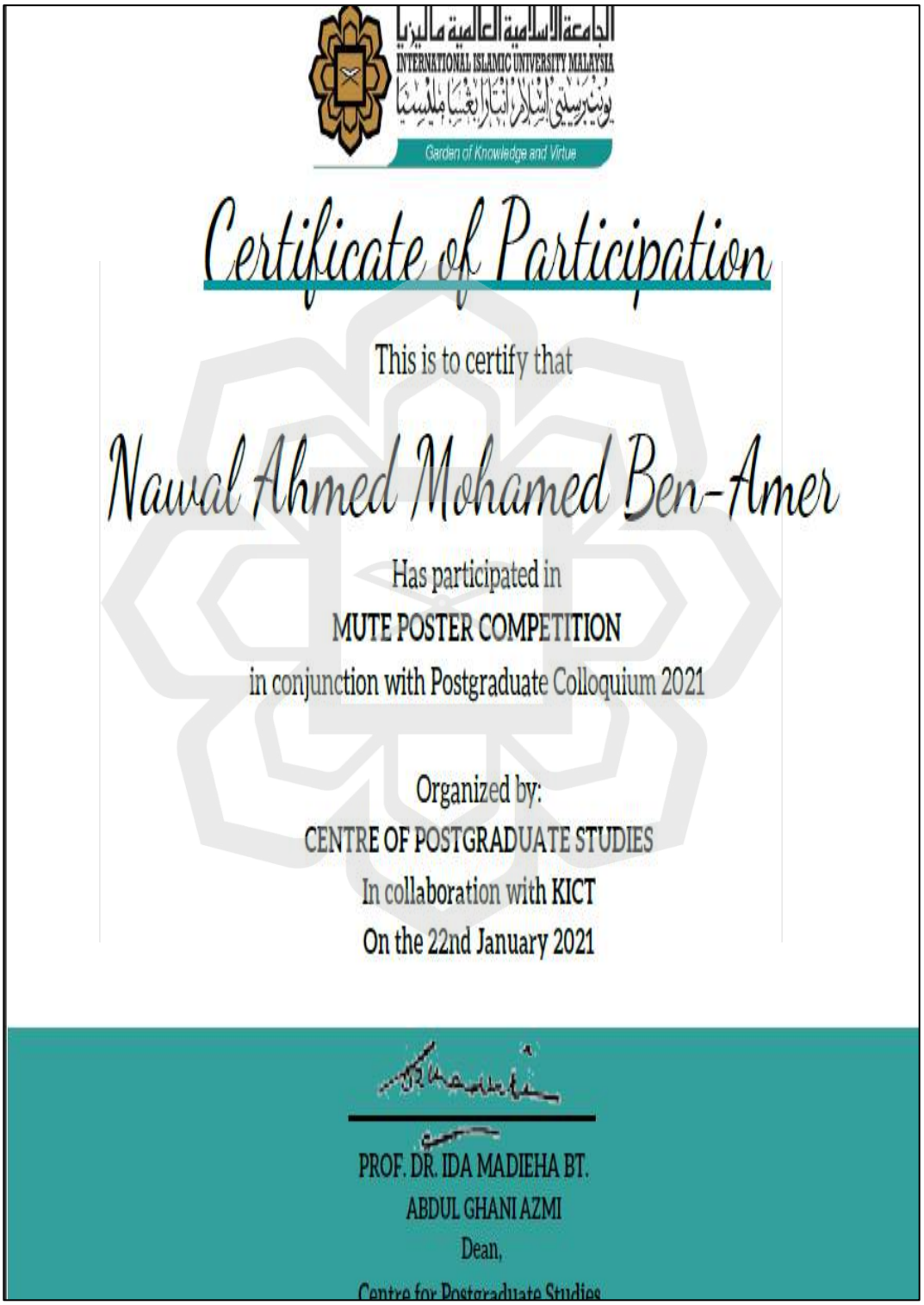
الجامعة الإسلامية العالمية ماليزيا
INTERNATIONAL ISLAMIC UNIVERSITY MALAYSIA
Garden of Knowledge and Virtue

Certificate of Participation

This is to certify that

Nawal Ahmed Mohamed Ben-Amer

Has participated in

MUTE POSTER COMPETITION

in conjunction with Postgraduate Colloquium 2021

Organized by:

CENTRE OF POSTGRADUATE STUDIES

In collaboration with KICT

On the 22nd January 2021

PROF. DR. IDA MADIEHA BT.
ABDUL GHANI AZMI
Dean,
Centre for Postgraduate Studies

APPENDIX XIII: ACHIEVEMENTS

Medical Research Symposium 2023

Poster No. PNC008

INTERNATIONAL VIRTUAL 2023 MEDICAL RESEARCH SYMPOSIUM

RETINOIC ACID TARGETING DGAT2 IN NON-ALCOHOLIC FATTY LIVER DISEASE

Nawal Ahmed Mohamed[1], Zunariah Buyong[1], Nor Zamzila Abdullah[1], Asmah Hanim Hamdan[1], Jamalludin Ab. Rahman[1], Sirajudeen Kuttulebbai Naina Mohamed Salam[1]

[1]*International Islamic University Malaysia, Kulliyyah of Medicine, Malaysia*

- Nonalcoholic fatty liver disease (NAFLD) is caused by triglyceride (TG) accumulation in the hepatocyte.
- Liver storage of vitamin A is decreased in NAFLD.
- Retinoic acid (RA) decreased liver steatosis.
- RA also suppressed DGAT2 hepatic expression in NAFLD animal model.

Introduction:

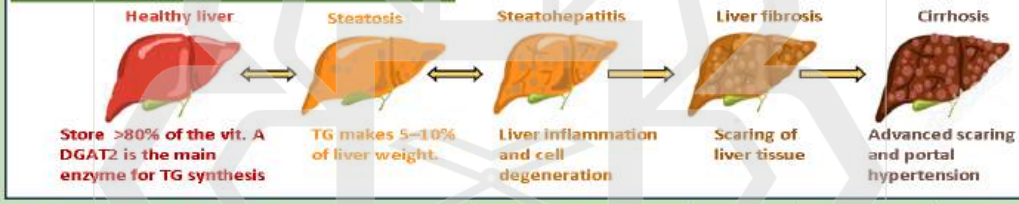

36 rats divided into 4 groups. CD: Control diet; HCD: High Cholesterol Diet; HCD + Vehicle (V) and HCD + Retinoic Acid (R). HCD + RA received subcutaneous RA twice weekly for four weeks.

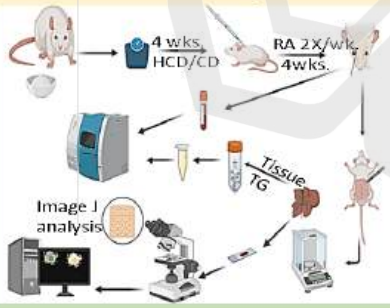

Liver tissue TG was significantly reduced in RA treated animals compared to HCD rats

DGAT2 expression in HCD group treated with RA was significantly lower than HCD only group

Group	Tissue TG	DGAT2 expression
CD	76.4±21.3**	7.0±1.4**
HCD	230.4±39.4	21.5±1.9
HCD+V	212.7±48.1	21.7±1.8
HCD+RA	102.3±19.3**	12.1±1.8 **

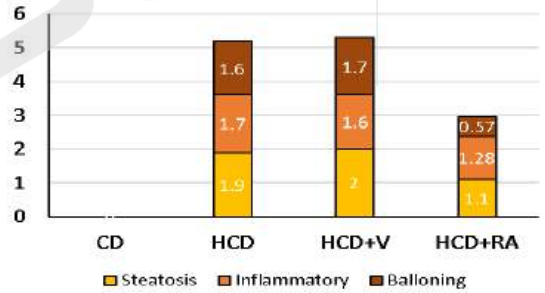

Discussion & Conclusion:

- RA was successfully shown mitigating TG deposition in the liver. A similar result reported by Zarei et al., (2020) based on semiquantitative analysis on histopathological changes.
- None of the previous studies on RA reported its effect on DGAT2 expression.
- Our results reveal therapeutic opportunity of RA in improving TG accumulation in the liver through inhibiting DGAT2.

References:

Leila Zarei, Negin Farhad & Ata Abbasi (2020): All-Trans Retinoic Acid (atRA) effectively improves liver steatosis in a rabbit model of high fat induced liver steatosis, Archives of Physiology and Biochemistry, DOI: 10.1080/13813455.2020.1743725

Acknowledgement:

IIUM Research Management Centre for providing financial support under RMCG20-064-0064. Medical Laboratory Technologists & Staff, Department of Basic Medical Sciences, Pathology Laboratory Medicine, and Postgraduate Office Kulliyyah of Medicine, International Islamic University Malaysia, Malaysia.